EFFECTS OF GAMMA RADIATION ON FETAL DEVELOPMENT IN THE RAT.

A Thesis

Presented to the Faculty of Graduate Studies,

University of Manitoba, in Partial Fulfillment

of the Requirements for the Degree of

Master of Sciences

by

Anne Elizabeth Strock

September, 1991

ISBN 0-315-77745-1

EFFECTS OF GAMMA RADIATION ON FETAL DEVELOPMENT IN THE RAT

BY

ANNE ELIZABETH STROCK

A thesis submitted to the Faculty of Graduate Studies of the University of Manitoba in partial fulfillment of the requirements of the degree of

MASTER OF SCIENCE

Dedicated with love and thanks to my parents,

Arthur and Dorothy Strock.

ACKNOWLEDGEMENTS

I wish to express my thanks to Mr. B. Sam and Dr. P. Daeninck for their guidance in animal care and treatment procedures, Linda Snell for teaching me histological processing techniques, Paul Perumal for teaching me film processing and developing, and Roy Simpson for his expertise in photography. As well, I am deeply grateful to Donna Love and Bill Pylypas for their generous assistance in various lab procedures.

Special thanks to Drs. Judy Anderson and Jean Paterson for their assistance, encouragement, and support throughout the course of my studies, and Dr. J. Thliveris for his advice in assessing histological data. I would also like to express my sincere appreciation and thanks to Dr. J.E. Bruni for his excellent teaching in neuroanatomy, and expert guidance in assessing my data.

I would also like to thank the Department of Anatomy for awarding me an Anatomical Research Fund Graduate Student Scholarship during the final year of my studies.

To my advisor, Dr. T.V.N. Persaud, I express my deepest appreciation and thanks for his endless patience, encouragement, and guidance in introducing me to a new realm of knowledge.

I would like to acknowledge my friends and family who have offered me encouragement, support, and understanding, all of which is much appreciated. Special thanks to Helen Strock and Hugh Penwarden, to whom I am indebted for instilling in me the confidence to see this project to completion.

ABSTRACT

The teratological effects of *in utero* exposure to 0.5 Gy (50 rads) on gestational day 15 was investigated in Sprague-Dawley rats at 4 hours, 48 hours, and 5 days after irradiation. A Theratron Cobalt Unit was used for whole body exposures of the pregnant animals. Control animals were confined to a treatment chamber for a comparable time period but were not irradiated. The following parameters were investigated: maternal weight, litter size, embryolethality, fetal growth, litter sex ratio, placental weight, gross external morphology, and the histological changes in the cerebral cortex, the main olfactory bulbs, the corpus callosum, the hippocampal formation, the cerebellum, as well as in the placenta.

There were no significant differences in any group as compared to age-related controls with respect to maternal weight, litter size, embryolethality, litter sex ratio or external morphological development. Significant differences were found in fetal weight, crown-rump length, and placental weight. Although the brain in all specimens showed acute irradiation effects, only the cerebral cortex and main olfactory bulbs revealed irradiation-induced changes at later fetal stages. Placental changes were observed 4 and 48 hours after irradiation, but not at the 5 day interval.

The present findings were compared to observations from other related teratological studies. The fetus as

a model for investigating irradiation-induced effects in the brain is discussed, and a hypothesis for the role of the placenta in irradiation-induced teratogenesis is proposed.

TABLE OF CONTENTS

1. INTRODUCTION AND OBJECTIVES

This project is one of four components of a preliminary study conducted in the Department of Anatomy, and supported by the Atomic Energy Commission of Canada.

The purpose of these studies, was to assess the effects of a "low dose" of ionizing radiation on the embryonic and fetal rat, with particular emphasis on the developing nervous system. Although controlled irradiation teratogenetic studies have been conducted for almost 60 years, only in recent years have investigators focused on the teratogenetic effects of low dose levels. Low dose level research is needed in order to establish safety protocols for medical exposures and, home and occupational environments. Currently, little is known about the full spectrum of low dose ionizing radiation effects on the unborn child.

In all four components of the project, pregnant Sprague-Dawley rats were irradiated with 0.5 Gy (50 rads) of gamma radiation at various stages of the gestational period. Irradiated offspring were assessed at different intervals of the prenatal and postnatal periods. The other three completed components of this project include:

1) irradiation on gestational day 9.5 and assessed 4 hours, 48 hours, and 10 days post-irradiation.

2) irradiation on gestational day 15 and assessed on postnatal days 7 and 26.

3) irradiation on gestational day 18 and assessed on

postnatal days 7 and 26.

This component of the study involved whole body irradiation of pregnant Sprague-Dawley rats on gestational day 15 with a 0.5 Gy (50 rads) dosage of gamma radiation. Fetuses were recovered at 4 hours, 48 hours, and 5 days post-irradiation.

Most experimental studies involving irradiation during pregnancy have dealt with the postnatal offspring, and only a few have assessed prenatal developmental effects. From this study, we hope to gain insight into fetal outcome following irradiation with a relatively low dose of ionizing radiation (0.5 Gy = 50 rads) on gestational day 15. The following were investigated: fetal growth, external morphological development, placentation, and neurogenesis. The brain areas selected for histological studies have included the cerebral cortex, the main olfactory bulbs, the corpus callosum, the hippocampal formation, and the cerebellum. These brain areas were selected on the basis of other reports of gestational day 15 radiosensitivity at higher dose ranges, and/or their predicted developmental vulnerability to a gestational day 15 exposure.

Prenatal assessment of radiation effects may provide information on the pathogenesis of developmental defects which have been observed in the postnatal period. Furthermore, the data obtained from this investigation will be applied to experiments utilizing lower ionizing radiation dose ranges in rats, as well as a series of

proposed studies on the prenatal irradiation effects on the postnatal brain development and behavior of monkeys.

2. REVIEW OF THE LITERATURE

2.1. IONIZING RADIATION

2.1.1. Properties of Ionizing Radiation

Ionizing radiation is a term used to describe specific types of energies, which possess enough photon energy to cause the ejection of electrons from atoms or molecules in living tissue. Ionization is a property of x-rays, gamma rays, and particulate radiation. Ionization within living tissue can cause variable, dose-dependent degrees of mutations and chromosomal abnormalities, carcinogenetic changes, cell-killing, and alterations of cell and/or tissue growth (Prasad, 1974; Brent, 1986; Hall, 1988).

Gamma rays and x-rays are both forms of electromagnetic radiation, whose short wavelengths and high frequencies provide sufficient photon energy to ionize in biological material. Gamma rays and x-rays are essentially identical in biological effect. Their different names simply reflect the different ways they are manufactured. X-rays are produced by acceleration of electrons to high energy levels. The kinetic energy of the electrons is converted into x-rays. Gamma rays represent the excess energy derived from radioactive isotopes, as they attempt to reach a stable form (Hall, 1988; Cobb, 1989). It should be noted that other forms of electromagnetic radiation such as ultraviolet, infrared, visible light, microwave, and radiowaves are very different from gamma or x-rays.

Due to the long wavelength and low frequency characteristics of these radiant energies, as compared to x-ray and gamma rays, they do not possess the photon energy required for ionization in tissue. Instead, the primary biological effect imparted by these forms of radiation is excitation of atomic or molecular electrons (Brent, 1986).

Particulate radiation is a term used to collectively describe sub-atomic particles of various masses and charges. These would include protons, alpha-particles, neutrons, and heavy charged ions. Teratological studies involving particulate radiation have not been considered in this review because of the differences that exist between particulate and electomagnetic ionizing radiation. It may suffice to say that for a given dose, particulate radiation is more destructive to absorbing tissues, as it produces a much higher rate of ionizing events within biological material, compared to electromagnetic ionizing radiation (Upton, 1982; Hall, 1988).

2.1.2. Units of Measure

There are several units of measure used to quantify doses of ionizing radiation. The oldest unit is the roentgen (R) which is a measure of the quantity of ionization induced in air. It is not used in current teratology/radiobiology literature, as it is not an accurate measure of the amount of ionizing radiation absorbed in tissue. However, Hall (1988) claims that in the case of x-rays and gamma rays, one roentgen results in an absorbed dose of roughly one

rad in soft tissue or water. The most commonly used units to express absorbed dose are the rad and the gray (Gy). The rad is equivalent to 100 ergs per gram of tissue, whereas the gray is equivalent to one joule per kilogram of tissue or, 100 rads. Although the appropriate international unit of absorbed dose is the gray, the rad is still used to a great extent in everyday radiobiology practice (Upton, 1982; Hall, 1988; Cobb, 1989).

In literature concerning radiation protection and human risk estimation, the rem and the sievert are units commonly used. These units were introduced so that different types of radiation could be compared for their biological effects. The rem is the amount of any radiation that produces an effect equivalent to one rad of gamma rays in biological tissue. Similarly, one sievert is equivalent to effects produced by one gray (Upton, 1982).

Although many authors refer to low dose and high dose levels, these terms are really quite arbitrary (Hicks and D'Amato, 1980). Low level radiation is a term that has been used in describing annual background radiation accumulations which are as low as 2.0 to 3.6 millisieverts (Upton, 1982; Clarke and Southwood, 1989). In contrast, Bayer and Altman (1975), in a study of the granule cell population in the rat brain, use the term low level radiation when describing fractionated daily doses of 150 to 200 rads. In an extensive study of rat olfactory lobe morphology following x-irradiation, Halasz (1986) used the term low

level to describe fractionated doses of 50 to 200 rads, which cumulated in doses ranging from 250 to 1070 rads per animal.

2.1.3. Sources of Ionizing Radiation

Humans and other organisms are constantly exposed to ionizing radiation derived from both man-made and natural sources. Natural background radiation is primarily composed of emissions of radioactive elements in the earth's crust, cosmic rays, as well as emissions from radioactive isotopes that occur naturally in the body. Man-made sources would include routine medical diagnostic exposures, consumer products such as television sets and smoke detectors, various building materials and phosphate fertilizers, as well as global fallout from nuclear weapons, leakage from nuclear reactors, and occupational exposure. For the average person in the United States, the total annual background radiation exposure is about 3.6 millisieverts (Clarke and Southwood, 1989). This dose level is really quite minute when one considers that a typical dental x-ray provides a dose of 1 millisievert to the cheek (Upton, 1982).

The hazardous effects of background radiation are too small to detect. There are still many unanswered questions concerning effect thresholds and, the cumulative and heritable effects of background radiation exposure (Upton, 1982; McClellan, 1988; Cobb, 1989).

Persons who receive medical radiation treatment

would be exposed to much higher annual doses of ionizing radiation. Fractionated doses can cumulate into exposures of hundreds to thousands of rads for some radiotherapy treatments (Hicks and D'Amato, 1966; Brent, 1986). As well as medical exposure, individuals subjected to a single dose exposure of ionizing radiation in the 50 rad (0.5 Gy) range may include victims of nuclear weaponry or nuclear accidents. In some occupations, such as radium mining and medical technology for example, workers may also be exposed to higher than average cumulative doses (Brent, 1986; Cobb, 1989).

2.1.4. Biological Effects

The biological outcome for tissues subjected to ionizing radiation is dependent on the degree of damage to "critical targets" within the absorbing cells, and the capacity of the cell to repair itself. Critical targets can be defined as those discrete cellular structures which, if damaged, threaten the functional capacity, reproductive capability, or longevity of the cell. Probably the most critical target of all cell molecules is the chromosomal DNA molecule, although some radiobiologists suspect that the nuclear membrane is equally as important (Upton, 1982; Hall, 1988).

As gamma and x-rays are absorbed into biological tissue, they give up their photon energy through interactions with "free" electrons (electrons whose binding energy is small compared with the photon energy). The photon

energy is therefore dissipated, having given part of its energy to the electron as kinetic energy. The photon, with whatever energy remains, continues on a deflected path to take part in further interactions. The net outcome of the proton/free electron interactions is the production of a number of fast moving electrons. These fast moving electrons can damage the cell "critical targets" directly, or indirectly. First, they are capable of directly breaking chemical bonds which are vital to the functional and/or reproductive capacity of the chromosomes in their path. In the indirect effect, fast moving electrons can ionize other atoms or molecules of the absorbing tissue, causing the production of chemically unstable ions and free radicals (an atom or a molecule that contains an unpaired electron). These secondary ions and free radicals can subsequently cause damage to chromosomal material by breaking essential chemical bonds. These events, which take only a fraction of a second to occur, may ultimately be expressed as biological damage (Hicks and D'Amato, 1966; Upton, 1982; Hall, 1988).

Radiation damage to the DNA molecule can result in single or double strand breaks of the double helix structure, base deletions, or deletions of chemical cross-links of the two DNA strands. In some cases, given adequate time, nutrition, and an intact cellular environment, the damaged chromosome can be repaired by enzymatic processes in the cell. In cases where repair is not achieved, the

chromosome break will be replicated and passed on to subsequent cell generations. In other cases, misrepair can occur. During misrepair, broken chromosome fragments erroneously rejoin with other chromosomal fragments or with the wrong chromatid piece. Consequently, gross distortions of the chromosome may result in heritable mutation within the cell progeny. These chromosomal aberrations can also lead to abnormal segregation of chromosomes as the cell undergoes mitosis. Abnormal segregation may eventually lead to loss of the affected chromosome, and/or death of the cell as it attempts to reproduce. These radiation induced chromosomal aberrations can be observed in human lymphocytes after a gamma ray dose as low as 25 rads (Upton, 1982; Hall, 1988).

According to Hall (1988), unlike other traumatizing agents such as hyperthermia, ionizing radiation does not typically cause instantaneous cell death. Instead, as implied above, cells seriously affected by ionizing radiation die while attempting the next, or some subsequent mitosis. For this reason, ionizing radiation induced cell death is often referred to as mitotic-linked, or reproductive death. It should be noted, however, that there may be a few exceptions to this reproductive death rule. Hall (1988) claims that large fractions of the small human lymphocyte can be killed by relatively small doses of radiation. As this cell type does not divide, it is assumed that the small human lymphocyte dies an instantaneous

interphase death.

2.1.5. Radiosensitivity of Cells and Tissues

For the purposes of this study, the biological endpoints which define radiosensitivity of a cell or tissue are the observable effects of cell death and/or, alterations in the normal proliferation and differentiation of cells or tissues. Multiple factors influence the radiosensitivity of a cell exposed to ionizing radiation. Some of these factors include the type of ionizing radiation used, as well as the severity of the initial damage done to the DNA molecules within the cell. Other factors which must be considered when predicting cell radiosensitivity include the irradiation dose, the inherent radiosensitivity of the cell, the dose rate, and the stage of the cell cycle the cell is in during irradiation exposure (Hall,1988).

Numerous types of proliferative, mammalian cell lines have been studied both *in vitro* and *in vivo*, to determine the relationships between radiation dose and the proportion of cells that survive within an exposed given tissue. This relationship is expressed as the cell-survival curve, (Fig. 2-1) where the dose is plotted on a linear scale and the surviving fraction is plotted on a logarithmic scale. The typical curve for gamma or x-ray exposures in both *in vitro* and *in vivo* studies of various normal or neoplastic tissues, for a dose range of up to 700 rads (7.0 Gy), resembles that shown in Figure 2-1. The curve can be described as possessing an initial

Figure 2-1: **AN EXAMPLE OF A TYPICAL MAMMALIAN CELL-SURVIVAL CURVE**

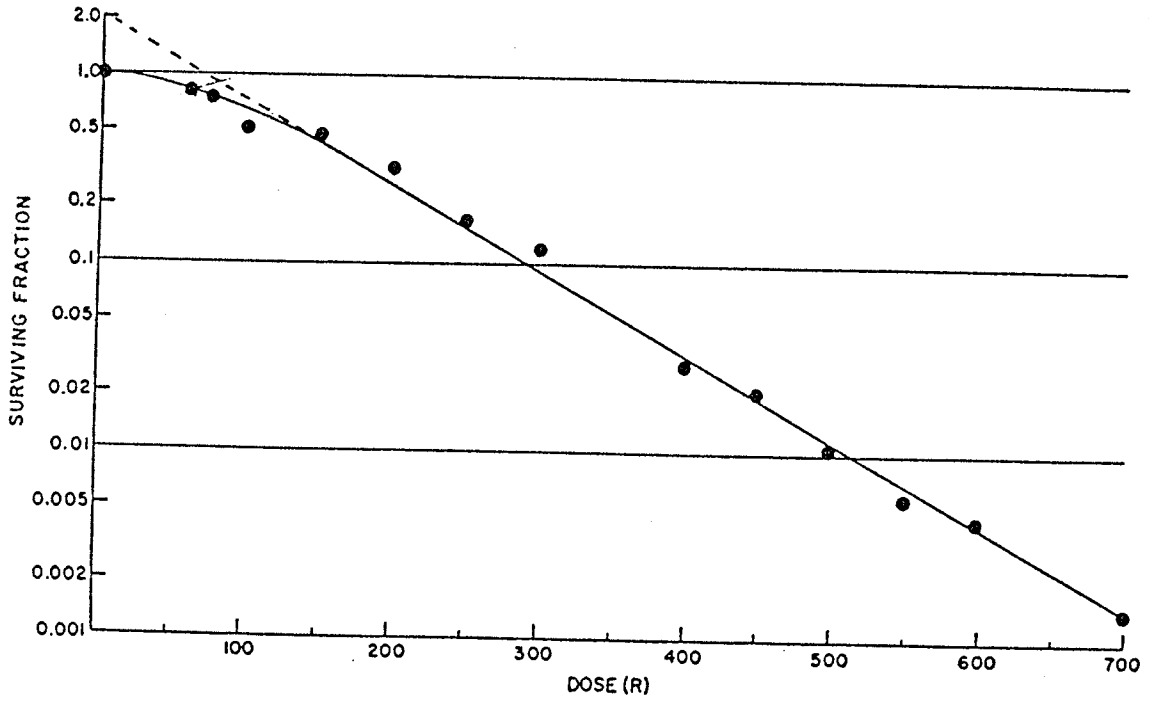

(From: Hall, 1988).

"shoulder" or bend in the lower doses ranges. As the dosage approaches the 100 to 200 rad range (1 to 2 Gy), the relationship becomes a straight line in this log-linear plot. Essentially, it could be said that in dose ranges of approximately 100 to 700 rads (1 to 7 Gy), cell killing becomes an exponential function of dose. As stated, this curve is very similar for a variety of mammalian cells examined. However, differences do exist between cells in the size and slope of the initial "shoulder" at dose ranges between 1 and about 100 rads (0.01 to 1 Gy). These differences in "shoulder" sizes between cells probably represents the inherent differences in radiosensitivities between cells (Hall, 1988). Hall also states, that since the most minute dose of radiation probably produces an effect, true threshold doses cannot be established. He suggests that the "shoulder" of the slope may represent a "quasi-threshold" dose for the cell type in question.

Inherent radiosensitivities of cells have been studied in a number of mammalian cell types. Although there are likely exceptions to some general observations, efforts have been made to classify the relative sensitivities of various tissues based on histopathologic observations. The most radiosensitive mammalian cell type is the primitive dividing stem cell. An apparent "moderate dose" (Hall, 1988, pp. 362) will cause a proportion of these cells to die a mitotic or reproductive death. The biological outcome of the irradiated tissue or organ as a whole is

dependent on the dose size, and/or the remaining stem cell population's ability to replenish the lost daughter cell population sufficiently, to ensure the functional properties of the organ or tissue.

The most radioresistant cells of the mammalian system are the highly differentiated, fixed postmitotic cells. An example of such a cell type is the mature neuron. Extremely high doses in the thousands of rads range is required to cause significant death of neurons in the adult organism (Rugh, 1965; Prasad, 1974; Hall, 1988). Connective tissue and blood vessels are considered to be intermediate in sensitivity between the most sensitive and most radioresistant parenchymal cell types. This is significant in that if a given dose does not affect the parenchymal population of the organ or tissue, secondary effects may be imposed on this population through the higher radiosensitivity of the stroma (Hall, 1988).

Another factor to be considered that may influence the radiosensitivity of a cell is the dose rate. Simply, the dose rate refers to the method of radiation delivery. A given dose of ionizing radiation can be delivered in one exposure, or in fractionated and protracted exposures where the dose is cumulatively achieved by providing a number of smaller dose exposures at different time intervals. When doses are fractionated, it is probable that there would be a lower number of cells with lethal damage and a higher proportion of cells with sublethal damage per

fractional exposure, as compared to a single dose exposure. Because some cells with sublethal damage are capable of repair, the overall biological outcome for the cell population is reduced. It should be noted, however, that this dose-rate effect only applies when the given dose per exposure is lower than about 100 rads (1 Gy). At higher doses per exposure, lethal damage is more probable. As well, the time interval of successive exposures is an important consideration. If the time interval is sufficiently protracted to allow total repair of the sublethally damaged cells, then the dose rate effect can occur. If however, a subsequent exposure is given prior to the repair of sublethal damage, irradiation effects may be cumulative, and an increase in cell death may occur (Hall, 1988). In this study, the dose rate delivery method used was most like that of a single dose exposure in terms of probable biological effect. Only studies concerned with a single dose exposure were considered for this review.

Studies of individual mammalian cells indicate that cell radiosensitivity is also dependent on the cell age in the mitotic cycle (Hall, 1988; Hicks and D'Amato, 1966 and 1980). The cell cycle can be divided into four distinct phases. The first is termed the S or synthesis phase. During this discrete phase, the nuclear DNA is replicated. The next phase in the cell cycle is called the second gap or G2 phase. It corresponds to the interval between the S phase and metaphase and therefore, includes

prophase, where the cell prepares for mitosis. The next phase, representing the remaining stages of mitosis and cytokinesis, is called the M phase. Following the M phase, is the first gap or the G1 phase of the cell cycle. This phase is generally longer than the other phases of the cell cycle. During the G1 phase, daughter cells grow and perform their specialized functions within their respective tissue population. These cells eventually continue in the cell cycle by entering the S phase. Other classes of cells, that lose their capacity for mitotic division such as the mammalian neuron, move from the G1 phase and enter a G zero phase. Some cells that enter a G zero phase may grow and differentiate, and remain in this protracted functional state for the entire life of the organism. Alternatively, other cell types that enter the G zero phase are capable of reentering the cell cycle under conditions of suitable extrinsic and/or intrinsic stimuli (Hicks and D'Amato, 1966 and 1980; Wheater et al, 1987).

Single cell survival has been assessed during high doses of radiation throughout the various stages of the cell cycle. Mammalian cells generally tend to be most radiosensitive during, or close to the M phase. The G2 phase is also a considerably radiosensitive period. As well as increasing the probable death of cells in this phase, radiation during the G2 phase can also cause delays in the mitotic process by halting cells in late prophase just before visible mitosis begins. If the G1 phase is

of an appreciable length, a sensitive period is evident early in this phase, followed by a radioresistant period toward the end of G1. Mammalian cells tend to be the most radioresistant during the S phase. As mentioned previously, highly differentiated cells which move out of the reproductive cell cycle into the G zero phase are also highly resistant to the cell-killing effects of ionizing radiation (Hicks and D'Amato, 1966; National Research Council, 1980; Hall, 1988). These patterns of vulnerability throughout the cell cycle are generally assumed to be true for most proliferative populations, and therefore, can be assumed to apply to most proliferative tissue populations of the embryo and fetus.

The radiosensitivity patterns of the developing mammalian central nervous system (CNS) is slightly different. Radioautographic studies using tritiated thymidine indicate that proliferative cells in these tissue populations tend to be most radiosensitive during late G2 and early G1 phases rather than in the M phase (Hicks and D'Amato, 1966 and 1980). In the case of G1 phase cells, cell death is instantaneous, as these cells have no mitotic future. They remain radiosensitive while still undifferentiated and migrating to their permanent maturation site of the CNS (Hicks and D'Amato, 1966 and 1980; Altman, 1969a, 1969b; Bayer and Altman, 1974 and 1975; Bayer, 1980a, and 1983). Studies indicate that doses as low as 12 rad (0.12 Gy) can cause observable cell death of late G2 and

early G1 neuronal cells of some mammalian species (Hoshino and Kameyama, 1988). Not until doses ranging from 300-500 rads (3-5 Gy) are cells in G zero, S phase, and M phase decimated in developing nervous tissue (Hicks and D'Amato, 1980).

2.1.6. Factors Influencing the Radiosensitivity of Embryonic and Fetal Tissue

Cell populations considered highly radiosensitive are those which exhibit a high degree of mitotic activity, and are undifferentiated or in the process of differentiation. These cell population characteristics are common to all developing organs and tissues at some point in prenatal life. It follows, therefore, that the developing embryo or fetus is at greater risk of insult from ionizing radiation than the adult organism (Ritenour, 1986).

Prenatal ionizing radiation exposure has been a known initiator of abnormal development and congenital malformations since the turn of the century, although adequately controlled experimentation of prenatal effects did not occur until 1935 (Job et al, 1935). Since that time, studies of radiation teratogenesis have revealed that ionizing radiation can cause: 1) embryonic, fetal, or neonatal death, 2) congenital malformations, and 3) growth alterations (particularly growth retardation) of specific organs and structures, and/or of the offspring as a whole. For a given single dose, the probability of detecting any one or a combination of these effects is

primarily dependent on the dose size and the age of the embryo or fetus at the time of gestational exposure (Mullenix et al, 1975; Brill, 1982; Brent, 1986; Ritenour, 1986; Schull et al, 1990).

Timing of gestational exposure is an extremely important factor in estimating prenatal risk. For every developing tissue, organ, and structure, different developmental timetables exist. As well, within each individual timetable of development for various structures, there are periods of greater vulnerability to teratogenic insult, as well as periods of greater capacity for repair. Differences in the timing of gestational exposure can therefore, greatly alter the ultimate biological outcome for the fetus or embryo. For example, radiation-induced cell death, or organ maldevelopment may be of little consequence to a specific organ because the gestational day of irradiation does not intrude on the developmental timetable of that organ. If irradiation damage occurs in a non-critical stage of the organ developmental timetable, biological outcome may also be minimal, as the organ may be able to replace damaged cells, and/or correct developmental impediments at that particular time of development. Conversely, if radiation exposure occurs during a more critical period of development for the organ, radiation-induced effects may be more severe. If, at this stage, the tissue is no longer capable of recovering cell loss or reversing malformation effects, permanent cell depletion and/or

malformation would be the biological outcome of the radiation insult. Consequently, to adequately predict the radiation effects on a given gestational day, one must consider what organs and tissues are developing at that time, and what developmental stages these specific cell populations are in. The size of the radiation dose will also influence the magnitude of the initial tissue reaction, and thus, the ultimate biological effect (Brill, 1982; Brent, 1980 and 1986; Kameyama and Hoshino, 1986).

Many teratological studies have been carried out in laboratory animals with irradiation doses ranging from about 10 to 400 rads (0.1 to 4.0 Gy), on varying gestational days. Some of these studies, with special emphasis on the effects of irradiation on gestational day 15 in the rat will be presented, following a review of the developmental features of the rat fetus on gestational day 15.

2.2. THE RAT FETUS ON GESTATIONAL DAY 15

In any teratological or developmental review, it is important to consider the methods by which various investigators have timed pregnancies in laboratory rodents. This refers to the dating of the first 24 hours following mating as either gestational day 0 or 1. A recent survey of scientists and the literature in the field of developmental neurobiology reveal that both designations are used with almost equal frequency, indicating that no standardized methodology exists (Paxinos et al, 1991). In the present

study, the morning of finding spermatozoa in the vaginal smears was considered to be the first day of gestation. As this factor is important for accurately comparing the data in the literature, gestational age will be adjusted to this study when necessary. This will be indicated by (adjusted).

The normal gestational period of the rat is between 21 and 23 days. The gestational period can be divided into five stages. The preimplantation stage corresponds to gestational day 0 to 5.5; implantation is from gestational day 5.5 to 8.0; early organogenesis is from gestational day 8.0 to 10.0; late organogenesis is from gestational day 10.0 to 13.0; the fetal period extends from gestational day 13.0 to birth (Brill, 1982). Gestational day 15 of the rat, therefore, represents the early fetal stage. The developmental events of gestational day 15 will be outlined with respect to those features relevant to this study.

2.2.1. Placental Development

The chorioallantoic placenta of the rat begins to develop on about gestational day 10, when the allantoic blood vessels begin to invade and separate maternal blood vessels of the uterine decidua (Bridgeman, 1948a; Davies and Glasser, 1968). By gestational day 15 (Fig. 4-14a and 4-16a), all the histological zones of the definitive placenta, and their cytological constituents can be identified with conventional light microscopy (Bridgeman,

1948a; Blackburn et al, 1965; Davies and Glasser, 1968). Moving from the fetal to the maternal decidua side of the placenta, these zones or regions include the chorionic plate region, the labyrinthine zone, the basal zone, and the decidua basalis (Davies and Glasser, 1968; Muntener and Hsu, 1977). See Figures 4-14a and 4-16a, 4-17, and 4-18 for gestational days 15, 17, and 20, respectively.

The chorionic plate is a region composed primarily of connective tissue. In section, the connective tissue is interrupted with the passing of the branches of the umbilical arteries and veins. Between the chorionic plate and the labyrinth, narrow spaces or clefts which lack maternal blood can be seen. These spaces are called the intraplacental clefts. At later stages of pregnancy, these clefts join with each other forming the intraplacental space (Muntener and Hsu, 1977).

The next distinguishable area is the labyrinthine zone. This is the area where both maternal vascular channels and fetal vessels are found. The branches of fetal vessels in this region are separated from the maternal blood by septa of connective tissue, and by a trilaminar trophoblastic epithelium. The layer of the trilaminar epithelium which is in contact with maternal blood (often referred to as layer #1), is cellular in nature while the other two deeper layers are syncytial (Bridgeman, 1948a; Kirby and Bradbury, 1965; Davies and Glasser, 1968; Hernandez-Verdun, 1974; Muntener and Hsu, 1977). As mitosis is seen only in layer

#1, it is assumed that the subsequent growth of the labyrinth area, which continues until term, is due to the proliferation of this layer (Davies and Glasser, 1968). Other factors which contribute to growth of this region include progressive increases of the maternal blood content of the region (Blackburn et al, 1965), and hypertrophy of the cellular constituents of this zone (Bridgeman, 1948b).

The next region of the placenta is the basal zone, although it is sometimes referred to as the junctional zone, the reticular zone or the trophospongium. The basal zone consists of three different cell types. The most predominant cell type is the small basophilic cell. These are presumed to be cytotrophoblastic extensions of the labyrinthine zone. Later in gestation, these cells often develop into giant cells as do some of the layer #1 cells of the labyrinthine trophoblasts. The second cell type found in this zone are the giant cells which lie adjacent to the decidua basalis. These cells form a layer several cells in thickness and tend to be more numerous in the peripheral portions of the placenta. The third cell type found in the basal zone are the clear or glycogen cells (Davies and Glasser, 1968). In the gestational day 15 placenta, these cells are numerous and arranged in small groups or islands. From about gestational day 17, these glycogen cells progressively lose their glycogen content, and appear pyknotic. They are replaced with an eosinophilic substance called fibrinoid

which is presumably a glycoprotein or mucopolysaccharide as this substance is P.A.S. positive. The line demarcated by the progressively pyknotic glycogen cells, represents the ultimate point of cleavage between the maternal and fetal components of the placenta during parturition (Blackburn et al, 1965). In addition to these cellular constituents of the basal zone, maternal blood spaces surrounded by giant cells or small basophilic cells can also be seen in this zone (Davies and Glasser, 1968).

The final zone evident in histological sections is the decidua basalis. Due to mesometrial growth of the placenta on gestational days 12 to 14, the decidua basalis of the 15 day rat placenta has thinned, and will eventually become is a narrow fibrous band (Blackburn et al, 1965).

Blackburn and colleagues (1965) found that the normal rat placenta demonstrates two periods of rapid increases in weight between gestational days 15 to 21. The first increase is between gestational days 15 to 17, while the second is from gestational days 19 to 21. In comparing wet placental weights with dry placental weights, they concluded that weight increases are primarily due to hypertrophy and hyperplasia of the placenta cellular constituents, particularly the labyrinthine trophoblast.

2.2.2. External Morphology

By gestational day 18.5, the rat fetus has achieved its definitive external form. From gestational day 18.5 until parturition there is further growth of the fetus,

Table 2-1: **EXTERNAL MORPHOLOGICAL CHANGES OCCURRING ON GESTATIONAL DAY 15 IN THE RAT**

STRUCTURE	GESTATIONAL DAY DEVELOPMENT COMMENCES	DEVELOPMENT COMPLETED
eyelid formation	15.5	18.5
ear (pinna) development	14.0	18.5
growth of fused mandible	13.0	17.5
tongue development	14.5	17.0
palate fusion	14.5	18.0
vibrissary papillae appear	14.5	18.0
mammary papillae appear	14.5	15.5
hair papillae appear	15.5	18.0
forepaw digit differentiation and separation	14.5	17.0
hindpaw digit differentiation and separation	16.0	18.5
gut herniates and reduces	13.5	18.0
cloaca closes	16.0	17.0

(extrapolated from Christie, 1964; Edwards, 1968; Shepard, 1989).

* all dates refer to the time at which the structure can be observed.

with no further visible developmental progress occurring (Christie, 1964; Edwards, 1968; Shepard, 1989). Crown-rump length ranges for various gestational ages were described by Christie (1964). Roughly, the rat fetus grows 2 mm in length during gestational day 15; 2.5 mm during gestational day 16; 3.0 mm during gestational day 17; and 4.5 mm during gestational day 18.

On gestational day 15, the rat fetus is entering the final stages of external morphological development. These changes are outlined in Table 2-1 as well as in Appendices III a,b and c. Figure 4-1 depicts the rat fetus on gestational days 20, 17, and 15. For any one of these structural changes, gestational day 15 may be assumed to represent a critical period of morphological development and for teratogenesis to occur.

2.2.3. Brain Development

The mammalian brain possesses a long developmental timetable which begins in the early period of organogenesis and extends into postnatal life. In the rat, neurogenesis begins when the neural folds of the ectodermal plate are evident by about gestational day 9.5. Fusion of the neural folds begins at the diencephalic-mesencephalic junction on gestational day 10.5. Closure of the anterior neuropore and rhombencephalon is completed by gestational day 11.5, with closure of the posterior neuropore following on gestational day 12.0 (Christie, 1964; Edwards, 1968). Following day 12.0, various areas and regions of the brain

develop within their own developmental timetables.

This section will briefly outline the developmental events during gestational day 15 of the various brain areas relevant to this study. As the cerebral cortex appears to be the most thoroughly researched in terms of developmental neurobiology and irradiation teratogenesis, it will be discussed first.

2.2.3.1. Cerebral Cortex

At the time of the onset of the closure of the cerebral vesicle, the wall of the vesicle is about 1 to 2 cells in thickness. The basal ends of these radially arranged, elongated epithelial cells are attached to a basement membrane under the pial surface, while the apical ends of these cells line the lumen of the cerebral vesicle and are anchored together by terminal bars. From about gestational day 10 to 15, these cells proliferate, thus increasing the thickness of the vesicle wall and forming a pseudostratified columnar neuroepithelium (Fig. 4-2a) (Berry, 1974).

The S phase of the epithelial cell cycle occurs while the cell nucleus is located at the basal end of the cell. As the cell passes through the G2 phase, the nucleus migrates to the apical end of the cell. Concurrent to the G2 phase, the cell loses its basal attachment. It then rounds up in the juxtaventricular area, and enters mitosis. After separation of the daughter cells during the G1 phase, the nuclei of these cells migrate in a basal

direction with the concurrent growth of the basal processes. These processes re-attach to the subpial basement membrane, and eventually, the proliferation cycle is repeated (Berry, 1974; Schultze and Korr, 1981; Smart and McSherry, 1982). This proliferation zone of the cortex is called the ventricular zone (Boulder Committee, 1970).

The ventricular zone is believed to give rise to neurons, neuroglia, cells of the future ependymal and subependymal regions, and the epithelium of the choroid plexus (Schultze and Korr, 1981). Lineage relationships between neurons and glia destined for the cerebral cortex are still uncertain (Alvarez-Buylla, 1990). The popular notion has been that glial cells and neurons are generated from separate pools of stem cells in the ventricular zone (Rakic, 1986). In many studies, it has been found that a single neuroblastic progenitor cell is capable of generating several classes of neurons (Levitt et al, 1981; Smart and McSherry, 1982; Luskin et al, 1988; Alvarez-Buylla, 1990; McConnell, 1990). Recent studies, however, have suggested that in some regions of the brain, a single stem cell may be capable of generating both neurons and some types of glial cells (Price and Thurlow, 1988; Gray et al, 1990; McConnell, 1990; Walsh and Cepko, 1990). Variations in the results have been attributed to species differences, regional differences, or differences in gestational dates.

Migration of neurons from the ventricular zone

to more superficial areas of the cortical substance continues from gestational day 13 through the early neonatal period (Berry, 1974). The outward radial migration movements of post-mitotic neurons are guided by the close apposition to the surface of specialized glial elements called radial glial cells. These cells arise early and lie within the ventricular zone with a centrally directed process attached to the juxtaventricular border, and a radially ascending process which crosses the width of the cerebral wall and branches subpially. The neuronal-glial interaction is probably due to a highly selective affinity between glial and neuronal surfaces. Once ascent of the neuron is complete, the neuron detaches from the glial fiber at its marginal or laminar destination (Rakic, 1988; Caviness, 1989; Gadisseux et al, 1989; Gadisseux et al, 1990; Gray et al, 1990; Liesi, 1990; Rakic, 1990; Walsh and Cepko, 1990).

Late on gestational day 13, the first neurons, which arise in the ventricular zone, can be seen in their post-migration positions, intermingling with corticopetal fibers between the pial surface and the ventricular zone (Berry, 1974: Raedler et al, 1980). This zone corresponds to the marginal zone of the developing cortex (Boulder Committee, 1970). The marginal zone first appears in the ventro-lateral area of the future cortex. The marginal and all other developmental zones to be discussed develop in a ventral to dorsal direction, presumably due to the relationship between incoming corticipetal fibers and

the initiation of migrations and differentiation (Marin-Padilla, 1978; Raedler et al, 1980; Smart and McSherry, 1982). By gestational day 15, all neurons of this primordial marginal zone have completed their proliferation and migration cycles (Marin-Padilla, 1978).

Marin-Padilla (1978) proposed that the earliest migrating cells of the marginal zone which are located closest to the pial surface, are the Cajal-Retzius cells of lamina I of the definitive cortical plate. Meanwhile, the cells in the lower portions of this primordial marginal zone are the neurons, referred to as subplate neurons, which will eventually occupy lamina VII. These cells of the subplate include large polymorphic and stellate neurons.

Neuron production of the ventricular zone continues, with those neurons generated on gestational days 15 and 16 representing the earliest forming neurons of the definitive cortical plate. Following migration of neurons from the ventricular zone, laminae IV to II of the cortical plate are formed in an inside-out manner. Neurons of lamina IV can be identified at their definitive destinations on gestational day 16; lamina V on gestational day 17; lamina IV on gestational day 18; and laminae III and II forming on gestational days 19 to 21 (Berry and Rogers, 1965; Berry, 1974). Migrating neurons therefore pass through the previously formed laminae to reach their destinations in more superficial positions of the developing cortical plate (Hicks et al, 1959; Angevine and Sidman, 1961; Berry

and Eayrs, 1963; Berry and Rogers, 1965).

By gestational day 17 (Fig. 4-4a), five distinct zones (including the cortical plate) can be recognized. From the pial to the ventricular surface, there is the previously described marginal zone, the developing cortical plate, the intermediate zone consisting of various corticopetal and corticofugal fibers, the subventricular zone, and the ventricular zone (Boulder Committee, 1970; Raedler et al, 1980). The subventricular zone, which appears on gestational day 17 in the rat, represents a second region of mitotically active cells and is located superficially to the ventricular zone. Cells of this zone are believed to be stem cells of the ventricular zone which have lost their apical attachment. Unlike the ventricular zone, cells of the subventricular zone lack a radial arrangement of precursor cells. As well, mitotically active cells do not demonstrate the nuclear migration movements typical of ventricular zone progenitors (Raedler et al, 1980; McConnell, 1990). The subventricular zone is believed to primarily serve as a major pool of glial cell precursors (Berry, 1974; Lewis, 1979; Sturrock and Smart, 1980; Caviness, 1989); however, some authors suggest that this zone may also give rise to some classes of neurons (Altman and Das, 1966; Boulder Committee, 1970). With subsequent growth of the cortical plate and intermediate zone, the subventricular and ventricular zones progressively decrease in thickness (Raedler et al, 1980). See figure 4-4b.

In summary, developmental events of the rat cerebral cortex on gestational day 15 include the final stages of venticular progenitor cell proliferation, the end of the migration passage of fetal subplate neurons, as well as the early stages of neuronal production and subsequent migration to the deepest cortical lamina (lamina VI) of the cortical plate. Gestational day 15 also precedes the development of identifiable intermediate and subventricular zones.

2.2.3.2. Main Olfactory Bulb

Neurogenesis of the main olfactory bulb in the rat spans from gestational days 12 to postnatal day 20 (Bayer, 1983). In addition, Altman (1969b) found that the subventricular layer of the lateral ventricles continues to contribute internal granular neurons to the main olfactory bulb via a "rostral migratory stream" beyond postnatal day 20, up to postnatal day 180. These late generated interneurons are thought to serve as renewal neurons for the olfactory internal granular cell population (Altman, 1969b; Bayer, 1983).

The output neurons (mitral and tufted cells) of the main olfactory bulb, are believed to arise prenatally from the neuroepithelium of the basal telencephalic ventricular zone. The majority of interneurons (granular cells) of the main bulb primarily arise postnatally from the subventricular zone of the basal telencephalon (Bayer, 1983).

Table 2-2: **GENERATION TIMETABLE FOR THE MAIN OLFACTORY BULB OUTPUT NEURONS AND INTERNEURONS**

CELL TYPE	GENERATION PERIOD	PEAK TIME OF GENERATION (% FORMED)	LAYER DESTINATION
mitral	gd. 12-18	gd. 15+16 (80%)	mitral cell layer (4)
internal tufted	gd. 12-20	gd. 16+17 (50%)	external plexiform layer (3)
external tufted	gd. 16-22	gd. 18+19 (65%)	external plexiform layer (3)
interstitial tufted	gd. 17 - pn. 1	gd. 20-22 (70%)	glomerular layer (2)
external granule	gd. 21 - pn. 19	pn. 1-7 (56%)	glomerular layer (2)
internal granule	pn. 1-20	pn. 1-13 (58%)	internal granule layer (6)

(extrapolated from Bayer, 1983).

gd. = gestational day

pn. = postnatal day

By gestational day 19 (Figure 3-1) in the rat, all six layers of the adult main olfactory bulb can be discerned, although not all cytological constituents are present (Zeman and Innes, 1963, Pellegrino et al, 1981; Bayer, 1983; Halasz, 1986; Paxinos et al, 1991). Moving from superficial to deep layers of the adult rat main olfactory bulb, layers include the olfactory nerve fiber layer, the glomerular layer, the external plexiform layer, the mitral cell layer, and the internal plexiform layer. The innermost layer of the adult main olfactory bulb is the internal granular layer. As the internal granule cells do not arise until the postnatal period, the area deep to the internal plexiform layer in prenatal rats is occupied by the migrating cells arising from the olfactory ventricular zone, and the ventricular zone itself (Zeman and Innes, 1963; Hinds, 1968a; Bayer, 1983).

In Table 2-2, the gestational dates for the development of these various output neurons and interneurons of the main olfactory bulb, as derived by Bayer (1983), are listed. As can be seen from Table 2-2, gestational day 15 represents the date of peak production of the mitral cells of layer four. It may also be important to note that at the time of peak production of mitral cells, the olfactory lobes are just beginning to be visibly discernible on the rostral aspect of the telencephalon (Hinds, 1968b; Bayer, 1983).

2.2.3.3. Corpus Callosum

Although several studies have determined the origins and destinations of corpus callosum commissural fibers in both the rat (Jacobson and Trojanowski, 1974; Wise, 1975; Wise and Jones, 1976; Ivy and Killackey, 1981; Jensen and Altman, 1982) and the mouse (Yorke and Caviness, 1975; Silver et al, 1982; Schmidt and Lent, 1987), gestational dates for the developmental events of the corpus callosum have just been provided for the mouse (Silver et al, 1982). As the origins, genesis, and terminations of the callosal axons of the mouse are similar to the rat, Rugh's (1968) extrapolation tables for mouse to rat embryonic ages have been used in this review.

Retrograde studies of the rodent corpus callosum demonstrate that callosal fibers generate from laminae II to VI of the cortical plate, with the heaviest concentration of cells of origin in laminae III and V. These fibers are early generated axons of immature pyramidal neurons which grow out from their cortical laminar positions and travel through the intermediate zone to the medial walls of the cerebral hemispheres (Jacobson and Trojanowski, 1974; Wise, 1975; Yorke and Caviness, 1975; Wise and Jones, 1976; Ivy and Killackey, 1981). By about gestational day 19 in the rat (Rugh, 1968; Silver et al, 1982), the commissural fibers have reached the midsagittal zone of the cerebral hemispheres and by the day of birth (Fig. 4-8), most have crossed into the contralateral hemisphere (Wise and Jones, 1976).

Silver et al (1982), found that normal crossing of the callosal fibers from their hemisphere of origin to the contralateral hemisphere, was dependent on the presence of a glial cell scaffolding or "sling" which spans between the two cerebral hemispheres. Rostral to the lamina terminalis, glial cells can be seen arising from the ventricular zone of the medial aspect of the lateral ventricle walls, and migrating to a position below and lateral to the longitudinal cerebral fissure. This sequence of proliferation and migration of glial "sling" cells progresses in a caudorostral direction and begins on gestational day 13 to 14 in the mouse (rat equivalent= gestational days 14.5 to 15). Callosal fibers are guided between hemispheres by the glial "sling" and crossing of callosal fibers is believed to be completed by a few days after birth, as the glial "sling" disappears at this time (Silver et al, 1982).

By parturition, most growing axon terminals lie within the subcortical plate regions of the contralateral hemisphere. Studies indicate that growth of callosal fibers into the cortical plate and the subsequent establishment of synaptic connections is dependent on the maturation of post-synaptic pyramidal cells. Maturation of these cells begins in the deeper cortical laminae and proceeds in an inside-out progression with lamina II callosal neurons establishing synaptic connections last. Callosal fiber connections are complete within the first postnatal week.

Although there are differences between cortical regions, the cells of origin of callosal fibers tend to have the same topographic pattern of distribution as the callosal terminals (Jacobson and Trojanowski, 1974; Wise, 1975; Yorke and Caviness, 1975; Wise and Jones, 1976; Ivy and Killackey, 1981; Silver et al, 1982).

In summary, gestational day 15 in the rat represents the time of development of the glial "sling" which eventually facilitates the midsagittal crossing of callosal fibers. As well, as discussed previously in relation to cortical plate development, gestational day 15 may also represent the early developmental period of the deepest infragranular neurons of the cortical plate. Although slight, lamina VI of the cortical plate may contribute fibers to the corpus callosum.

2.2.3.4. Hippocampal Formation

The rodent hippocampal formation is an anatomically complex structure which undergoes significant cytological as well as morphological changes during late prenatal and early postnatal periods (Bayer and Altman, 1974). On gestational day 14, the neuroepithelium (ventricular zone) of the dorsomedial wall of the telencephalon begins to curve into the lateral ventricle. These bilateral curved segments represent the primordial hippocampal formation. Cytogenesis of this structure spans from about gestational day 15 to postnatal day 21. The dorsally located portion of the hippocampal ventricular zone will give rise to

part of the subiculum. The middle portion gives rise to Ammon's horn, while the dentate gyrus arises from the most ventral portion of the hippocampal neuroepithelium (Bayer and Altman, 1974; Bayer, 1980a; Bayer, 1980b). See Figure 4-9 for hippocampal formation development on gestational days 15, 17, and 20.

The neuroepithelial ventricular zone of the hippocampal formation can be easily distinguished on gestational day 15, as it comprises about 78% of the total primordial hippocampal volume. Cytologically, it resembles the ventricular zone of the developing neocortex. The ventricular zone grows in volume rapidly from gestational days 15 to 18, thereafter it begins to decrease in size until it disappears on postnatal day 1. A thin subventricular zone appears on about gestational day 17 and continues to grow until gestational day 20. It disappears in the second postnatal week. Unlike the neocortex, however, the subventricular zone is never as prominent a feature in the hippocampus (Bayer, 1980b). Bayer (1980b) also suggests that in the postnatal period, cells which have migrated from the neuroepithelial zone near the origins of the choroid plexus, establish a secondary germinal matrix in the hilus of the dentate gyrus. This germinal zone is believed to give rise to the late-generated dentate granule cells.

Table 2-3 indicates the time of cellular origin for the different regions of the developing hippocampal

Table 2-3: **TIME OF ORIGINS FOR THE MAJOR HIPPOCAMPAL FORMATION CELL TYPES IN THE RAT**

ZONE	CELL TYPE	GESTATIONAL DAY OF ORIGIN
subiculum	deep pyramidal	gd. 15-17
	superficial pyramidal	gd. 17-18
Ammon's horn	pyramidal and other large neurons of stratum oriens, strata radiatum, and lacunosum-moleculare	gd. 15-17
	glia and small neurons of the above zones	pn. 1-14
	pyramidal cells of the stratum pyramidale	gd. 17-19
dentate gyrus	polymorphic and pyramidal cells of dentate hilus	gd. 15-19
	small neurons and glia of dentate hilus	pn. 1-16
	large neurons of dentate molecular layer	gd. 15-19
	small neurons and glia of dentate molecular layer	pn. 1-16
	granule cells of dentate granular layer (ectal limb before endal limb)	gd.17-pn.15

(extrapolated from Bayer and Altman, 1974; Bayer, 1980a; Bayer, 1980b)

gd. = gestational day

pn. = postnatal day

formation. It should also be noted that on approximately gestational day 17, the fimbria can first be identified in coronal section, in the ventral regions of the hippocampal primordia. Fimbrial fibers initially consist of septal afferents primarily from the medial and diagonal band nuclei, en route to the hippocampus. The cells of origin of these fibers arise from gestational day 14 to 16. The fimbria grows considerably on gestational days 18 to 19, due to the additions made by subicular pyramidal axons on their way to septal nuclei and the mamillary bodies. A third fimbrial growth spurt occurs on gestational days 21 to 22 due to the additions from Ammonic pyramidal neurons destined to terminate in the septum (Bayer, 1980b).

In summary, on gestational day 15, a number of important developmental events are occurring in the hippocampal formation. These include:

1) growth of the neuroepithelial ventricular zone.

2) early morphological differentiation of the hippocampal formation primordium.

3) early cytogenesis of the large neurons of the subiculum, strata oriens, strata radiatum, lacunosum-moleculare, dentate hilus, dentate molecular layer, as well as the cells of origin for fimbrial fibers.

2.2.3.5. Cerebellum

Like the hippocampal formation, the rodent cerebellum undergoes significant morphological and cytological development from gestational day 13 to about

Table 2-4: **TIMETABLE OF CYTOGENESIS FOR CEREBELLAR NEURONS IN THE RAT**

NEURON TYPE	GESTATIONAL DAYS OF DEVELOPMENT	GESTATIONAL DAY OF PEAK PRODUCTION	LAMINAR DESTINATION OF CELL BODIES
deep cerebellar nuclei neurons	gd. 13-16	gd. 14	medullary zone
Purkinje cells	gd. 13-17	gd. 15	Purkinje cell layer (cerebellar cortex)
golgi cells	gd. 19 to pn. 3	gd. 19 to 21	Purkinje cell layer
basket cells	pn. 5-11	pn. 6 to 8	molecular layer (cerebellar cortex)
stellate cells	pn. 7-13	pn. 9 to 11	molecular layer
granule cells	pn. 5- 21	pn. 6 to 15	internal granule layer

(extrapolated from Altman, 1969a; Altman and Bayer, 1978a)
gd. = gestational day
pn. = postnatal day

the 4th postnatal week. As can be seen in Table 2-4, neurons of the cerebellum arise in three waves throughout the developmental period. The distinct laminar pattern, and the folia characteristic of the mature adult cerebellum are not evident until the second postnatal week (Altman, 1969a; Altman and Bayer, 1978a).

The early cerebellar anlage appears in the region of the dorsolateral metencoele on gestational day 13. At this time, it is represented by a pair of plates composed of neuroepithelial cells. These cells are similar to those seen in other proliferative zones of the brain such as the cerebral cortex; the cells are pseudostratified in appearance, and those lying in the juxtaluminal position are mitotically active. The deep cerebellar nuclei neurons and a small percentage of Purkinje cells begin to arise from the proliferative neuroepithelium on this day (Altman and Bayer; 1978a).

Gestational day 15 represents the final days of deep cerebellar nuclei neuron production and the peak time of Purkinje cell production. Five defined zones can be identified at this period of development (Fig. 4-12a). Moving from superficial to deep areas in the cerebellar anlage, these zones include the superficial fibrous layer, the nuclear zone, the intermediate fibrous layer, the transitory zone, and the cerebellar neuroepithelium. The superficial fibrous layer represents the primordial marginal zone of the cerebellum. The nuclear zone is believed

to be composed of post-migratory deep cerebellar nuclei neurons. The intermediate fibrous zone is a transient fiber layer of unknown origin. It disappears by about gestational day 17 in the rat. The transitory zone represents early premigratory Purkinje cells. The cerebellar neuroepithelium is at maximal thickness from gestational days 15 to 17, however it starts to regress in size on gestational day 17 when Purkinje cell production comes to an end. It is no longer evident in the rat cerebellar regions by about the second postnatal week (Altman and Bayer, 1978a).

Several changes occur on gestational day 17 (Fig. 4-12b). As stated, the cerebellar neuroepithelium begins to regress in most regions with exception to areas limited to the ventrocaudal and laterocaudal margins of the cerebellar anlage, in the region of the choroid plexus primordium. This area called the germinal trigone, begins to give rise to a second germinal layer of the cerebellum called the external germinal layer on gestational day 17. Cells of the external germinal layer arise from the lateral and caudal aspects of the trigone, and continue to grow in a caudorostral direction as a continuous sheet of cells. The external germinal layer reaches the most anterior aspects of the cerebellum on gestational day 20. During the postnatal period, this external germinal layer gives rise to the stellate, basket, and granule neurons, and possibly the precursors of Bergmann's glial

cells. The external germinal layer regresses in the late postnatal period in region specific patterns, and has completely disappeared in all regions by postnatal day 30 (Altman, 1969a; Altman and Bayer, 1978a).

Gestational day 17 also represents the early migration stage of the Purkinje cells through the nuclear zone to occupy a more superficial position, under the external germinal layer. Through the guidance of radial glial cells, the undifferentiated Purkinje cells begin their en masse migration from the transitory zone which is essentially completed by gestational day 20. This migration obliterates the distinction between nuclear and transitory zones (Altman, 1969a; Altman and Bayer, 1978a).

By gestational day 20 (Fig. 4-12c), the Golgi cells of the future Purkinje layer have begun to arise from the regressing neuroepithelium. These cells are difficult to distinguish with conventional light microscopy at this age, due to the immature appearance of these, and surrounding cells. The external germinal layer is distinct at this time, and gaining in thickness as development progresses. Subjacent to the external germinal layer is the primordial molecular layer. Although the major constituents of this layer have not yet developed (i.e.., basket cells, stellate cells, and parallel fibers), climbing fibers originating from the olivary nuclei may occupy this layer at this time. Deep to this primordial

molecular layer is the Purkinje cells layer (Altman, 1969a; Altman and Bayer, 1978a and 1978b).

During the prenatal and early postnatal period, the Purkinje cell layer is many cells in thickness, and the cells themselves have not begun to differentiate. Although there is significant variation in the timing of events between regions in the postnatal cerebellum, Purkinje cell differentiation and conversion to the single-celled row configuration seen in the adult rat cerebellum begins during the second postnatal week (Altman, 1969a; Altman and Bayer, 1978a and 1978b).

In summary, gestational day 15 represents a very early stage of morphological and cytological differentiation in the rat cerebellum. Likely, the most critical events of gestational day 15 include the genesis of late arising deep cerebellar neurons, and the majority of cortical Purkinje neurons.

2.3. PRENATAL EXPOSURE TO IRRADIATION

2.3.1. Maternal Influences on Irradiation Teratogenesis and Placental Radiosensitivity

It has long been assumed that radiation effects on prenatal development are due to direct ionizations within the fetus or the embryo, rather than a secondary effect of maternal irradiation (Kalter, 1968; Prasad, 1974; Norton, 1986; Ritenour, 1986; Brent, 1980; Schull et al, 1990). Wilson and Karr (1951) found that direct irradiation of selected rat implantation sites, which

eliminates the variables involved in whole body maternal irradiation, was sufficient to produce prenatal malformations. Brent and McLaughlin (1960) found that whole body irradiation of pregnant rats on gestational day 10 (adjusted) with a 400 to 1400 rad (4 to 14 Gy) dose while shielding the embryos, failed to produce congenital malformations, although an increased resorption rate was observed at the higher dose ranges. In other experiments, doses from 60 to 400 rads (0.6 to 4 Gy) were used to determine the role of maternal irradiation vs direct effects on embryonic development, of the preimplantation and early implantation rat conceptus. It was concluded that higher litter lethality rates, congenital malformations, and changes in fetal weight observed in irradiated term rats, were due to irradiation of the ova or zygote rather than maternal organs of pregnancy (Brent and Bolden, 1967 and 1968).

Given that the placenta is a highly vascular and rapidly growing structure, it may be assumed that this structure would be highly radiosensitive and thus, contribute to the teratogenic effects of ionizing radiation (Rugh, 1965). No current studies have investigated this theory, presumably due to the fact that early investigators found that the placenta was highly radioresistant.

Foraker et al (1955) irradiated pregnant rabbits on gestational day 9 with a 1200 roentgen dose. Placental tissues were examined 5 days later. Foci of necrosis and degeneration of syncytial and perisyncytial cells were

found in the labyrinthine region; however, the authors stated that considering the size of the radiation dose, damage was of "modest proportion". Brent (1960), conducted a series of controlled experiments irradiating the placenta alone, the embryo alone, half of the placenta and embryo, or the entire implantation site on gestational day 13 (adjusted) of the rat. A dose of 400 rads (4 Gy) was used for all irradiations. At the end of the 17th day of gestation (adjusted), exposed fetuses in all groups were compared with each other as well as with controls for incidences of fetal mortality, congenital malformations, and differences in fetal weight. Placental irradiation alone did not contribute to any irradiation effects in the fetus as compared with controls, although in terms of fetal mortality, inclusion of the placenta in a total site exposure increased the fetal mortality rate over that of irradiation of the embryo alone. Placental inclusion in total site exposures did not, however, increase the incidence of malformations or low fetal weight, compared to exposures of the embryo alone. No histopathological or morphometric assessments were made of the placentas in this study.

Rugh (1965) reported that acute exposure of the "fully formed" fetal mouse placenta to 400 rads (4 Gy) of x-rays and examined 72 hours later did not cause any demonstrable changes to the chorionic or vascular epithelium of the placenta. At this stage of development, a dose of 800 rads (8 Gy) to the placenta was found

insufficient in causing fetal death. Furthermore, irradiation of the second trimester monkey placenta with 400 rads (4 Gy) failed to produce any histopathological effects. It was concluded that the placenta, despite its highly vascular elements, is "one of the most radioresistant organs concerned with the developing embryo and fetus" (Rugh, 1965).

Since the 1960's, few studies have focused on the maternal responses to whole body exposures, or to the histopathological and morphometric responses of the irradiated placenta. Rather, studies have focused primarily on the direct effects of irradiation on the ova, embryo, and fetus. In a few cases, maternal weight changes throughout pregnancy have been reported. Norton and Kimler (1988) found that following irradiation on gestational days 13, 15, or 17 with 1 Gy (100 rads) of gamma rays, pregnant rats failed to gain weight normally for a 24 hour period. By parturition, these irradiated animals had resumed their weight and no significant differences existed between irradiated and non-irradiated animals. This delay in maternal weight gain was not observed in the second part of Norton and Kimler's (1988) study, where dams were exposed to a dose of 0.75 Gy (75 rads). However, in a subsequent study (Norton et al, 1991), dams exposed to a 0.75 Gy (75 rads) dose on gestational day 15 also failed to gain weight for a 24 hour period. In both of these studies the significance of delays in maternal weight gain were

not explored nor explained. In a recent report, single dose exposures to 100 rads (1 Gy) or less was considered as having minimal maternal effects (Schull et al, 1990).

2.3.2. Fetal Lethality and Litter Size

An increase in litter mortality with a consequent reduction in litter size is a reported outcome of prenatal irradiation in experimental animals. The risk of reduction in litter size is both dependent on the dose of irradiation and the gestational time of exposure. Figure 2-2 represents Brent's (1980) literature survey of the litter mortality rate of the rat following both a 150 rad (1.5 Gy), and a 30 rad (0.3 Gy) dose from gestational day 0 through 20. An additional scale for the human gestational timetable has been provided to compare and approximate effects. As the graph reveals, the highest period of prenatal risk for both 150 and 30 rad (1.5 and 0.3 Gy) exposures in the rat is in the early preimplantation period (Russell and Russell, 1950; Brent and Bolden, 1967; Brent, 1980).

Two factors may account for the heightened mortality rates during this time period. First, very few cells at this stage of development are responsible for the continued viability of the conceptus (Ritenour, 1986). Secondly, cells in this early stage are dividing synchronously and therefore, will vary in their radiosensitivity in a synchronized manner, depending on the stage of the cell cycle during exposure. This latter point also explains the radiosensitivity shifts seen in the graph at this

Figure 2-2: **OFFSPRING MORTALITY CURVE AT 150 AND 30 R IN THE RAT**

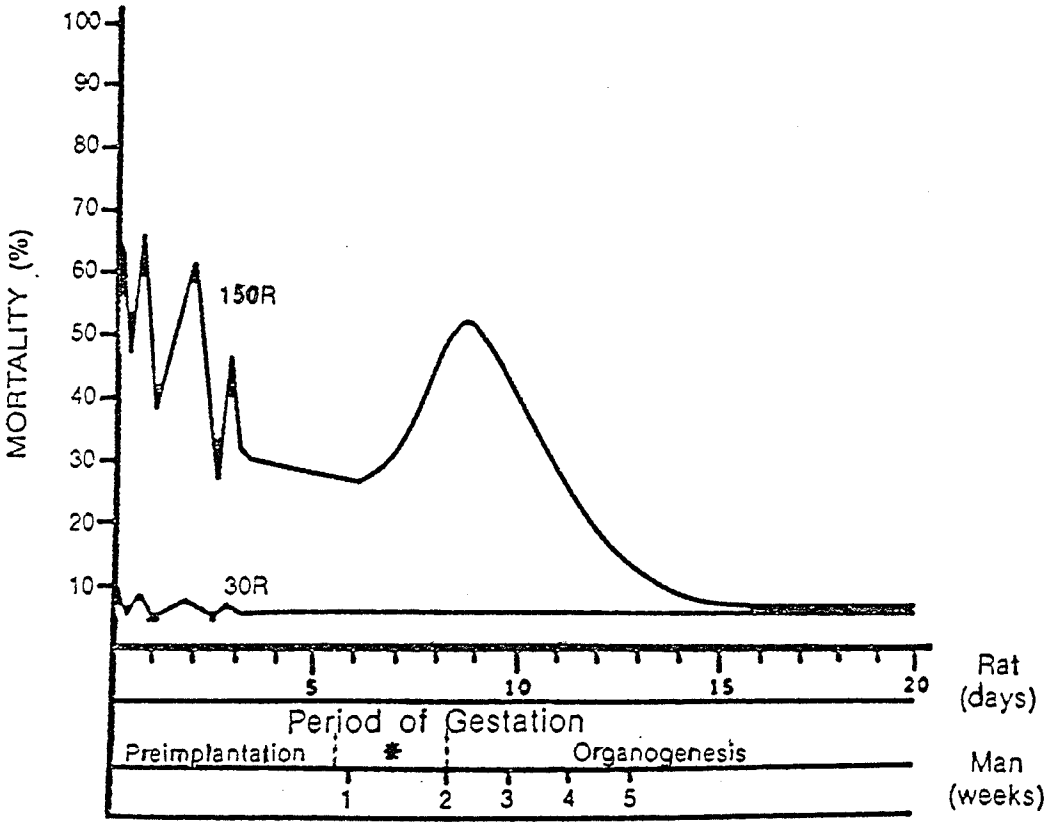

(From: Brent, 1980).

early stage for both 150 and 30 rad dose ranges (Brent, 1980). It is interesting to note, that those offspring that survive an irradiation exposure at this early developmental stage, do not demonstrate any detrimental effects of irradiation such as malformations or growth retardation at birth (Brent, 1980; Hicks and D'Amato, 1980; Mossman and Hill, 1982; Brent, 1986).

At the 30 rad (0.3 Gy) dose level, litter size is not altered by radiation exposure for the remainder of the gestational period. Following exposure to 150 rads (1.5 Gy), the embryo becomes somewhat more radioresistant during the implantation stage, but peaks again in radiosensitivity during early organogenesis. This is not surprising considering that the organ systems necessary for the prenatal and postnatal viability of the embryo are developing at this time. From about gestational day 10 to term, the mortality rate progressively decreases, thus rendering the rat fetus at lower risk to the lethal effects of a 150 rad dose as compared with other periods of gestation (Brent, 1980).

In general terms, a radiation exposure during the later stages of fetal life is more apt to result in viable fetuses than exposures during early embryogenesis or organogenesis (Mullenix et al, 1975; Mole, 1979). One possible exception to this general rule may be the fetus exposed to radiation on gestational day 17. Takeuchi et al (1981) reported a decrease in mean litter size following

a 100 rad (1 Gy) irradiation on gestational day 17. Jensh et al (1987) also reported a reduction in litter size of rats irradiated with 0.4 Gy (40 rads) on gestational day 17, although this difference was not statistically significant when compared with controls. Studies indicate that fetal lethality rates can be significantly increased throughout the fetal period by doses of 200 rads (2 Gy) or greater. In these cases, most fetuses will die at term or soon after birth, presumably due to damage to vital CNS structures (Hicks et al, 1959; Schull et al, 1990).

Specifically, on gestational day 15, the graph indicates a slight (approximately 8%) risk of fetal lethality following a 150 rad (1.5 Gy) irradiation dose. In dose ranges of 100 rads (1 Gy) or less, however, the rat fetus on gestational day 15 is not at risk for the lethal effects of a radiation exposure (Brent, 1980; Takeuchi et al, 1981; Norton, 1986; Norton and Kimler, 1988). It may be assumed therefore, that the threshold dose which may alter the litter size on gestational day 15 is greater than 100 rads (1 Gy), although the exact value of this threshold has not been established.

2.3.3. Fetal Growth

Intrauterine growth retardation is a common consequence of prenatal irradiation. Some investigators suggest that neonatal weight is one of the most sensitive indicators of prenatal irradiation (Jensh et al, 1986; Norton, 1986). Brent (1980) found in the rat that prenatal

exposures to 150 rads (1.5 Gy) from implantation (gestational day 5.5) to term reduced the birth-weights of the offspring, compared to controls. Studies have shown that those animals irradiated during the fetal period demonstrate a slower rate of postnatal growth recovery than those irradiated at earlier periods of gestation (Rugh et al, 1964; Brent, 1980; Takeuchi et al, 1981).

Norton and Kimler (1988) found with a 1 Gy (100 rads) dose on either gestational days 13, 15, or 17, gestational day 15 irradiated offspring showed the most significant reduction in weight at birth, compared to the controls. On gestational day 15, an irradiation dose of 0.25 Gy (25 rads) has no effect on the weight of the offspring. However, radiation doses of 0.50 Gy (50 rads) and greater cause a dose-related reduction in birth-weight (Norton and Donoso, 1985; Norton, 1986). Studies which have evaluated the postnatal growth recovery of offspring irradiated on gestational day 15 indicate that recovery is also dose-related. Offspring irradiated with 0.50 Gy (50 rads) recover from low birth-weight by postnatal day 14 (Norton and Donoso, 1985; Norton, 1986). A gestational day 15 exposure of 0.75 Gy (75 rads) has been reported to result in persistent weight reductions up to three to four months of age (Norton and Donoso, 1985; Norton et al, 1991), while a dose of 1.25 Gy (125 rads) has been reported to result in persistent weight reductions until five or six months of age (Mullenix et al, 1975).

2.3.4. Fetal External Morphology

Figure 2-3 presents a survey concerning the incidence of gross congenital malformations observed in the mouse and the rat following a 100 rad (1 Gy) single exposure on each day of the gestational period (Brent, 1980). The black arrow on the right side of the ordinate indicates the approximate 2% control incidence of congenital malformations observed in rats. The white arrow on the left side indicates the slight increase in the incidence of malformations observed in a specific strain of mice following radiation exposure on gestational day 1, as reported by Russell et al (as cited by Brent, 1980). Other than these latter studies, no increased incidence of malformations has been reported following radiation with 100 rads (1.0 Gy) prior to gestational day 8 (Brent, 1980).

A dramatic increase in congenital malformations is indicated during the early organogenic period (gestational days 8-10) because this is the period of early induction for many organs and systems. Many investigators have assessed the incidence of malformations induced during this period, as well as late organogenesis, utilizing doses ranging from 25 rads (0.25 Gy) to 400 rads (4 Gy). Studies show that irradiation on specific days during this period result in highly reproducible patterns of anomalies. Malformations involve structures or organs undergoing a rapid rate of growth and differentiation at the time of irradiation. For example, gestational day 8 in the rat is the period

Figure 2-3: **OFFSPRING MALFORMATION CURVE AT 100 R IN THE RAT**

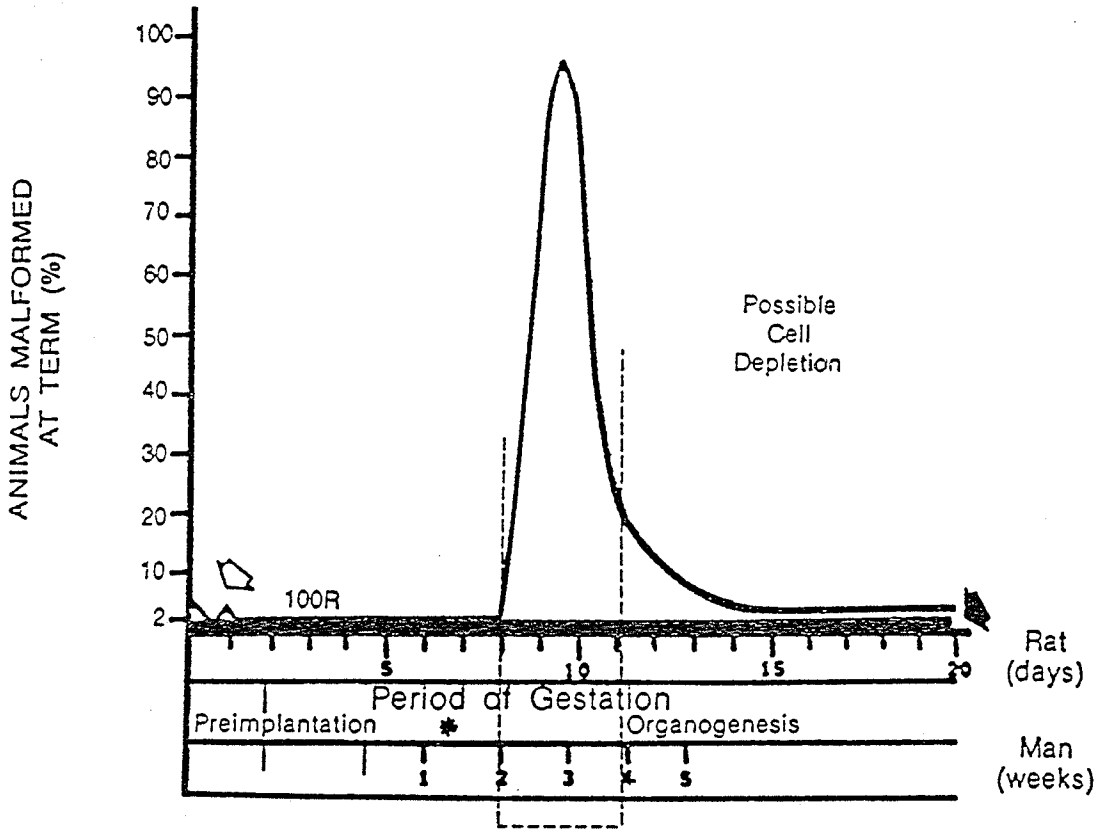

(From Brent, 1980).

of induction of the neural plate. Irradiation on gestational day 8 disrupts the normal development of the forebrain and cranium resulting in such severe malformations as anencephaly or exencephaly. The severity and frequency of malformations for a given day during organogenesis, is dependent on the radiation dose (Job et al, 1935; Wilson and Karr, 1951; Hicks, 1953; Hicks et al, 1957 and 1959; Cowan and Geller, 1960; Roizin et al, 1962; Hicks and D'Amato, 1961, 1966, and 1980; Brizzee, 1967; Konermann, 1982; Tribukait and Cekan, 1982; Kameyama and Hoshino, 1986; Takeuchi and Takeuchi, 1986; Persaud and Bruni, 1990). The lowest dose reported in the literature that can increase the incidence of gross congenital malformations during organogenesis is 25 rads (0.25 Gy) (Hicks and D'Amato, 1963; Yamazaki, 1966; National Research Council, 1980; Brizzee et al, 1982; Konermann, 1982).

During late organogenesis (gestational days 10-13), the incidence of congenital malformations decreases dramatically. By about gestational day 15 and through the remainder of the fetal period, the incidence of congenital malformations is only slightly increased above control levels. Congenital malformations are not frequently induced after irradiation with 100 rads (1 Gy), but there is a high probability of irreversible cell loss during this period, at this dose range. The brain and retina tend to be most affected from irradiation during the fetal stage due to their protracted developmental period as

compared with other organ systems (Wilson and Karr, 1951; Hicks, 1953; Hicks et al, 1957 and 1959; Cowan and Geller, 1960; Brent, 1980; Ordy et al, 1982; Ferrer et al, 1984; Kameyama and Hoshino, 1986; Persaud and Bruni, 1990).

2.3.5. Fetal Brain Development

Few studies have examined the acute effects of ionizing radiation on the fetal brain, all of which have focused on the ventricular zone of the developing telencephalon. Whether or not findings of the telencephalon region can be generalized to other irradiated brain regions is not known. Notwithstanding the different doses of irradiation used at different gestational days of telencephalic development, some general remarks regarding the acute effects to the telencephalon can be made.

Following irradiation exposure, regardless of gestational day or dose, no observable effects can be detected within 1 hour post-irradiation (Hicks and D'Amato, 1961; Hoshino and Kameyama, 1988). At one to two hours post-irradiation, a reduction in the number of mitotic cells has been reported at dose ranges of 50 to 200 rads (0.5 to 2 Gy) (Hicks and D'Amato, 1961; Hayashi and Kameyama, 1979; Brizzee et al, 1982; Tribukait and Cekan, 1982). A few electron microscopy studies have been conducted at this post-irradiation period. Findings of these studies suggest that ultrastructural changes are not evident until 1.5 to 2 hours post-irradiation. These changes included disruption of the nuclear membrane with an increase in

homogeneous density of the nucleus. Plasma membranes of cells were often frayed and irregular, while the cytoplasm contained numerous ribosomal aggregations (Hicks and D'Amato, 1961; Brizzee et al, 1982).

Hayashi and Kameyama (1979) studied the mouse telencephalon, irradiated with 25 or 100 rads (0.25 or 1 Gy) at various intervals of the fetal period. After irradiation with low dose levels during the early cortical proliferation and migration stage of development, cytoplasmic ribosomal aggregations were evident prior to the appearance of nuclear pyknosis. This was not the case following irradiation at later fetal stages, indicating that the sequence of acute radiation-induced ultrastructural changes depended on the gestational day of exposure. During this early developmental period of the cortex, there is general consensus that pyknotic changes of irradiated cells can first be observed by light microscopy at 2 hours post-irradiation. The peak incidence of pyknotic changes occurs within 4 to 6 hours, with doses ranging from 25 to 200 rads (0.25 to 2 Gy) (Hicks and D'Amato, 1961 and 1980; Brizzee et al, 1982; Kameyama and Hoshino, 1986; Hoshino and Kameyama, 1988). Within 2 to 5 hours post-irradiation, mitosis at the juxtaluminal border resumes, and by 24 hours post-irradiation, clearance of cellular debris is evident. Generally, the time required for irradiated tissue to resume the microscopic appearance of control levels is dependent on irradiation dose. Tissues irradiated

with 50 rads (0.5 Gy) and lower appear to recover within 24 hours, while tissues irradiated with 150 to 200 rads (1.5 to 2 Gy) require 48 to 72 hours to recover to control levels (Berry and Eayrs, 1963; Hicks and D'Amato, 1980; Hoshino and Kameyama, 1988).

Aside from these reports of acute irradiation effects, most prenatal irradiation studies of the developing brain have assessed the offspring during the postnatal rather than the fetal period. Regardless of the assessment period, however, there is general consensus in the literature that gestational days 13 in the mouse, and 15 in the rat are the periods of greatest radiosensitivity for the developing cerebral cortex in these species (Hicks et al, 1957; Cowan and Geller, 1960; Hayashi and Kameyama, 1979; Takeuchi et al, 1981; Brizzee et al, 1982; Konermann, 1982; Norton and Donoso, 1985; Kameyama and Hoshino, 1986; Hoshino and Kameyama, 1988; Norton and Kimler, 1988; Schull et al, 1990).

As outlined earlier, these periods in both the mouse and the rat represent the first stages of cortical neuron development and migration. Studies of irradiation on gestational day 13 in the mouse, or gestational day 15 in the rat have yielded a wide range of dose dependent developmental defects of the cerebral cortex as observed in the postnatal period. At doses of 100 rads (1 Gy) or greater reports include acute rosette formation with subsequent postnatal development of ectopic cortical masses,

severe reductions of cortical thickness (usually associated with microcephaly), neuronal depletion, decreased dendritic arborization, and disturbances of dendritic alignment with decreased neuronal connectivity (Hicks, 1953; Hicks et al, 1957 and 1959; Cowan and Geller, 1960; Hicks and D'Amato, 1961 and 1966; Takeuchi et al, 1981; Brizzee et al, 1982; Norton and Donoso, 1985; Kameyama and Hoshino, 1986; Norton and Kimler, 1988; Schull et al, 1990; Fukui et al, 1991).

Fewer studies have been conducted with dose ranges of less than 100 rads (1 Gy). It has been found that during the early stages of neuronal production and migration in the rat and the mouse, a radiation dose of 25 to 30 rads (0.25 to 0.30 Gy) is sufficient to cause permanent depletion of cortical neurons. Also, irradiation with a dose as low as 25 rads (0.25 Gy) during early corticogenesis can cause a reduction of the number of cortical cell dendritic branches, shorter dendritic processes, and derangement of arborization patterns (Hicks and D'Amato, 1963; Kameyama and Hoshino, 1986; Konermann, 1986; Hoshino and Kameyama, 1988; Schull et al, 1990). Fukui and colleagues (1991), recently found that a 0.48 Gy (48 rads) in utero dose on gestational day 16 (adjusted) to rats caused a temporary delay in the number of dendrites arising in cortical cells postnatally. A permanent decrease in the mean length of dendrites was observed after the 12th postnatal week.

In terms of the overall architecture of the postnatal rat cortex following gestational day 15 or 16 irradiation, dose levels of 0.45 to 0.50 Gy (45 or 50 rads) have been reported to cause significant reductions in cortical thickness. These reductions have been attributed to reduced neuronal populations and associated neuropil density (Norton and Donoso, 1985; Reyners et al, 1986; Fukui et al, 1991). In addition, during early corticogenesis in the rat and the mouse, irradiation doses of as little as 0.1 to 0.25 Gy (10 to 25 rads) have been reported to cause disturbances in the spatial arrangement of cortical neurons of the postnatal rat (Hicks and D'Amato, 1963; Konermann, 1986; Hoshino and Kameyama, 1988; Norton et al, 1991).

Persaud and Bruni (1990) observed abnormally arranged loci of neurons, primarily in infragranular cortical layers of 26 day old rats which were irradiated in utero on gestational day 15 with 0.5 Gy (50 rads). This anomaly was seen in 33% of all irradiated 26 day old offspring. However, it was not observed in 7 day old offspring irradiated on gestational day 15 with 0.5 Gy (50 rads).

As noted previously, there is general consensus that the late G2 and early G1 primitive neurons are the most radiosensitive elements of the developing brain. Little is known, however, about the relative radiosensitivity of the glial and vascular elements of the developing brain (Kameyama and Hoshino, 1986; Schull et al, 1990; Dr. R.P.

Jensh, personal communication). Although many postnatal manifestations of fetal irradiation of the brain may be attributed to delayed mitotic division, delayed maturation, or death of primitive neurons, other factors such as glial death, vascular changes, interruption of migratory activity, alterations of dendritic growth, and reduced synaptogenesis cannot be excluded. The literature therefore suggests that some of the manifestations of prenatal irradiation cannot be detected until later in the postnatal period, when full maturation of central nervous system structures have been achieved (Brent, 1986; Konermann, 1986; Schull et al, 1990).

Other than Halas z (1986), there have been no systematic histological studies reported on the development of the olfactory lobes of experimental animals following prenatal irradiation. Successive prenatal exposures, cumulating in hundreds to thousands of rads were used in order to determine the prenatal vs postnatal sequence of neuronal development in the olfactory lobes. Consequently, this data is of limited practical application.

Earlier investigators have reported reduction in the size of the olfactory lobes and rosette formation following doses ranging from 150 to 250 rads (1.5 to 2 Gy); however, detailed descriptions of these findings have not been included (Hicks, 1953; Cowan and Geller, 1960; Brizzee and Brannon, 1972; Tamaki and Inouye, 1976). Persaud and Bruni (1990), reported that exposure to 50

rads (0.5 Gy) on gestational day 15, did not induce pathohistological changes in the olfactory lobes when assessed on postnatal day 7. However, abnormal neurons were observed in the region of the olfactory nuclei in a few 26 day old specimens.

Abnormal development of the rat corpus callosum is a frequently reported outcome following fetal irradiation with high dose levels. Changes in the corpus callosum following prenatal irradiation from gestational days 9 to 18 using doses ranging from 100 to 300 rads (1 to 3 Gy) have been reported (Hicks, 1953; Cowan and Geller, 1960; Brizzee, 1967; Brizzee and Brannon, 1972; Tamaki and Inouye, 1979). The most sensitive period for maldevelopment of the corpus callosum is gestational days 14 to 17 in the rat (Mullenix et al, 1975; Schmidt and Lent, 1987; Schull et al, 1990). Studies of irradiation effects during this sensitive prenatal stage indicate that doses of 200 rads (2 Gy) or greater may cause total agenesis of the corpus callosum (Hicks et al, 1959; Cowan and Geller, 1960; Schmidt and Lent, 1987). Doses in the 100 to 200 rad (1 to 2 Gy) range may cause reductions of callosal thickness, reductions of the rostrocaudal callosal length, and/or an inability of fibers to cross the midsagittal zone into the contralateral hemisphere. These changes have been assumed to be caused by reductions of the cortical neurons which contribute axons to the corpus callosum, and/or disturbed development of the

midsagittal glial sling (Hicks, 1953; Cowan and Geller, 1960; Mullenix et al, 1975; Schmidt and Lent, 1987).

In lower dose ranges, Persaud and Bruni (1990) found only 1 offspring with an underdeveloped corpus callosum among the offspring of rats irradiated with 50 rads (0.5 Gy) on gestational day 15. Konermann (1986) found that irradiation of mice with 25 to 100 rads (0.25 to 1 Gy) on gestational day 13 caused a dose-related reduction in the thickness of the corpus callosum in postnatal offspring. No other assessments of corpus callosum development have been conducted at dose ranges under 100 rads (1 Gy).

Very little information exists regarding the effects of prenatal irradiation on the development of the hippocampus and associated structures. With dose ranges of 200 rads (2 Gy) or greater on gestational day 16, ectopic clusters as well as cell deficits have been reported in the postnatal hippocampal pyramidal cell layer. These deficits have been associated with an overall reduction in the size of the hippocampus (Hicks, 1953; Cowan and Geller, 1960; Ferrer et al, 1984). Using a 200 rad (2 Gy) dose of ionizing radiation to determine the proliferative and migratory patterns of cells during hippocampal development, Bayer (1980b) found that the germinal epithelium of the hippocampal formation was most radiosensitive on gestational day 15. Radiosensitivity of this proliferative zone was found to decrease progressively throughout the remainder of gestation.

Persaud and Bruni (1990) found histological abnormalities in 57% of 26 day old offspring irradiated on gestational day 15, and in 33% of 26 day old offspring irradiated on gestational day 18. No abnormalities were noted in the 7 day old offspring in these groups. Although lamination of the hippocampus was not disturbed, circumscribed areas of dark pyknotic neurons as well as areas of reduced numbers of cells were seen in both hippocampal pyramidal cell layers and dentate granule cell layers. These cellular changes were not confined to any particular rostrocaudal area, and were often bilateral.

Few systematic studies of prenatal irradiation effects on the cerebellum exist. With doses ranging from 100 to 400 rads (1 to 4 Gy), developmental alterations of the cerebellum can be induced from gestational day 13 through the end of the second postnatal week in the rat. These earlier studies indicated that prenatal irradiation disturbed the basic shape and size of the postnatal cerebellum, while postnatal exposure caused deficits in the intrinsic cellular architecture, especially the granular cell layer (Hicks, 1953; Hicks et al, 1959; Cowan and Geller, 1960; Altman, 1969a; Tamaki and Inouye, 1976). In dose ranges of 100 rads (1 Gy) and greater, gestational day 15 represents the peak day for irradiation induced reductions of Purkinje cells (Das, 1977; Altman and Bayer, 1978a; Schull et al, 1990).

Das (1977) found that a 170 rad (1.7 Gy) irradiation

of the cerebellum on gestational day 15 caused considerable degeneration to the proliferative neuroepithelium, as observed 6 hours post-irradiation. Although some fragmentary regeneration of the neuroepithelium was observed by 2 days post-irradiation, postnatal assessment revealed a 50% reduction in the number of cerebellar Purkinje cells. Other short and long term post-irradiation observations made in this study included a reduced surface area spread of the external germinal layer (thickness of this layer was not affected), a 40% reduction in the number of granule cells in the internal granular layer, and significant reductions in the size of molecular and medullary zones. Despite these reductions, however, irradiated cerebellum demonstrated normal trilaminar organization and folia development in the postnatal period (Das, 1977).

As the external germinal layer has not begun to develop until gestational day 17 in the rat, Das (1977) suggested that the reduced surface area and the subsequent reduced output of granule cells from this layer was due to depletion of the Purkinje cells. It was suggested that the Purkinje cells of the cerebellum have a inductive influence on the growth and mitotic activity of the external germinal layer. Reductions of the molecular layer were assumed to be due to stunted Purkinje dendritic growth as well as a reduction in the parallel fiber component arising from a depleted compliment of granule cells. Medullary zone reduction was assumed to be due to a reduction

in ascending fibers from the spinal cord, inferior olivary nuclei, pontine nuclei, and other nuclei of the brainstem. A reduction in the number of descending axonal processes of Purkinje cells also likely contributed to the reduced size of this zone (Das, 1977).

Persaud and Bruni (1990) found different postnatal effects following a 50 rad (0.5 Gy) irradiation exposure on gestational day 15. Although no reductions of Purkinje cells were evident, variable sized islands of reduced numbers of granule cells in the granular cell layer were observed. These changes were not seen in 7 day old offspring, however, 14% of irradiated offspring revealed these changes on postnatal day 26. Similar, but less severe lesions were also observed in 22% of 26 day old offspring irradiated on gestational day 18 with 50 rads (0.5 Gy).

2.3.6. Postnatal Behavior

According to postnatal behavioral studies, single exposures to rats in utero at doses ranging from 25 to 200 rads (0.25 to 2 Gy) may result in impairments of sensory function, motor capabilities, learning, memory, and emotionality (Mullenix et al, 1975; Tamaki and Inouye, 1976; D'Amato and Hicks, 1980; Ordy et al, 1982; Jensh, 1986; Norton, 1986; Norton and Kimler, 1987 and 1988; Schull et al, 1990; Norton et al, 1991).

In many studies gestational day 15 has been identified as the most sensitive period for induction of postnatal behavioral changes. Some of these changes

include delays in motor development, hypoactivity (usually, later in postnatal life these animals develop hyperactivity), impaired maze learning, and a characteristic "hopping" rather than alternate gait pattern (D'Amato and Hicks, 1980; Jensh, 1986; Norton, 1986; Norton and Kimler, 1988; Schull et al, 1990; Norton et al, 1991). In some cases, attempts have been made to correlate behavioral alterations with irradiation induced developmental disturbances of the brain. In most of such studies, morphological and histological assessment has been carried out on the cerebral cortex only (Norton and Kimler, 1987 and 1988; Norton et al, 1991).

3. MATERIALS AND METHODS

3.1. EXPERIMENTAL ANIMALS

3.1.1. Animals

Sixty-one virgin, female rats of the albino Sprague-Dawley strain were used in this study. The weights of the animals ranged between 200 and 300 grams.

3.1.2. Environment

The rats were housed in wire mesh cages with a maximum of four animals per cage. All animals received food and water ad libitum.

The animal holding room was maintained at a temperature of 20° Centigrade (+/- 2° C). A constant day/night cycle was maintained with a 12 hour light cycle extending from 0800 hrs. to 2000 hrs., followed by a 12 hour dark cycle from 2000 hrs. to 0800 hrs.

All animals used in this study were allowed to acclimatize to the animal holding environment for a period of at least one week, prior to being utilized in these experiments.

3.1.3. Mating and Determination of Pregnancy

Six male albino rats of the Sprague-Dawley strain were used for breeding in this study. Timed pregnancies were obtained by housing three female rats with one male overnight. Female rats were removed from the breeding cages at approximately 0900 hours the following morning, and vaginal smears were taken. Pregnancy was confirmed by the presence of spermatozoa in the vaginal smear.

As copulation was assumed to have taken place midway between the dark cycle at approximately 0200 hours, the day of determined pregnancy was designated day 1 of gestation. Weights of pregnant animals were taken and recorded at this time. Pregnant animals were then earmarked for identification, and housed together to a maximum of four animals per cage. The pregnant rats were then left undisturbed until the time of irradiation or sham-irradiation treatment.

3.2. EXPERIMENTAL DESIGN

3.2.1. Groups

Once pregnancy was confirmed, animals were randomly assigned to one of six groups. Each group consisted of ten pregnant animals with exception to the first group (#1), which consisted of eleven animals. These groups are summarized as follows:

GROUP #1 Untreated Controls - gestational day 15+5 days (day 20).

GROUP #2 Irradiated - gestational day 15+5 days (day 20).

GROUP #3 Untreated Controls - gestational day 15+48 hours (day 17).

GROUP #4 Irradiated - gestational day 15+48 hours (day 17).

GROUP #5 Untreated Controls - gestational day 15+4 hours.

GROUP #6 Irradiated - gestational day 15+4 hours.

3.2.2. Irradiation Treatment

The animals were irradiated with a dose of 50

rads (0.5 Gy) between 1700 hours and 1800 hours on gestational day 15.

Prior to irradiation treatment, the animals were weighed and their weights recorded. They were then placed in a specially constructed, clear, Lucite box measuring 20.0 cm x 10.0 cm x 7.0 cm. This box is divided into three equal compartments measuring 10.0 cm x 6.5 cm x 7.0 cm each, thus allowing for treatment of up to three animals at a time. The small size design of each compartment was to ensure minimal air-space around each pregnant animal, and therefore, maintenance of optimal backscatter conditions. Ample breathing holes were located in the outer walls and roof of each Lucite compartment.

The animals were irradiated using a Theratron F Cobalt Unit which is housed in the Manitoba Cancer Foundation, Health Sciences Centre. Because this equipment is utilized for radiotherapy treatments, it is calibrated and its performance is checked by the Medical Physics Department of the Cancer Foundation on a regular basis. The calibration has been carried out according to the TG 21 protocol as recommended by the American Association of Physicists in Medicine. The ionizing chamber and electrometer (measuring instruments) have been calibrated by the National Research Council of Canada.

To ensure uniform dose distribution throughout the irradiated rats, two parallel opposed fields first in a postero-anterior direction, then in an antero-posterior

direction totalling 50 rads (0.5 Gy) were used. The surface to source distance, regardless of the number of rats irradiated at one time, was 75.0 cm for both planes of exposure.

Since anywhere from one to three rats could be exposed at one time, the field size (area of Lucite compartments occupied) varied accordingly. The actual field sizes were 20.0 cm x 10.0 cm x 7.0 cm, 13.5 cm x 10.0 cm x 7.0 cm, and 10.0 cm x 6.5 cm x 7.0 cm for irradiation of three, two, or one rat, respectively.

Once the rectangular field size was determined for a given treatment, Table A2 (Appendix Ia) was used to determine an equivalent square field. For example, when irradiating three animals, the square field equivalent of 20.0 cm x 10.0 cm would equal 13.0 cm x 13.0 cm.

The next step in exposure time calculations was to determine the percent depth dose. This is the percent of the total irradiation source dose that penetrates a given depth of tissue. The Lucite box was 7 cm deep yet because both an antero-posterior and a postero-anterior exposure were used to achieve thorough dose distribution, the depth was assumed at the mid-point, or 3.5 cm deep. Using the % Depth Dose Table (Appendix Ib), and the example used above of a three rat exposure, the percent depth dose would equal 86.4%.

To calculate the actual given dose, the formula Given Dose = Total Dose Desired/Percent Depth Dose x 100,

was used. For a three rat irradiation therefore, the given dose = 50 rads / 86.4% x 100 = 57.9 rads (0.579 Gy).

Finally, the time required for total exposure was calculated. Time= Given Dose/Absorbed Dose Rate x 60. Due to ongoing cobalt decay, the tables used to determine absorbed dose rate are changed every two months. At the time of irradiation exposure for animals in this study, absorbed dose rates were 112.0 rads/min, 111.2 rads/min, and 107.6 rads/min for irradiation of three, two, or one animal, respectively. To complete the above example, the total time of exposure for a three animal irradiation was: 57.9 rads / 112.0 rads per min. x 60 = 31.0 seconds. Since animals were irradiated with both antero-posterior and postero-anterior exposures, each exposure would be 15.5 seconds in this example.

All rats in this study received total dose exposures of less than one minute.

3.2.3. Untreated Controls

On gestational day 15, between 1700 hrs. and 1800 hrs., one to three control animals were weighed and placed in the Lucite treatment box. The total time of confinement for both irradiation treated, and sham-irradiated controls was twenty to thirty minutes.

3.2.4. Hysterotomy and Fetectomy

Depending on their group assignment, pregnant animals were prepared for surgery either 4 hours, 48 hours, or 5 days after irradiation or control procedures. For

the 48 hour and the 5 day groups, these procedures were initiated between 1600 hours and 1700 hours on their respective days.

Prior to being anesthetized, animals were weighed and their weights recorded. This third and final weighing was not done on animals in the 15+4 hour groups, as an initial sample in these groups did not indicate any weight changes within four hours from treatment or control procedures.

After weights were recorded, animals were anesthetized with an intraperitoneal injection of Nembutal (sodium pentobarbital) at a dose of 50 mg per kg of body weight. Once animals proved to be unresponsive to mechanical stimulation, a midline and two transverse abdominal incisions were made. After uteri and fetuses were examined in situ, the uterine horns were cut open on their anti-mesometrial side, and the fetuses and placentas were removed. Fetuses and placentas were weighed separately and immersed in a mixed aldehyde fixative solution (Appendix IIa). Following fetectomy, dams were sacrificed by severance of the respiratory diaphragm and abdominal aorta while still anesthetized.

3.2.5. Fixation Procedures

As mentioned, placental and fetal tissues were immersed in a mixed aldehyde fixative following fetectomy. An initial sample of fetuses demonstrated that whole body immersion was adequate to ensure total fixation of the brain in the 15+4 hours and 15+48 hours groups. As this

was not the case for the 15+5 days fetuses, they were decapitated prior to immersion.

After approximately one month of fixation time, about half of the fetuses and all placentas from each litter were transferred into a straight phosphate buffer solution, in preparation for paraffin embedding procedures. The remaining fetuses were transferred into a dextrose rinse solution (Appendix IIb), as part of the standard procedure for Epon plastic embedding. For the latter group, the dextrose solution was changed every two to three weeks to prevent mold growth.

3.3. TERATOLOGICAL EVALUATION

3.3.1. In-Situ Assessment

As mentioned previously, after the abdominal incisions were made, the uterine horns and fetuses were examined *in situ*. At this time, the number of implantation sites, as well as resorption sites, were counted and recorded. All fetuses were also tested for response to mechanical stimulation in order to determine the live birth to stillbirth ratio.

3.3.2. Examination of External Morphology

At the time of this study, no known standardized assessments of external morphology existed for fetuses aged 15 to 20 gestational days, although there are assessments available for the rat at earlier stages of embryonic development (Brown and Fabro, 1981). Consequently, criteria for evaluation of the fetuses in this study were developed

based on extrapolation from the available literature. The primary sources used to design these assessments included the work of Christie (1964), Wilson (1964), and Edwards (1968). Control fetuses in this study served as additional reference resources when designing external morphological criteria (see Appendices IIIa, IIIb, and IIIc, for criteria used to assess gestational day 15+4 hour litters, 15+48 hour litters, and 15+5 day litters, respectively).

Each criterion was designed to yield a "yes" response if fetal development was considered to be normal for fetal age, while a "no" response indicated abnormal development. Each fetus in a given litter was recorded in this manner and one form was used for each litter. When a "no" response was recorded for any one fetus in a litter, the observed defect was described in detail under the "comments" section of the form. A total of 61 litters (862 fetuses) were assessed in this manner using a binocular dissection microscope.

In addition to assessment of external morphology, crown-rump measurements of each fetus were taken using an ocular micrometer disc, and recorded on the litter assessment forms. This data, however, could only be collected for gestational day 15+4 hour and 15+48 hour fetuses, as the 15+5 day fetuses were decapitated at the time of fetectomy.

The male to female sex ratios were also determined for the gestational day 15+5 day litters. Using the fetal sexing method outlined by Wilson (1964), measurements of

the distance between the genital tubercle and anus were taken using the ocular micrometer. The distance is approximately one mm in females and twice as much in males.

3.3.3. Histological Processing of the Brain

After the external morphological assessments were completed, a number of fetuses were randomly selected from each litter for brain tissue processing. Whole brains and a rostral portion of the spinal cord were dissected out of fetuses using a binocular dissection microscope and blunt probe. The gross morphology of each brain was examined. This initial sample of brains, destined for Epon plastic embedding, were then temporarily stored in a dextrose solution (see Appendix IIb for Epon plastic recipe, and Epon plastic embedding protocol for light microscopy).

Approximately five Epon embedded brains per group were then sectioned on a Reichert OMU 2 ultramicrotome, using handmade half inch glass knives. Each brain was sectioned coronally from its rostral to caudal extent at a thickness of 0.5 to 1.0 micron. Approximately five sections were saved between intervals of 30 sections. These sections were left for 24 hours to dry then were stained with methylene blue - azure II. As the quality of sections and/or staining of these initial slides was seldom deemed adequate for histological and morphological comparisons, the Epon plastic embedding method was abandoned, and the remaining brains were embedded in paraffin. Although the plastic sections provided greater definition of histological structures,

paraffin sectioning proved to be a more expedient method for obtaining large numbers of tissue sections.

Two fetuses were randomly selected from each litter for paraffin embedding of the brain for a total of 122 specimens. All of the brains were dissected out of the fetal craniums, in the manner previously described. These brains were then processed for paraffin embedding according to the procedure outlined in Appendix IIc. From a total of 122 embedded specimens, a minimum of 10 brains from each group were selected for sectioning. Whole brain, coronal, serial sections were made at thicknesses of 8.0 microns for gestational day 15+48 hours and 15+5 day brains, and 5.0 microns for gestational day 15+4 hour brains. An AO Spencer microtome and steel knife were used. After a minimum of 24 hours drying time, slides were then stained with thionin according to the procedure outlined in Appendix IIc.

3.3.4. Microscopic Evaluation of Brain Sections

All slides were assessed using a binocular, Nikon light microscope. For each area of the brain subject to examination in this study, several coronal planes of section were viewed in order to evaluate the rostral to caudal extent of each structure. Due to the pronounced ventral curvature of the 15+4 hour brains, olfactory lobes had to be horizontally sectioned in this group, in order to maintain the coronal sectioning plane for the rest of the brain. The gestational day 15+5 day control and irradiated

brains were the first to be studied.

For a given plane of section, all control and experimental slides were matched for anatomical location. Control slides were then studied to familiarize the investigator with the morphology and histology of reference structures in question. All identifying numbers on control and experimental slides were then covered with masking tape, and slides were mixed. With each slide assessed, the investigator made a determination as to whether the slide belonged to a control or experimental group. Justifications for decisions were recorded. This same procedure was used in assessing 15+48 hour slides and 15+4 hour slides. It should be noted that those slides made from Epon plastic embedding were used when possible, for the purpose of identifying cell types, shapes, and possible effects of irradiation.

As the number of brains sectioned and examined varied per group, the following is a summary of the total n value per group:

15+5 day controls - 13 paraffin embedded + 3 Epon embedded
= 16 brains examined.

15+5 day irradiated - 12 paraffin embedded + 3 Epon embedded
= 15 brains examined.

15+48 hour controls - 10 paraffin embedded + 3 Epon embedded
= 13 brains examined.

15+48 hour irradiated - 10 paraffin embedded + 3 Epon embedded
= 13 brains examined.

15+4 hour controls - 10 paraffin embedded + 3 Epon embedded
= 13 brains examined.

15+4 hour irradiated - 10 paraffin embedded + 3 Epon embedded
= 13 brains examined.

3.3.5. Brain Measurements

Some quantifiable data were collected on the 15+5 day brain sections. First, olfactory mitral cell counts were conducted on four control and four irradiated brains. Sections were matched for anatomical location, and assurance of a comparable coronal plane. Counts were conducted at one level of section, approximately 312 microns caudal to the rostral tip of the olfactory lobe. A 20x80 ocular micrometer rectangle was used as indicated in Figure 3-1, with the 20 micrometer edge lined up horizontally, and level to the most dorsal tip of the olfactory ventricle. All mitral cell counts were done with a x40 power objective. Mitral cells could be easily identified, as their spherical shape, and pale staining cytoplasm made them readily distinguishable from neighbouring cells in this field.

The developmental zones of the frontal, parietal and occipital cortices were also measured in the 15+5 day fetuses. As no stereotaxic atlas of the fetal rat brain exists, the anatomical landmarks used by Norton and Kimler (1988) to designate the dorsal components of frontal, parietal, and occipital cortical areas in the adult rat were also used in this study. These landmarks included: anterior commissure midsagittal crossing for frontal cortex, the

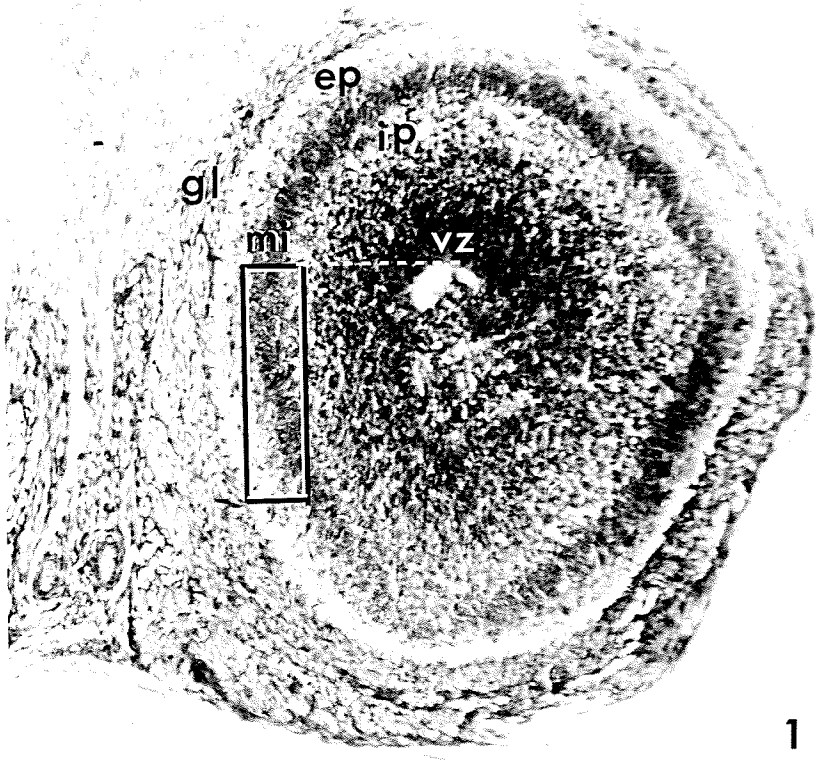

1

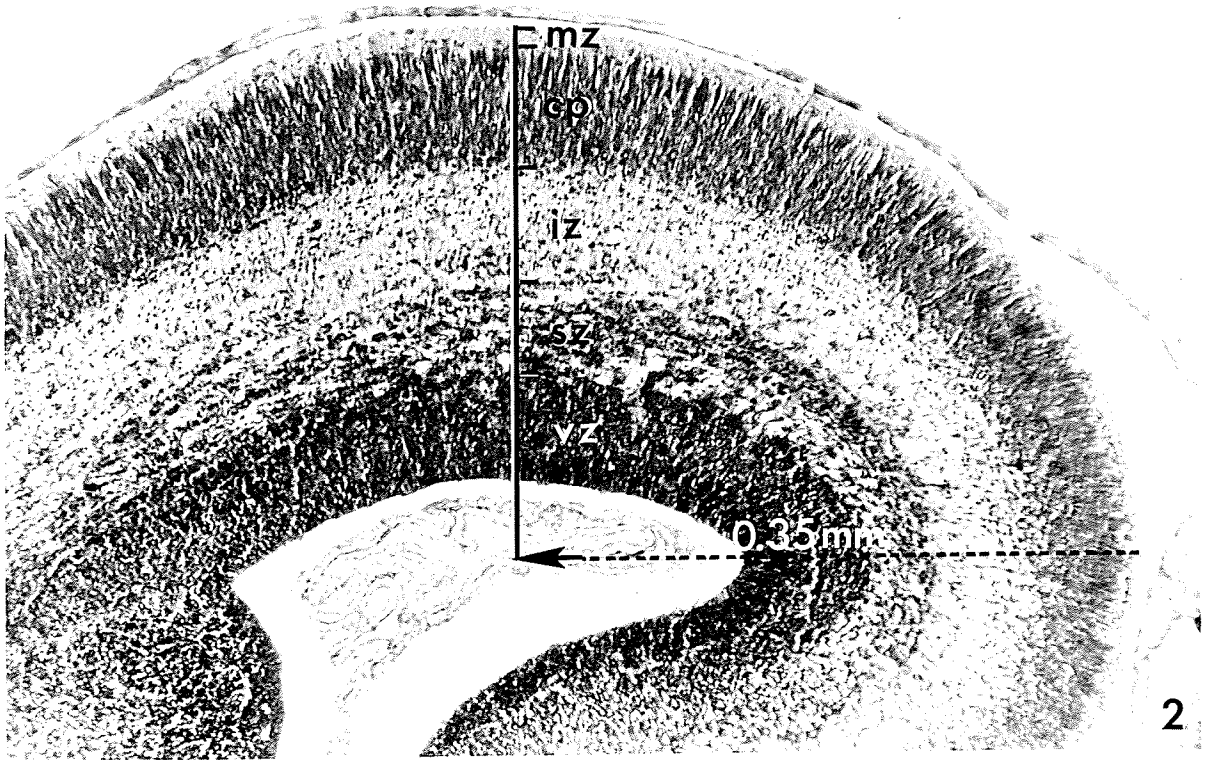

2

level just caudal to the interventricular foramen for parietal cortex, and the level of the posterior commissure for occipital cortex. All sections used for measurements were matched for exact anatomical location and comparable coronal plane of section. Five control sections and ten experimental sections were used for frontal cortex measurements; seven control and ten experimental sections were used for parietal measurements; seven control and seven experimental sections were used for occipital measurements. For all three cortical areas, thickness measurements were made on the cortical plate, the intermediate zone, the subventricular zone, the ventricular zone, and the total thickness of these four zones. The marginal zone was not included in these measurements, due to difficulty in differentiating the limits of this zone in most specimens.

A Zidas-Zeiss digitizing pad was used, at x128 magnification (x10 objective). As depicted in Figure 3-2, the point of measurement was determined at a distance of 0.35 mm from the most medial midsagittal extreme of the cortex. Measurements were made in a line parallel to the midsagittal plane. To ensure accuracy of measurements, each zone measurement was repeated x4, and the average of these four measurements was recorded.

The rostrocaudal extent of the midsagittal crossing of the corpus callosum in gestational day 15+5 day irradiated, and control brains was also measured. As all brains in these groups were serial sectioned at a thickness of 8

microns, the number of sections in which the corpus callosum was seen crossing the midline were counted. Callosal measurements were done on ten irradiated and ten control brains.

3.3.6. Histological Processing of Placentas

One placenta was randomly selected from each litter for a total of 61 specimens. Placentas were then bisected with a razor blade at the level of the central artery. The two halves of each placenta were then processed for paraffin embedding in a Fischer Histomatic tissue processor. Both halves of the placenta were then embedded together with their medial edges facing the embedding block. Two consecutive sections of 7.0 microns were mounted on glass slides and allowed to dry for 24 hours. These slides were then stained with haematoxylin and eosin by the procedure outlined in Appendix IId.

3.3.7. Microscopic Evaluation of the Placenta

As with the brain sections, sections of control placentas were studied in order to familiarize the investigator with the normal placenta morphology and histology at the various gestational ages examined in this study. For each age group, identifying numbers on control and experimental slides were then covered with masking tape and the slides were mixed. A determination was made as to whether the slide belonged to either the control or irradiation treated group. Justifications for decisions were recorded.

3.4 STATISTICAL ANALYSIS

The NWA Stat Pak (Northwest Analytical Inc., Portland, Oregon) was used for statistical analysis in this study. Student t-test comparisons between control and irradiated specimens were performed for each of the following parameters: maternal weights, number of live fetuses per litter, fetal weights, placental weights, crown-rump lengths, mitral cell counts, and rostrocaudal lengths of corpus callosi.

Chi-square comparisons were made between control and irradiated specimens to determine differences in the number of resorptions per litter, the number of dead fetuses per litter, the frequency of gross external morphological anomalies, the frequency of brain effects observed, and the frequency of placental effects observed. Inherent in this statistical program, the Yates' correction factor was applied to all chi-square comparisons.

Two types of statistical assessments were made on the 15+5 day cortical thickness measurements. First, a three-way analysis of variance was used to provide a general picture of measurement trends. The three parameters compared in this analysis include: A) control vs irradiated, B) frontal vs parietal vs occipital, and C) cortical plate vs intermediate zone vs subventricular zone vs ventricular zone vs thickness total. As well as these comparisons, factor combinations of AxB, AxC, BxC, and AxBxC were also performed. Once the general picture of measurement trends

were determined, one-way analysis of variance comparisons were made between each cortical zone measurement and its comparable control measurement.

For all statistical comparisons, a 0.05 significance level was employed.

4. RESULTS

4.1. MATERNAL WEIGHTS

As outlined previously, weights of pregnant dams were taken at the time of determined pregnancy, prior to irradiation or sham-irradiation procedures, and prior to the time of fetectomy. Tables 4-1, 4-2, and 4-3 show the mean weights $\pm$ the standard error of the mean for 15+5 day, 15+48 hour, and 15+4 hour groups, respectively. As these tables depict, no significant differences between maternal weights of irradiated and control groups were detected at these gestational intervals.

4.2. FETAL LETHALITY AND LITTER SIZE

From the 11 litters yielded from Group #1 dams, (control fetuses recovered on gestational 15+5 days) a total of 142 viable fetuses were recovered. The comparable irradiation group (Group #2) yielded 135 viable fetuses from 10 litters. In Groups #3 and #4 (15+48 hour controls and irradiated), 149 and 147 viable fetuses were recovered, respectively. In the 15+4 hour groups, control litters resulted in 140 viable fetuses, while 149 live fetuses were recovered from irradiated litters.

Tables 4-4, 4-5, and 4-6, reveal that a 50 rad (0.5 Gy) dose of ionizing radiation on gestational day 15 had no impact on the mean number of viable fetuses per litter, nor the total number of resorptions or deaths found in each irradiation group, as compared with their age-related controls. Out of a total of 61 litters, only 2 dead fetuses

were found; one in Group #4 (15+48 hour irradiated), and another in Group #5 (15+4 hour controls). The total number of resorptions per animal group was found to be almost equal for 15+5 day and 15+48 hour control vs irradiated groups. In the 15+4 hour groups, however, irradiated litters yielded a total of 12 resorptions while only 7 resorptions were observed in controls. This difference did not prove significant with chi-square comparison.

To assess the differences between the number of resorptions observed across the different gestational age groups, control resorption frequencies and irradiated resorption frequencies were compared separately with chi-square analysis. No significant differences were found across gestational ages for either control or irradiated groups.

4.3. FETAL GROWTH

Table 4-7 shows the mean weights of fetuses at each of the post-irradiation intervals examined in this study. No significant differences existed between the irradiated and control fetuses of the 4 hour post-irradiation groups. However, irradiated fetuses in both the 15+48 hour and 15+5 day groups were significantly lighter in weight when compared with controls (P is less than 0.001). This weight differential was assumed to be a treatment effect.

Table 4-8 shows the mean crown-rump lengths of the 15+4 hour and the 15+48 hour groups. As explained earlier, crown-rump measurement data were not collected

for the 15+5 day offspring. Although no differences were detected in the mean weights of offspring 4 hours post-irradiation, crown-rump measurements were significantly reduced in this group (P is less than 0.05). Irradiation-induced stunting was also significant at the 48 hour post-irradiation interval (P is less than 0.001).

4.4. ASSESSMENT OF EXTERNAL MORPHOLOGY

Figure 4-1 shows the normal external morphological development and relative sizes of fetuses at the different gestational ages examined in this study. Data collected utilizing the external morphological assessment forms developed for this study (Appendices IIIa, b, and c), are compiled in Table 4-9. Some explanation of the defects observed is required.

Partial exencephaly was a term used to describe a cranial anomaly observed with varying frequency in all 15+4 hour and 15+48 hour groups. As revealed in gross examination, this defect typically appeared as a rounded mass of tissue, usually located in the midsagittal frontal area of the cranium, or occasionally unilaterally, in the approximate region of the rostral, fronto-temporal junction. Skin overlaying these masses was not interrupted, and in no instances were other associated cranial or facial anomalies observed. In order to accurately diagnose this anomaly, one 15+4 hour control specimen and one 15+48 hour irradiated specimen were coronally sectioned for microscopic assessment. In both instances, whole fetal heads were embedded in

paraffin, and serial sectioned at 8 micron thicknesses throughout the rostrocaudal extent of the anomaly. Microscopic evaluation of the sections revealed that these anomalous "bulges" consisted of both meningeal and neural tissue, herniating through the primitive skull. Consequently, these anomalies are best described as partial exencephalies or brain herniations, as they contained neural tissue, and were limited to a specific region of the cranium.

Out of 862 fetuses assessed, three paw deformities were observed. In the anomalous 15+48 hour control and 15+48 hour irradiated fetuses, the deformity consisted of a pronounced unilateral forepaw flexion as compared with other specimens in these groups. One fetus in the 15+4 hour control group demonstrated brachydactyly of the right hindpaw, with an observable shortening of the right hindlimb.

Two unilateral malformations of the eyelids were observed in the 15+5 day irradiated group. In both instances, full closure of the palpebral fissure was not complete as would be expected at this gestational age. As well, in both of these specimens, the upper eyelids of the affected eyes demonstrated what would be best described as a partial lateral cleft. These eyelid malformations were assumed to have caused the incomplete closure of the palpebral fissures. The remaining defects listed in Table 4-9 are self-explanatory.

In general, this particular strain of rat appears

to have a naturally low incidence of morphological malformations. No statistically significant differences in the frequency of observed morphological defects existed for any irradiation group as compared with their age-related controls, nor between gestational ages. Equally as important, irradiated offspring did not demonstrate any significant delay in the developmental rhythm of external morphological events as compared with age-related controls.

4.5. LITTER SEX RATIOS

As part of the external morphological examination, all fetuses yielded from the 15+5 day groups were sexed, in order to determine whether a 50 rad (0.5 Gy) irradiation exposure on gestational day 15 may alter the litter sex ratio. Of 142 control offspring in this post-irradiation interval, 48% of offspring were male, while 52% were female. Of 135 irradiated offspring, 49% were male while the remaining 51% were female. Irradiation did not appreciably alter the sex distribution of offspring in this study.

4.6. HISTOLOGICAL EVALUATION AND MEASUREMENTS OF BRAIN REGIONS

All brains randomly selected for either paraffin or Epon embedding were examined for gross morphological defects. No gross morphological defects were found in any of the six study groups, although in a few of the visibly smaller irradiated fetuses (approximately seven irradiated specimens from all groups combined), overall brain size was also reduced. As the relative weights of the these

smaller brains were not examined in relation to body weights, it could not be determined as to whether these smaller brains represent a true microcephaly.

4.6.1. Cerebral Cortex

In the 15+4 hour groups, the cerebral cortex was characterized by a relatively thick ventricular zone, and a smaller primordial marginal zone as depicted in Figure 4-2a. These zones appeared larger in lateral cortical areas; however, they tapered in size in a lateral to dorsal directions. As well as this lateral to dorsal size gradient, there also appeared to be a decrease in relative primordial cortex thickness in a rostral to caudal (frontal to occipital) direction. Mitotic cells were most readily apparent along the juxtaventricular border of the primordial cortex, although an occasional mitotic figure was often observed within the substance of the ventricular zone and/or in the region bordering the ventricular and primordial marginal zones. The majority of non-mitotic cells of the ventricular zone consisted of round to oval-shaped cells with light staining cytoplasm and small, dark staining nuclei (Fig. 4-3a). These cells, presumably representing S, G1, and G2 phase cells, appeared to be arranged in a radial pattern from the ventricular surface, extending throughout the ventricular zone.

The primordial marginal zone consisted of a thin band of irregularly arranged cells usually 3 to 5 cells in thickness. Cell shapes and sizes varied considerably

in this zone, although most resembled the presumptive S, G1, and G2 cells of the ventricular zone in terms of size, shape, and staining propensity (Fig. 4-3a). Cells of the 15+4 gestational day marginal zone likely represent the early generated neurons (and perhaps glial cells) of lamina 1 and subplate layers. It is also possible that in lateral cortical regions, some of these cells may also have been the early generated neurons of lamina 6; the earliest generated cells of the definitive cortical plate.

The fibrous constituents of the primordial marginal layer were not adequately stained by methylene blue - azure II nor thionin stains, therefore assessment of the fibrous components of this zone could not be carried out. The superficial border of the marginal zone was characterized by numerous meningeal blood vessels containing nucleated fetal red blood cells (Fig. 4-2a). Vessels could also be identified in the substance of the ventricular zone but to a lesser extent than in superficial marginal regions (Fig. 4-3a). At this gestational age, control slides revealed a very low incidence of naturally occurring cell death as demonstrated by the infrequent number of pyknotic cells in all control cortical regions.

Figures 4-2b and 4-3b depict a typical segment of the dorsal frontal cortex in fetuses irradiated on gestational day 15 and recovered 4 hours post-irradiation. All irradiated specimens at this post-irradiation interval demonstrated numerous pyknotic cells characterized by

shrunken cells containing circular, or irregularly shaped homogeneously staining masses. The number of pyknotic figures was subjectively assessed to be similar between lateral and dorsal cortical regions, as well as frontal to occipital regions.

As shown in Figures 4-2b and 4-3b, pyknotic figures tended to be localized in the ventricular zone, in a region just superficial to the juxtaventricular mitotic area, and extending to the most superficial limits of the ventricular zone. Very rarely were pyknotic cells observed in the juxtaventricular mitotic area, or in the marginal zone of any cortical region. At this post-irradiation interval, mitotic activity did not appear to be disturbed in any of the cortical regions assessed, as there appeared to be a comparable compliment of mitotic cells in both control and irradiated specimens.

As far as could be determined with conventional light microscopy, the vasculature of the primordial cerebral cortex appeared unaffected four hours after a 50 rad (0.5 Gy) irradiation, as endothelial cells appeared intact (Fig. 4-3b). Due to the absence of any observed macrophages or other phagocytotic cells (with the exception to the occasional monocyte), clearance of cellular debris was not believed to have commenced by this post-irradiation interval.

Figure 4-4a is an example of a typical dorsal segment of frontal cortex from a 15+48 hour (17 day) fetus. As demonstrated in this figure, five developmental zones

were evident at this gestational age. The fiber rich marginal zone contained a few elongated, horizontally oriented cells, as well as a few round to oval shaped cells like those observed in the 15+4 hour groups.

The cortical plate has become a distinctive entity at this gestational age, although differentiation of cortical plate laminae was not possible at this time. The majority of plate cells had not yet begun to differentiate and were homogeneous in appearance. Most consisted of round to oval-shaped cells with light staining cytoplasm and small nuclei. These particular cells appeared much like those cells observed in both the subventricular and the ventricular zones.

Another cell type was evident at this gestational stage. These cells were smaller, spherical, with dark-staining cytoplasm. They were observed in low numbers with an apparently random distribution in the cortical plate, intermediate zone, subventricular zone, and ventricular zone regions. Although the identity of these smaller cells is not known for certain, their random distribution indicated that they may represent migrating and/or early differentiating neuronal and/or glial cells.

Deep to the cortical plate, a thin intermediate zone consisting of both corticofugal and corticipedal fibers as well as migrating cells could be seen. The subventricular zone was also apparent on this gestational day. This zone could be easily differentiated from the ventricular zone

as it lacked the radial orientation of cells typical of the ventricular zone, although cell types appeared quite similar in these two areas. Some mitotic figures could be seen in the subventricular zone. The ventricular zone appeared the same as it did in the 15+4 hour groups with exception to the fact that it was thicker, and mitotic activity at the juxtaluminal border appeared somewhat reduced.

As before, a very low number of naturally occurring pyknotic cells were observed in the 15+48 hour control specimens. Cortical growth gradients still persisted in lateral to dorsal directions however, rostrocaudal gradients appeared less pronounced.

Those specimens irradiated on gestational day 15 and recovered 48 hours post-irradiation were indistinguishable from the corresponding controls. No differences were detected in terms of zonal organization, cell appearances, regionally estimated cell densities, mitotic activity, nor pyknotic cell frequency for any cortical area examined.

Figure 4-4b shows a normal dorsal segment of frontal cortex on gestational day 15+5 days (day 20). By gestational day 20, significant growth in thickness had occurred in both the cortical plate, and the intermediate zone, while the relative thicknesses of the subventricular and ventricular zones appeared reduced. The lateral to dorsal, as well as the rostrocaudal growth gradients of the developing cortical zones appeared to exist only for

the intermediate zone. Other developmental regions were subjectively assessed to be of almost equal size in both lateral to dorsal, and rostral to caudal directions.

The cytological constituents of the developmental cortical zones on this gestational day were similar to those described for the 15+48 hour specimens. Although lamination of the cortical plate had not yet commenced, cells of this region appeared to have assumed a radially oriented organization, much like the radial arrangement of cells seen in the ventricular zone of previous gestational stages. The small, spherical, dark-staining cells described previously were now quite numerous in the deeper regions of the cortical plate, and throughout the intermediate zone. The larger cells of the cortical plate (presumptive young neurons) were still homogeneous in appearance. However, they appeared to be slightly darker staining than they were at earlier gestational stages. This increase in staining intensity could be due to either an early maturation process, or an increase in the relative cell density of this region.

Mitotic figures appeared more abundant in the subventricular zones of these specimens, and an occasional mitotic figure was often observed in the intermediate zone. Mitosis at the juxtaluminal border of the ventricular zone was still evident, but at a lower rate than that seen at earlier gestational stages. As before, pyknotic figures were rarely seen in control specimens at this age, however,

when observed, cell death appeared to occur primarily in the intermediate and subventricular zones.

Like the gestational day 15+48 hour irradiated group, no differences existed between control and irradiated 15+5 day cortical specimens on microscopic evaluation. As differences in cortical thickness have been a reported postnatal outcome in other radiation studies, thickness measurements of the developmental zones and total thickness measurements were carried out according to the procedure outlined in Chapter 3.

Table 4-10 shows the significance values derived from the three-way analysis of variance done on these cortical samples. Several developmental trends are evident from this data. Factor C comparisons indicate that there are normally occurring significant differences between the thicknesses of the cortical plate vs the intermediate zone vs the subventricular zone vs the ventricular zone, and vs the zone total thicknesses within each cortical region. As indicated in Table 4-11, in frontal cortical areas, the intermediate zone measured as the largest zone in terms of relative thickness, followed by the cortical plate. Control measurements of frontal areas indicated a small size differential between subventricular and ventricular zones, however the ventricular zone appeared to be slightly larger in these samples.

Table 4-12 indicates a less pronounced thickness differential of zone measurements in the parietal cortical

region, compared to the frontal cortical region. Here, the intermediate zone was only slightly larger than the cortical plate. Again, subventricular thickness and ventricular thickness differences were small, with the subventricular zone measuring slightly more than the ventricular zone in control specimens for this cortical area.

As indicated in Table 4-13, thickness relationships of the individual occipital zonal areas were quite different. Here, the cortical plate was the largest, followed by the ventricular zone. The intermediate zone and subventricular zone in the occipital cortical region were almost equal in thickness.

Factor B comparisons revealed that there are normally occurring significant differences between the thickness measurements of frontal vs parietal vs occipital cortical areas. As shown in Tables 4-11, 4-12, and 4-13, a total thickness gradient does exist in decreasing fashion from frontal to occipital cortical areas. As would be expected therefore, Factor B x Factor C comparisons reveal naturally occurring significant differences between the zonal measurements of the three cortical regions. For individual zonal measurements, the most profound thickness differences appear to be between frontal and parietal cortical areas, with the frontal zone measurements being larger than the parietal zone measurements. From the parietal to occipital regions, a decreasing thickness gradient

appeared to only exist for the intermediate and possibly, the subventricular zones.

As indicated in Table 4-10, when all control and irradiated specimen measurements were compared (Factor A), significant differences existed. However, Factors AxB reveal that irradiation did not alter the normal total thickness relationships between frontal vs parietal vs occipital regions. As well, as indicated by Factor AxBxC comparisons, irradiation did not alter the normal individual zone size relationships between the three cortical regions. Rather, as deduced by the significance of AxC comparisons, irradiation appears to have altered the measurement of one or more zones, compared to its regionally comparable control counterpart, and thus, may have altered the normal relationship between zonal measurements within that particular region or regions. One-way analysis of variance comparisons were therefore made to further specify irradiation effects on cortical zone development.

Tables 4-11, 4-12, and 4-13 reveal that irradiated specimen measurements were generally slightly reduced for all compared zones with exception of the ventricular zones from all three regions, the cortical plate of the parietal region, and the intermediate zone for the occipital region. The only statistically significant differences found, however, were between the control and irradiated subventricular zones of frontal and parietal cortical regions. In both cases, the irradiated subventricular zones were thinner

(P is less than 0.001). In the case of the frontal cortex, the irradiation-induced reduction of the subventricular zone did not alter the size gradient order of cortical plate vs intermediate zone vs subventricular zone vs ventricular zone measures. In the case of the parietal cortex, the significant reduction of the subventricular zone rendered this zone the smallest of zones in the irradiated specimens; whereas, the ventricular zone is the smallest zone within controls for this particular cortical area.

In summary, although the cytology and spatial organization of the developing cerebral cortex appeared normal in specimens five days after a 50 rad (0.5 Gy) *in utero* radiation exposure, significant reductions in the thicknesses of both the frontal and parietal subventricular zones were revealed. There were no apparent effects on occipital cortical regions 5 days post-irradiation.

4.6.2. Main Olfactory Bulbs

Figure 4-5a shows a horizontally sectioned 15+4 hour control olfactory bulb. As in the developing cerebral cortex, a ventricular zone could be identified. The olfactory bulb ventricular zone was very similar in appearance to that of the cerebral cortex. Spherical to oval-shaped cells with pale-staining cytoplasm and small nuclei were radially arranged from the ventricular surface, and mitotically active cells could be observed at the juxtaventricular border.

Rostral to the ventricular zone in these sections, similarly appearing cells, organized in a more random pattern, could be seen. These cells were assumed to be early arising and migrating mitral and possibly, internal tufted cells, as these two cell types are apparently the first to arise within the main olfactory bulbs. As all of these cells were homogeneous in appearance at this developmental stage, it was impossible to differentiate between cell types in these sections. Some cells appeared to have reached the most superficial limits of the main olfactory bulbs; an area limited by what was assumed to be the primitive surrounding olfactory nerve fiber layer and adjacent mesenchyme.

On examination of several serial control sections, no growth gradients were revealed in terms of numbers of mitotic figures, nor relative cell distribution densities. As in the cerebral cortical regions, blood vessels containing nucleated fetal blood cells could be seen in the ventricular zone. Because of the relatively few pyknotic cells observed in control specimens, naturally occurring cell death was assumed to be low at this stage of development in the main olfactory bulbs.

Figures 4-5b and 4-5c show a typical section of the main olfactory bulb, 4 hours after a 50 rad (0.5 Gy) radiation exposure. Similar to the cortices of irradiated specimens, numerous pyknotic figures typified the main olfactory bulbs of all irradiated offspring. Pyknotic cells

appeared shrunken, and contained spherical or irregularly shaped homogeneously staining masses. As depicted in Figure 4-5b, cell shrinkage was quite severe in most samples of this brain region, to the extent that the radial arrangement of ventricular zone cells appeared disorganized. Pyknotic cells appeared to be most numerous in the ventricular zone substance and presumptive migration zone of the bulbs. Occasionally, pyknotic cells were seen in the superficial limits of the bulbs, yet rarely in the juxtaventricular, mitotically active area of the ventricular zone. Upon serial examination, it was concluded that distribution of pyknosis was equal throughout the main olfactory bulbs. The number of mitotic cells, which are limited to the juxtaluminal ventricular border at this stage of bulb development, were subjectively assessed as comparable in irradiated vs control specimens. The endothelial linings of bulb blood vessels appeared unaffected by radiation insult (Fig. 4-5c). As no macrophages were observed in irradiated bulb sections, it was assumed that debris clearance had not commenced by this post-irradiation interval.

Figure 4-6a, is a coronal section of a gestational day 15+48 hour (day 17) olfactory bulb from a control specimen. Considerable anatomical development had occurred in this brain region by this gestational stage. The glomerular, external plexiform, and mitral layers could be identified Fig. 4-6b).

Of all the cytological constituents of the main olfactory bulb on this gestational day, the post-migratory mitral cells could be the most easily identified due to their laminar location, and the fact that they appeared to have undergone some maturation, making them distinguishable from neighbouring cells (Fig. 4-6b). Post-migratory mitral cells appeared "bubble-like", in that they were quite spherical in shape, had paler-staining cytoplasm, with darker-staining cell membranes, compared with neighbouring cells. At this stage, no spatial organization appeared to exist for the cells of the mitral layer.

Other than in the juxtaventricular border of the olfactory ventricular zone, few mitotic figures were evident in other olfactory bulb regions. When occasionally present in other regions, mitotic cells were only observed in the glomerular layer.

When examining irradiated olfactory bulb sections of 15+48 hour specimens, all but 2 of the 13 specimens examined were indistinguishable from controls. Figure 4-6c represents one of the specimens deemed different from controls. In this, and the other anomalous specimen, many of the cells of the mitral cell layer did not have their characteristic "bubble-like"appearance, and instead, appeared to be shrunken and/or irregularly shaped, and considerably darker staining than control mitral cells. Consequently, mitral cell layers in these specimens appeared thinner than controls. These observations were consistent throughout

the rostrocaudal extent of the affected olfactory bulb specimens. As cell counts of mitral cells were not conducted at this post-irradiation interval, it could not be determined as to whether the perceived reduction of mitral layer thickness was due to a reduction of mitral cell numbers, or shrinkage of cells.

Besides these mitral cell changes seen in the 15+48 hour irradiated specimens, no other radiation-induced effects were observed in terms of relative cell densities, mitotic activity, laminar organization, or cell pyknosis. Although mitral layer changes observed were assumed to constitute an irradiation effect, chi-square analysis of 2 anomalous finding out of 13 irradiated specimens, as compared with 13 controls, was not statistically significant.

As was shown in Figure 3-1, the gestational 15+5 day (day 20) main olfactory bulb had essentially reached its definitive adult form, although not all cytological constituents (ie. granule cells) had arisen by this gestational day. Laminar organization was more distinctive at this gestational age as compared with earlier stages, and the internal plexiform layer could be identified.

Within the glomerular layer, 3 different cell types could be distinguished, based on their size, shape, and staining propensity (Fig. 4-7a). These cells were assumed to be the various tufted and glial cells known to exist within the glomerular layer. The same types of cells were observed in the fiber-rich external plexiform layer. These

cells could be either cells specific to this laminar location, or cells in migration to more superficial areas of the main olfactory bulb.

The mitral cell layer appeared much more compact and thicker than earlier gestational stages. Mitral cells still appeared "bubble-like" but were larger in size than the 15+48 hour cells. Small, spherical dark-staining cells were also observed in the mitral layer, and likely represented migratory cells of more superficial layers. Deep to the mitral layer, an internal plexiform layer could be identified. All cells deep to the internal plexiform layer, which likely represented proliferative and migrating constituents of the olfactory bulb, included the large pale-staining, and small spherical dark-staining cells similar to the migrating and proliferative zones of the cerebral cortex.

The mitotic activity at the juxtaventricular border of the olfactory ventricular zone appeared decreased from that at earlier stages. The only other mitotic figures apparent in these control sections, appeared in the glomerular layer and surrounding mesenchymal areas.

Out of 15 irradiated specimens assessed at this post-irradiation interval, four specimens were deemed qualitatively different than controls. Two of the four specimens affected were considered severe, due to the smaller gross size of these specimens and the strikingly decreased cell densities of essentially all the layers examined. (It should be noted that in these two specimens, overall

brain size was visibly smaller when compared to controls. The reduced size of the olfactory bulbs appeared proportional to the size of other brain regions in these irradiated specimens.) Figure 4-7b represents one of these severely affected specimens.

As can be seen in comparison with the non-irradiated control section (Fig. 4-7a), cell density appeared to be decreased in glomerular, external plexiform, mitral, internal plexiform, and migratory layers. The specific types of cells deficient in the glomerular, external, and internal plexiform layers was not assessed. Mitral cells of the mitral cell layer showed an obvious depletion in these specimens, compared with controls. As well, most of the cells in this layer appeared shrunken, irregularly shaped, and very dark staining; and they did not possess the characteristic appearance of control mitral cells. Although not evident in these figures, the proliferative ventricular zone appeared less affected, as cell density of this zone was comparable to controls, although somewhat smaller in overall size. Mitotic activity of these irradiated specimens appeared comparable to that of controls.

In the two more subtle of the affected irradiated specimens, the only qualitative difference appeared in the mitral cell layer. Mitral cell layers of these two specimens appeared normal for the most part, however, they contained multiple regions where the mitral cell density was low, and cells were shrunken, and dark-staining, much

like those seen throughout the mitral layers of the more severely affected specimens. These regional deficits were not consistently seen within any specific ventral, dorsal, medial, or lateral region of the mitral cell layer yet, deficits could be observed for some rostral to caudal distance in both of these affected specimens.

Chi-square comparisons of 4 affected out of 15 irradiated vs 16 control specimens proved to be significant at a P value of less than 0.05.

As t-test comparisons require that a group n value be greater than two, mitral cell counts on the 4 affected specimens were pooled, and compared with 4 similar-aged controls, utilizing the procedure outlined in Chapter 3. A significant difference (P was less than 0.05) was found between the number of mitral cells counted in control as compared to irradiated specimens. The mean number of cells and standard error of the mean in the control group was 40.8 $\pm$ 2.75, whereas in irradiated brains it was 27.5 $\pm$ 6.86. It is interesting to note that in the two severely affected specimens, the average number of mitral cells counted was 22; just slightly larger than half of the normal compliment of mitral cells for this 20x80 micrometer areas. The average cell count for the subtly affected specimens was 33, which constituted an approximate 18% reduction of mitral cells.

4.6.3. Corpus Callosum

Figure 4-8 shows the normal crossing of the genu

of the corpus callosum in a control, gestational day 15+5 (day 20) specimen. The most rostral point of crossing of the prenatal corpus callosum in the rat normally can be seen to occur at the level of the septal area, where the medial forebrain bundle and external capsule can be clearly distinguished (approximately 225 microns from the most rostral tip of the fetal rat brain). Caudally, the corpus callosum at this gestational age becomes progressively thinner, and appears to mesh with the fibers of the fornix. Upon microscopic evaluation of the midsagittal corpus callosum, it appeared that as well as a rostrocaudal thickness gradient, there was also a ventral to dorsal gradient in terms of fiber packing density. Ventral portions of the midsagittal area of the commissure appeared tightly packed, while fibers had a looser, lower density appearance in the more dorsal region.

In the midsagittal region, two different cell types were observed throughout its rostral to caudal depth. These cell types included the small, spherical, dark-staining cells seen and previously noted in both cortical and olfactory bulb regions, as well as thin, oval shaped cells, with pale-staining cytoplasm. Although the exact identities of these cell types could not be determined with certainty, it was assumed that they represented migrating neuronal, and glial elements.

As seen in Figure 4-8, a band of densely packed cells extend from the medial cortical ventricular zone,

and lie against the ventral border of the trunk of the corpus callosum. This band, which was thicker in lateral regions and tapering in thickness midsagittally, was composed of round to oval shaped cells, with pale-staining cytoplasm and small nuclei, similar in appearance to the cells of the cortical ventricular zone. Occasionally, pyknotic cells were seen within this band, although no consistent patterns of pyknotic cell distribution could be determined. As this band of cells was seen throughout the rostral to caudal extent of the crossing corpus callosum, it was assumed to be the "glial sling", which is thought to guide callosal fibers across the midsagittal region.

Following examination of 15 irradiated and 16 control specimens throughout the rostral to caudal extent of the crossing corpus callosum, it was found that the irradiated specimens were indistinguishable from controls. All specimens were qualitatively assessed in terms of relationships to anatomical landmarks, relative thickness, as well as both fiber, and cell densities. No differences were noted in terms of the appearance or distribution densities of the glial elements constituting the "glial sling".

Of these specimens examined, 10 control and 10 irradiated brains, which appeared similar in relative overall size, were selected to measure the rostrocaudal extent of corpus callosum crossing. Student t-test comparisons revealed no significant differences in crossing length,

with control mean lengths ± S.E.M. equalling 310.3 ± 40.9 microns, and irradiated mean lengths equalling 308.8 ± 36.8 microns.

4.6.4. Hippocampal Formation

Figures 4-9 a, b, and c, represent the prenatal rat hippocampal formation at gestational days 15+4 hours, 15+48 hours (day 17), and 15+5 days (day 20), respectively. All levels of section in these figures were in, or slightly caudal to the interventricular foramen region.

The gestational day 15+4 hour hippocampal formation (Figures 4-9a, 4-10a, and 4-11a), was primarily composed of a large ventricular zone. The ventricular zone of this region was cytologically very similar to that seen in cerebral cortical regions, although the relative cell packing density and thickness of this region appeared to decrease from a dorsal (subicular) to ventral direction. Cells were identical in appearance to those in the ventricular zones of regions previously described. They possessed a radial arrangement with mitotically active cells located along the juxtaventricular border.

Moving medially to more superficial regions of the primordial hippocampal formation, a fiber rich zone, continuous with the cerebral marginal zone could be seen. Within this region, there were a few randomly distributed cells which appear homogeneous, compared with the ventricular zone cells. These cells probably represented (in a dorsal to ventral direction) the early arising deep pyramidal

neurons of the subiculum, the large neurons of Ammon's horn, and the large neurons of the dentate gyrus. This so-called marginal zone of the hippocampal formation was limited medially by a mesenchymal region which separated the hippocampus from the ventricular zone of the third ventricle. This bordering area was rich in large blood vessels containing nucleated fetal blood cells.

Figures 4-10b and 4-11b, demonstrate a typical irradiated hippocampal formation at the gestational 15+4 hour post-irradiation interval. Like other regions of the brain examined at this post-irradiation interval, pyknotic figures were observed in all irradiated specimens. Pyknotic cells were characterized by shrunken cells, containing circular or irregularly shaped homogeneous masses. Unlike other brain regions however, pyknotic cell density in the hippocampal formation showed regional variation (Fig. 4-10b). The highest rate of pyknotic figures were observed in subicular regions with a progressive decline in pyknotic cell numbers in ventral directions. The most ventral regions of the hippocampal formation (presumptive proliferative zone of the dentate gyrus) rarely contained a pyknotic figure in these irradiated samples. In regions where pyknotic figures were present, they were restricted to the substance and superficial regions of the venticular zone. Pyknotic cells were never observed in either the juxtaventricular mitotically active area or in the marginal zones. These trends of pyknotic cell distribution existed for the

rostrocaudal extent of the hippocampal formation.

Figure 4-11b demonstrates two other features of the irradiated 15+4 hour hippocampal formation not seen in the other irradiated brain regions examined. First, a demonstrable decline in the number of mitotic figures was present in all irradiated specimens as compared to controls. This was true throughout the rostrocaudal extent of subicular, Ammon's horn, and dentate gyrus ventricular zones. Second, particularly in the region of Ammon's horn, small dark-staining flecks assessed to be cytoplasmic inclusions were also observed. There was no evidence of damage to endothelial cells in these irradiated samples, nor was there evidence of phagocytotic activity at this post-irradiation interval.

Figure 4-9b shows the normal developmental appearance of the gestational day 15+48 hour (day 17) rat hippocampal formation. The subicular region was more easily differentiated from Ammon's horn at this gestational age due to the presence of a well defined subicular pyramidal layer. As well, the dentate gyrus was just beginning to be visibly discernible. Between the dentate gyrus and the ventricular zone lies a zone of randomly distributed, homogeneous appearing cells. The cells of this zone were very similar in appearance to the cells of the ventricular zone. However, the cell density of this zone was less than that observed in the ventricular zone. These cells were assumed to be large undifferentiated neurons of strata

oriens, strata radiatum, and lacunosum-moleculare. Mitotic activity of the ventricular zone appeared to be restricted to localized regions in the hippocampal formation at this age, although the pattern of these regions was not established in this study. The control incidence of pyknotic cells was low for all hippocampal regions at this gestational stage.

One 15+48 hour control specimen did appear underdeveloped in that the zone of undifferentiated large neurons was visibly thinner, and the overall size of the hippocampal formation was reduced relative to other brain regions in this specimen and, as compared to other controls. With exception to this one anomalous control, no qualitative differences in the overall morphology, mitotic activity, cell appearances, or cell densities existed between the control and irradiated 15+48 hour hippocampal formation specimens.

Figure 4-9c shows the hippocampal formation of a 15+5 day control specimen. Considerable morphological changes have occurred by this gestational stage, however, the full adult configuration has not been achieved. The ventricular zone was somewhat attenuated, although the number of mitotic cells at the juxtaventricular border appeared to be the same as previous gestational stages.

Due to the well defined pyramidal layer of Ammon's horn which is continuous with the subicular pyramidal layer, the other laminae of the hippocampus could be identified.

The strata oriens, which lies between the ventricular zone and pyramidal cell layer, consisted of numerous, varying sized cells randomly distributed within a fiber-like meshwork. These cells likely represented the undifferentiated polymorphic cells of this region while the fibrous component of this layer probably consisted of the axon branches of these cells to the molecular layer and the alveus (alveus= a fiber tract more visible at later developmental stages).

Between the pyramidal layer and the dentate gyrus, the molecular layer could be seen. At this stage of development this region was primarily composed of undifferentiated, homogeneous appearing cells. In the adult rat, the molecular layer is much more fibrous in appearance as it contains numerous collaterals and dendritic branches from the pyramidal layer and other hippocampal regions. In the adult rat three strata can be identified. From the outermost region to the pyramidal layer these include the strata moleculare, the strata lacunosum, and strata radiatum. As depicted in Figure 4-9c, the entire region has been labelled as the lacunosum-moleculare, because in the adult, these two strata contain the majority of cells for the molecular layer.

At this stage of development, the dentate gyrus was clearly defined although the laminar pattern characteristic of this region had not yet developed. Cells of the dentate layer were similar to those seen in the molecular layer. The fimbria had also grown considerably at this gestational

stage. In coronal section, fibers appeared horizontally oriented, with a few circular and horizontally oriented cells dispersed between the fibers.

As with the 15+48 hour irradiated group, no differences were observed between the control and irradiated hippocampal formation specimens at the 15+5 day post-irradiation interval.

4.6.5. Cerebellum

Figures 4-12a, b, and c, depict the developing rat cerebellum at gestational day 15+4 hours, 15+48 hours (day 17), and 15+5 days (day 20) respectively.

Five distinct zones could be recognized in the 15+4 hour cerebellum. They included the superficial fiber layer, the nuclear zone, the transitional zone, the intermediate fiber layer, and the cerebellar neuroepithelium (Figs.4-12a and 4-13a). Cells of the cerebellar neuroepithelium were identical in appearance to the proliferative zone cells (ventricular zones) of other brain regions previously described. A radial organization of these cells was also evident, with mitotically active cells lining the juxtaluminal border of this zone. Mitosis appeared to be limited to this region of the cerebellum at this gestational stage. Cells of the nuclear zone and the transitional zone were indistinguishable in appearance from the cerebellar neuroepithelial cells, indicating that no differentiation had occurred by this gestational stage. Blood vessels appeared to be limited to the neuroepithelial layer of the cerebellar

primordium.

In all 15+4 hour irradiated specimens, numerous pyknotic cells were observed in the neuroepithelial region, while a few were observed in transitional and nuclear zones (Figs. 4-13b and c). In the neuroepithelial zone, pyknotic cells occurred in regions superficial to the mitotically active luminal border, and occurred most numerously in the lateral extensions of the cerebellar plate. This pattern was relatively consistent throughout the rostrocaudal length of the cerebellum. In the transitional and nuclear zones, no particular pattern of distribution existed. Mitotic activity appeared preserved in these irradiated specimens and, as indicated in Figure 4-13c, blood vessels appeared intact. Like other irradiated brain regions studied at this post-irradiation interval, no evidence of debris clearance was evident.

The 15+48 hour control cerebellum is shown in Figure 4-12b. This particular section shows the lateral limits of the germinal trigone, and the developing external germinal layer arising from the trigone. Other than mitotic cells, cells of the germinal trigone were indistinguishable in appearance from the cells of the attenuated cerebellar neuroepithelium. Very little mitotic activity was apparent in the cerebellar neuroepithelium at this time. Due to the compact, dark-staining nature of the external germinal layer, it could not be determined as to whether mitotic activity was occurring in this layer.

The Purkinje cell layer was recognized at this gestational stage, as a band of slightly higher density cells; they were indistinguishable in appearance from other cells in of the cerebellum at this time. The presumptive molecular layer (Fig. 4-12b) could only be observed in caudal regions of the cerebellum on gestational day 17.

By gestational day 15+5 days (day 20), the external germinal layer could be seen throughout the rostrocaudal extent of the cerebellum. The cerebellar epithelium had regressed to a few cells in thickness. Differentiation of cells within the substance of the cerebellum had not commenced, however, the Purkinje cell layer and cerebellar nuclei of the nuclear zone could be identified by their density patterns.

For both 15+48 hour and 15+5 day post-irradiation cerebellar sections, no qualitative differences from control specimens were found.

4.7. GROWTH AND HISTOLOGICAL EVALUATION OF PLACENTAL TISSUE

Table 4-14 shows the mean weights $\pm$ S.E.M. of placentas recovered from each post-irradiation group as compared with controls. As the table reveals, in the 15+4 hour groups, irradiated placentas had a significantly higher mean weight than the controls (P is less than 0.05). However, by the 48 hour post-irradiation interval, irradiated placentas weighed significantly less than controls (P is less than 0.001). By the 5 day post-irradiation interval,

differences in the mean weights between control and irradiated placentas no longer existed.

Figure 4-14a shows the normal appearance of the chorionic plate and labyrinthine zone of the 15+4 hour placenta. Fetal chorionic villi containing fetal blood could be seen arising from the chorionic plate, and penetrating into the labyrinthine zone. Within the labyrinthine zone, the trophoblastic layers of the fetal blood villi could be seen separating the fetal from the maternal blood channels. At this gestational stage, fetal red blood cells are nucleated and therefore, could be easily differentiated from maternal blood cells (Fig. 4-15a).

Figure 4-16a shows the remainder of the maternal side of the gestational day 15+4 hour control placenta which includes the basal zone and the decidua basalis. At this gestational stage numerous glycogen cells could be seen in the basal zone. As well, cytotrophoblastic (basophilic) cells could be seen dispersed throughout this zone, sometimes surrounding maternal blood pools. Giant cells typically formed a row separating the basal zone from the decidua basalis. However, in some controls they could also be seen dispersed within other regions of the basal zone. The decidua basalis was relatively thick at this gestational stage.

On examination of irradiated placentas of the 15+4 hour post-irradiation interval, 9 out of 10 placentas were considered to be qualitatively different from the

controls (P is less than 0.001 with chi-square comparison). These irradiated specimens typically demonstrated large gaps or spaces in the labyrinthine and basal zones (Figs. 4-14 and 4-16). Higher magnification views of the labyrinthine zones of these irradiated placentas (Fig. 4-15) revealed that the anomalous spaces were in fact, enlarged maternal blood channels. The enlarged channels were filled with a light-pink staining acellular substance. Maternal red blood cells could also be seen in these channels; however, they did not appear more numerous than in control maternal channels. The trophoblastic cells separating these enlarged maternal channels from fetal blood channels did not appear qualitatively different from controls. No changes in pyknotic cell frequencies or mitotic activity were evident.

In the basal zones irradiation-induced spaces were also filled with pale pink-staining acellular substance (Fig. 4-16b). As non-nucleated blood cells were also seen in these spaces, they were assumed to represent maternal blood pools. In some cases of irradiation-induced basal zone changes, the cytological organization of this zone appeared disturbed (Fig. 4-16b). However, due to the naturally random appearance of cells distributed in this zone as seen in some control specimens, it could not be determined as to whether cell depletion had occurred for either giant, glycogen, or cytotrophoblastic (basophilic) cells. Pyknosis was not a feature of this zone in irradiated specimens. The chorionic plate and decidua basalis was

indistinguishable in the placentas as compared with controls.

Figures 4-17a and b depict the normal morphological appearance of the gestational day 15+48 hour placentas. Figure 4-17a shows a portion of the chorionic plate, and the large labyrinthine zone characteristic of this gestational age. Figure 4-17b shows the basal zone and the attenuated decidua basalis. The glycogen cells of the basal zone on gestational day 17 tended to be arranged in small discrete islands, and the normal age-related degeneration of these cells could be seen.

Upon assessment of the gestational day 15+48 hour irradiated placentas, a subtle but statistically significant difference was observed in 6 irradiated placentas as compared to controls (P is less than 0.005 with chi-square comparison). As depicted in Figure 4-17c, small multiple areas of labyrinthine trophoblast showed differences in staining propensity. These areas stained a purplish-pink color instead of the characteristic blue stain of these cells seen in unaffected regions of the labyrinthine zone of the same specimens, and age-related control specimens. In these 6 affected placentas, areas of altered staining propensity most often appeared in the area of labyrinth close to the chorionic plate. No other qualitative differences existed in irradiated placentas of the 15+48 hour group.

The fetal side of the normal gestational day 15+5 day (day 20) placenta is depicted in Figure 4-18a, while the maternal side is shown in Figure 4-18b. The

labyrinthine zone was considerably larger than it was at earlier gestational ages. More giant cells could be seen in this zone at this time. In the basal zone, further degeneration of the glycogen cells pools could be observed. The decidua basalis was quite thin in many control specimens of this age group, and some small glycogen cell islands could be seen occasionally in this zone.

No qualitative differences were observed between control and irradiated placentas in the 15+5 day groups.

Table 4-1: **BODY WEIGHTS OF PREGNANT RATS IRRADIATED ON GESTATIONAL DAY 15 AND KILLED 5 DAYS POST-IRRADIATION**

	GESTATIONAL DAY 1	GESTATIONAL DAY 15	GESTATIONAL DAY 20
CONTROL (n = 11)	247.3 ± 5.1*	303.2 ± 5.9	357.1 ± 8.0
IRRADIATED (n = 10)	248.0 ± 12.1	306.4 ± 10.6	361.9 ± 10.0

* Mean ± S.E.M.

Student t-test comparisons. No significant differences between irradiated groups and controls.

Table 4-2: **BODY WEIGHTS OF PREGNANT RATS IRRADIATED ON GESTATIONAL DAY 15 AND KILLED 48 HOURS POST-IRRADIATION**

	GESTATIONAL DAY 1	GESTATIONAL DAY 15	GESTATIONAL DAY 17
CONTROL (n = 10)	248.3 ± 10.7*	307.4 ± 10.5	323.1 ± 10.2
IRRADIATED (n = 10)	238.1 ± 8.1	287.5 ± 6.9	300.1 ± 6.4

* Mean ± S.E.M.

Student t-test comparisons. No significant differences between irradiated groups and controls.

Table 4-3: **BODY WEIGHTS OF PREGNANT RATS IRRADIATED ON GESTATIONAL DAY 15 AND KILLED 4 HOURS POST-IRRADIATION**

	GESTATIONAL DAY 1	GESTATIONAL DAY 15
CONTROL (n = 10)	234.8 ± 4.7*	295.6 ± 7.0
IRRADIATED (n = 10)	243.6 ± 7.1	303.9 ± 6.1

* Mean ± S.E.M.

Student t-test comparisons. No significant differences between irradiated groups and controls.

Table 4-4: **LITTER SIZE AND LITTER MORTALITY OF PREGNANT RATS IRRADIATED ON GESTATIONAL DAY 15 AND KILLED 5 DAYS POST-IRRADIATION**

	VIABLE FETUSES/ LITTER	TOTAL NUMBER OF RESORPTIONS/GROUP	TOTAL NUMBER OF DEAD FETUSES/GROUP
CONTROL	12.9 ± 0.8* (n = 11)	15 (n = 142)	N/A (n = 142)
IRRADIATED	13.5 ± 0.6 (n = 10)	13 (n = 135)	N/A (n = 135)

* Mean ± S.E.M.

Student t-test comparisons for number of viable fetuses/litter.

Chi-square comparisons for total number of resorptions and dead fetuses/group.

No significant differences between the irradiated groups and the controls.

Table 4-5: **LITTER SIZE AND LITTER MORTALITY OF PREGNANT RATS IRRADIATED ON GESTATIONAL DAY 15 AND KILLED 48 HOURS POST-IRRADIATION**

	VIABLE FETUSES/ LITTER	TOTAL NUMBER OF RESORPTIONS/GROUP	TOTAL NUMBER OF DEAD FETUSES/GROUP
CONTROL	14.9 ± 0.7* (n = 10)	6 (n = 149)	N/A (n = 149)
IRRADIATED	14.7 ± 0.6 (n = 10)	8 (n = 147)	1 (n = 147)

* Mean ± S.E.M.

Student t-test comparisons for number of viable fetuses/litter.

Chi-square comparisons for total number of resorptions and dead fetuses/group.

No significant differences between the irradiated groups and the controls.

Table 4-6: **LITTER SIZE AND LITTER MORTALITY OF PREGNANT RATS IRRADIATED ON GESTATIONAL DAY 15 AND KILLED 4 HOURS POST-IRRADIATION**

	VIABLE FETUSES/ LITTER	TOTAL NUMBER OF RESORPTIONS/GROUP	TOTAL NUMBER OF DEAD FETUSES/GROUP
CONTROL	14.0 ± 1.1* (n = 10)	7 (n = 140)	1 (n = 140)
IRRADIATED	14.9 ± 0.6 (n = 10)	12 (n = 149)	N/A (n = 149)

* Mean ± S.E.M.

Student t-test comparisons for number of viable fetuses/litter.

Chi-square comparisons for total number of resorptions and dead fetuses/group.

No significant differences between the irradiated groups and the controls.

Table 4-7: **WEIGHTS OF FETUSES IRRADIATED ON GESTATIONAL DAY 15 AND RECOVERED 4 HOURS, 48 HOURS, AND 5 DAYS POST-IRRADIATION**

	FETAL WEIGHTS (g)		
	15+4 HOURS	15+48 HOURS	15+5 DAYS
CONTROL	0.22 ± 0.005* (n = 140)	0.54 ± 0.004 (n = 149)	2.41 ± 0.04 (n = 142)
IRRADIATED	0.22 ± 0.002 (n = 149)	0.49 ± 0.003** (n = 147)	2.26 ± 0.02** (n = 135)

* Mean ± S.E.M.

Student t-test comparisons. ** Significantly different from controls (P is less than 0.001).

Table 4-8: **CROWN-RUMP LENGTHS OF FETUSES IRRADIATED ON GESTATIONAL DAY 15 AND RECOVERED 4 HOURS, AND 48 HOURS POST-IRRADIATION**

	CROWN-RUMP LENGTHS (mm)	
	15+4 HOURS	15+48 HOURS
CONTROL	10.54 ± 0.074* (n = 125)	14.44 ± 0.048 (n = 132)
IRRADIATED	10.36 ± 0.040** (n = 149)	14.02 ± 0.046*** (n = 147)

* Mean ± S.E.M.

Student t-test comparisons. ** Significantly different from controls (P is less than 0.05).

*** Significantly different from controls (P is less than 0.001).

Figure 4-1: The normal external morphological appearance of the rat fetus on (a) gestational day 15+5 days (day 20); (b) gestational day 15+48 hours (day 17); (c) gestational day 15+4 hours.

(x2.3)

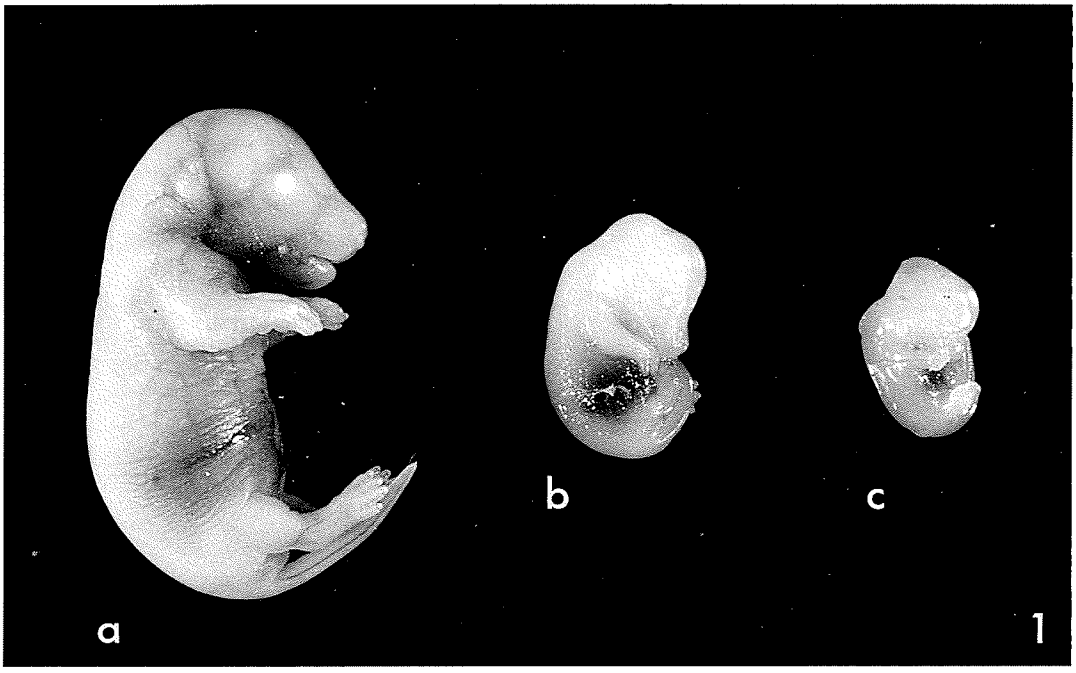
a
b
c
1

Table 4-9: **GROSS MORPHOLOGICAL DEFECTS OF FETUSES IRRADIATED ON GESTATIONAL DAY 15 AND RECOVERED 4 HOURS, 48 HOURS, AND 5 DAYS POST-IRRADIATION**

DEFECTS	15+4 HOUR CONTROL (n = 140)	15+4 HOUR IRRADIATED (n = 149)	15+48 HOUR CONTROL (n = 149)	15+48 HOUR IRRADIATED (n = 147)	15+5 DAY CONTROL (n = 142)	15+5 DAY IRRADIATED (n = 135)
PARTIAL EXENCEPHALY	3*	2	3	4	-	-
PAW DEFORMITIES	1	-	1	1	-	-
MICROPTHALMIA	-	1	-	-	-	-
ANOPTHALMIA	-	-	1	3	-	-
EVENTRATION OF THE LIVER	-	-	1	-	-	-
CLEFT LIP AND PALATE	-	-	-	-	1	-
CLEFT PALATE ONLY	-	-	-	-	1	-
SCOLIOSIS	-	-	-	-	1	-
EYELID MALFORMATIONS	-	-	-	-	-	2
EVENTRATION OF ABDOMINAL VISCERA	-	-	-	-	-	1

* Frequency of defect per group.

Chi-square comparisons. No significant differences between the irradiated groups and the controls.

Figure 4-2: Coronal sections through the dorsal areas of the frontal cerebral cortices from gestational day 15+4 hour fetuses.

a) Control cerebral cortex.
Epon embedded; methylene blue - azure II stain.
(x382.8)

b) Irradiated cerebral cortex showing numerous pyknotic cells.
Epon embedded; methylene blue - azure II stain.
(x382.8)

Marginal zone (mz); ventricular zone (vz); lateral ventricle (v).

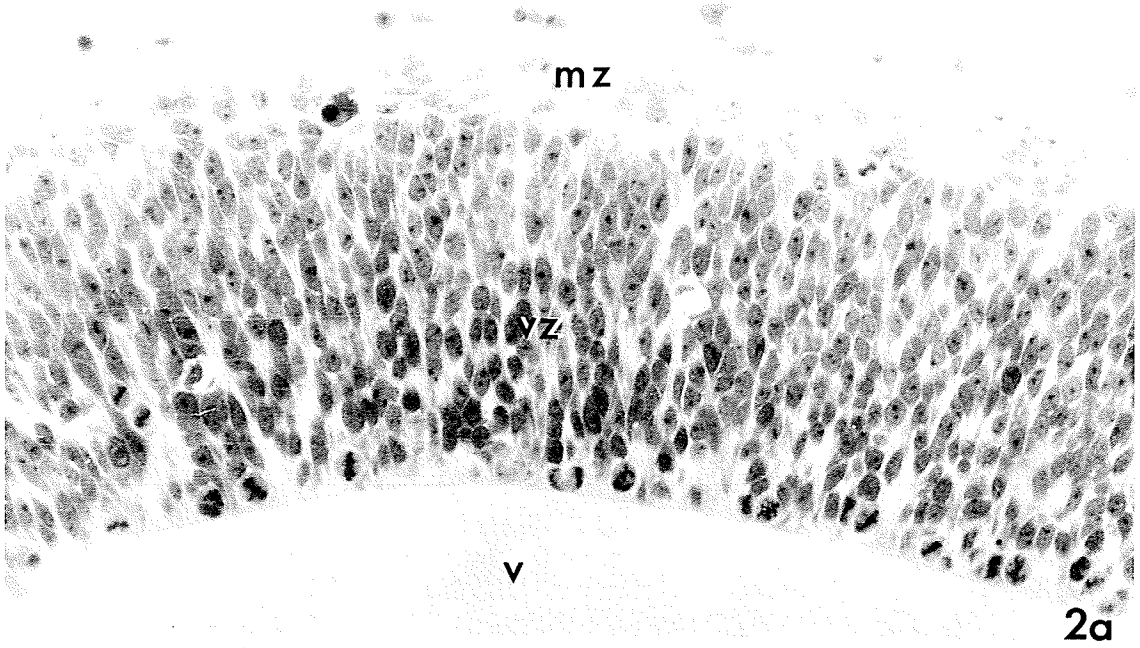

2a

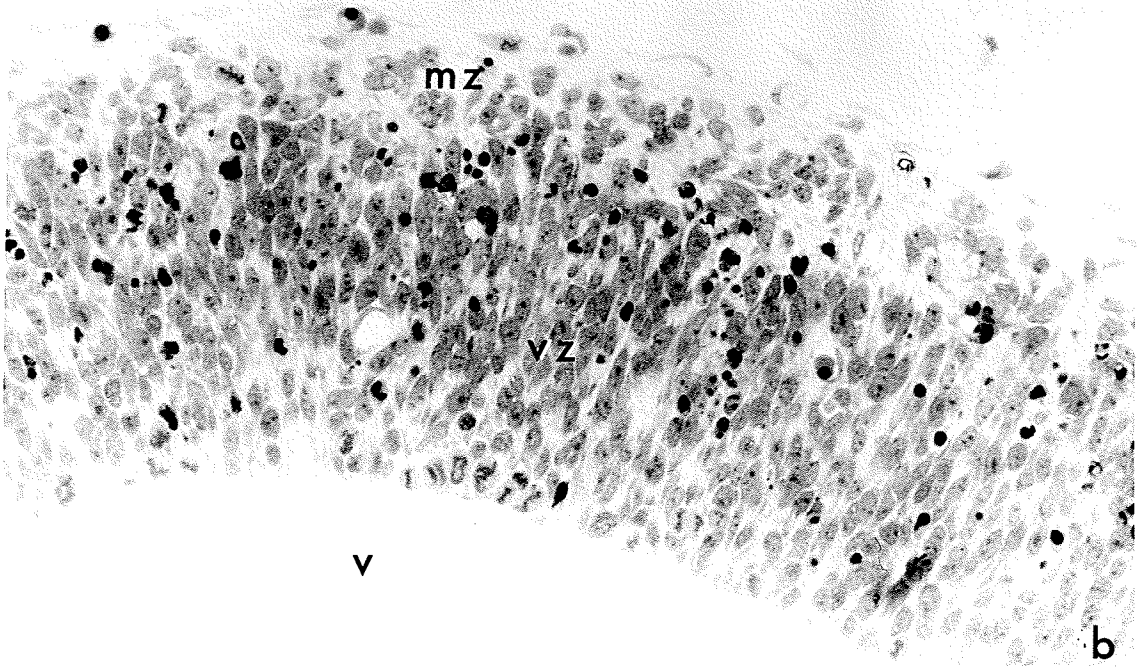

b

Figure 4-3: Higher magnifications of the dorsal cerebral cortices shown in Figure 4-2.

a) Control 15+4 hour cerebral cortex shown in Figure 4-2a. (x686.4)

b) Irradiated 15+4 hour cerebral cortex shown in Figure 4-2b. (x686.4)

Arrows indicate intact blood vessels. Marginal zone (mz); ventricular zone (vz).

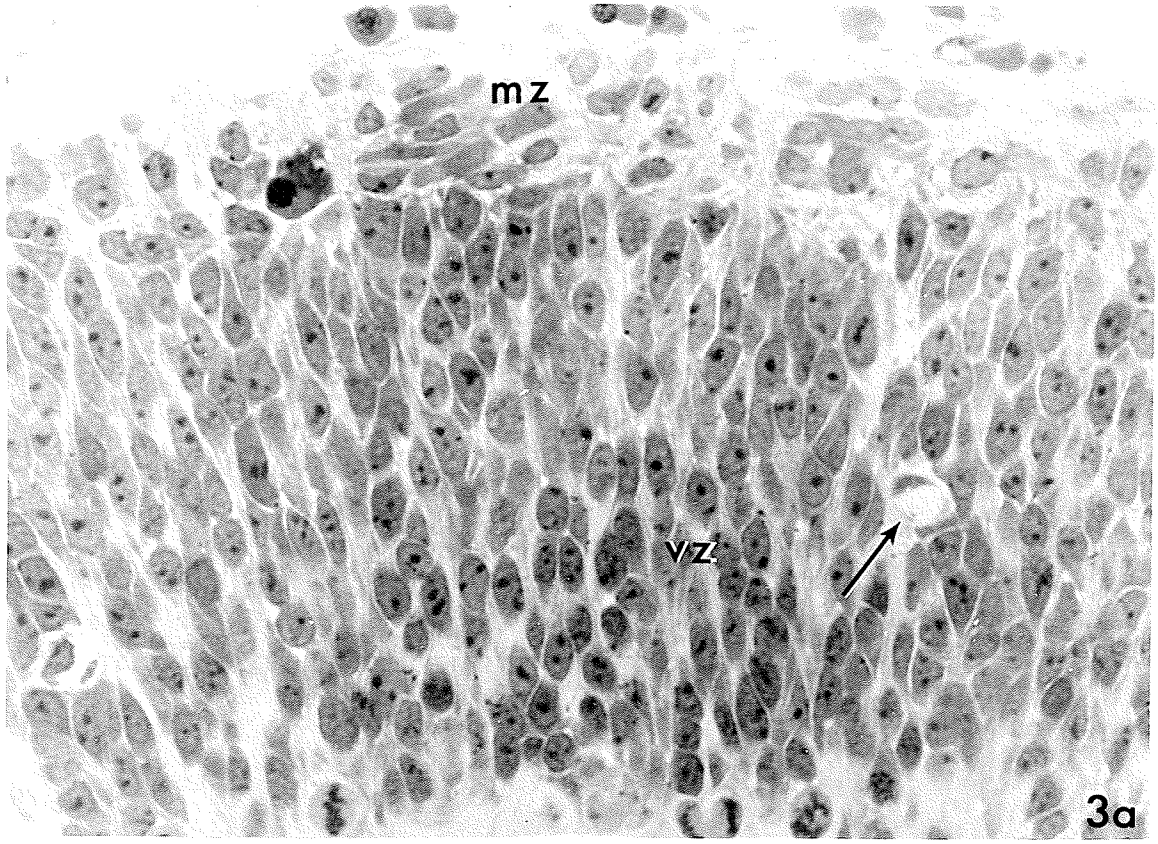
mz
vz
3a

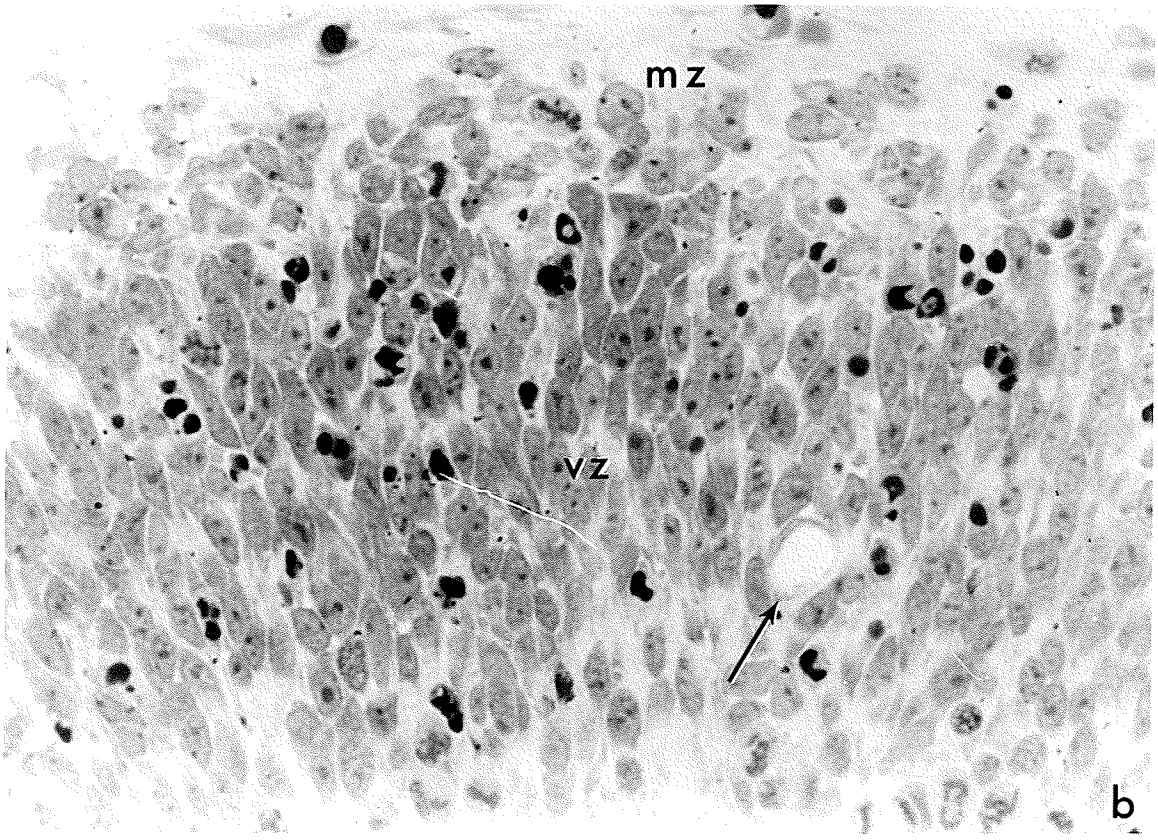
mz
vz
b

Figure 4-4: A coronal section through the dorsal area of the frontal cerebral cortex from:

(a) a gestational day 15+48 hour (day 17) control fetus.
Epon embedded; methylene blue - azure II stain.
(x171.6)

(b) a gestational day 15+5 days (day 20) control fetus.
Paraffin embedded; thionin stain.
(x68.6)

Marginal zone (mz); cortical plate (cp); intermediate zone (iz); subventricular zone (sz); ventricular zone (vz); lateral ventricle (v).

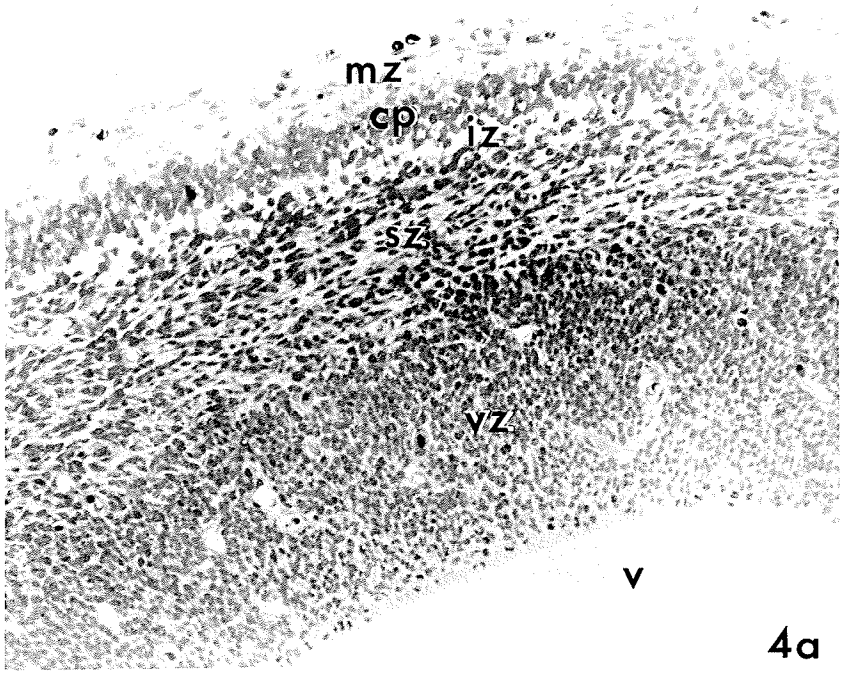

4a

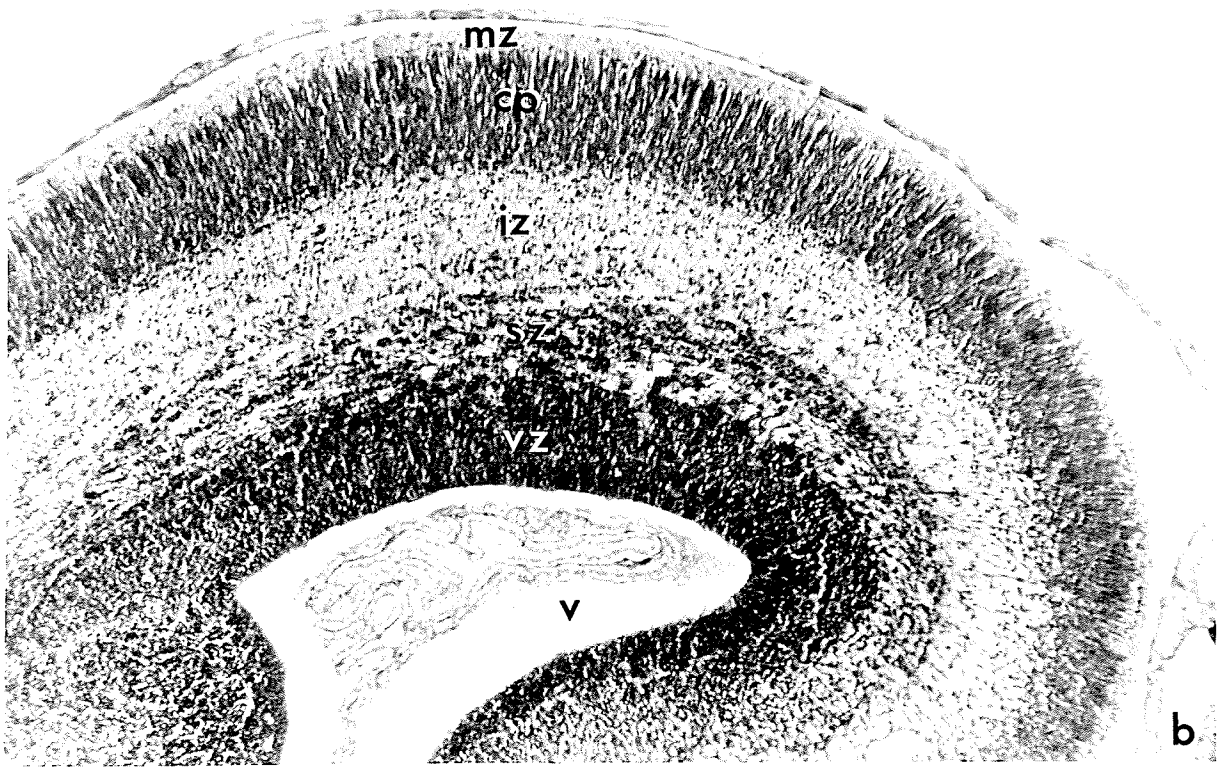

b

Table 4-10: **THREE-WAY ANALYSIS OF VARIANCE ON CORTICAL MEASUREMENTS OF FETUSES IRRADIATED ON GESTATIONAL DAY 15 AND RECOVERED 5 DAYS POST-IRRADIATION**

FACTOR COMBINATIONS	P VALUE
FACTOR A = control X experimental	P = 0.0006*
FACTOR B = frontal X parietal X occipital	P = 0.0000*
FACTOR C = cortical plate X intermediate zone X subventricular zone X ventricular zone X total	P = 0.0000*
A x B	P = 0.2251
A x C	P = 0.0076*
B x C	P = 0.0000*
A x B x C	P = 0.8914

* Significant differences exist between factor parameters.

Table 4-11: **THICKNESS MEASUREMENTS OF FRONTAL CORTICAL ZONES OF FETUSES IRRADIATED ON GESTATIONAL DAY 15 AND RECOVERED 5 DAYS POST-IRRADIATION**

	CORTICAL PLATE (mm)	INTERMEDIATE ZONE	SUBVENTRICULAR ZONE	VENTRICULAR ZONE	TOTAL
CONTROL (n = 5)	0.083 ± .003*	0.096 ± .005	0.073 ± .002	0.077 ± .002	0.325 ± .006
IRRADIATED (n = 9)	0.078 ± .002	0.091 ± .004	0.060 ± .001**	0.079 ± .002	0.309 ± .007

* Mean ± S.E.M.

One-way ANOVA comparisons. ** Significantly different from controls (P is less than .001).

Table 4-12: **THICKNESS MEASUREMENTS OF PARIETAL CORTICAL ZONES OF FETUSES IRRADIATED ON GESTATIONAL DAY 15 AND RECOVERED 5 DAYS POST-IRRADIATION**

	CORTICAL PLATE (mm)	INTERMEDIATE ZONE	SUBVENTRICULAR ZONE	VENTRICULAR ZONE	TOTAL
CONTROL (n = 7)	0.074 ± .002*	0.077 ± .003	0.067 ± .002	0.064 ± .003	0.281 ± .007
IRRADIATED (n = 10)	0.075 ± .002	0.073 ± .002	0.055 ± .001**	0.068 ± .002	0.271 ± .005

* Mean ± S.E.M.

One-way ANOVA comparisons. ** Significantly different than controls (P is less than .001).

Table 4-13: **THICKNESS MEASUREMENTS OF OCCIPITAL CORTICAL ZONES OF FETUSES IRRADIATED ON GESTATIONAL DAY 15 AND RECOVERED 5 DAYS POST-IRRADIATION**

	CORTICAL PLATE (mm)	INTERMEDIATE ZONE	SUBVENTRICULAR ZONE	VENTRICULAR ZONE	TOTAL
CONTROL (n = 7)	0.073 ± .002*	0.059 ± .002	0.058 ± .003	0.064 ± .002	0.254 ± .007
IRRADIATED (n = 7)	0.071 ± .003	0.059 ± .003	0.053 ± .002	0.064 ± .001	0.248 ± .007

* Mean ± S.E.M.

One-way ANOVA comparisons. No significant differences between the irradiated group and the controls.

Figure 4-5: Horizontal sections through the main olfactory bulbs of gestational day 15+4 hour fetuses.

(a) Control olfactory bulb.
Epon embedded; methylene blue - azure II stain.
(x343.2)

(b) Irradiated olfactory bulb showing numerous pyknotic cells.
Epon embedded; methylene blue - azure II stain.
(x343.2)

Olfactory ventricle (v); olfactory ventricular zone (vz); olfactory nerve fiber layer (onf).
The arrow in (a) shows a normal blood vessel with its endothelial lining.
Area outlined in (b) shows the enlargement area for Figure 4-5c (next page).

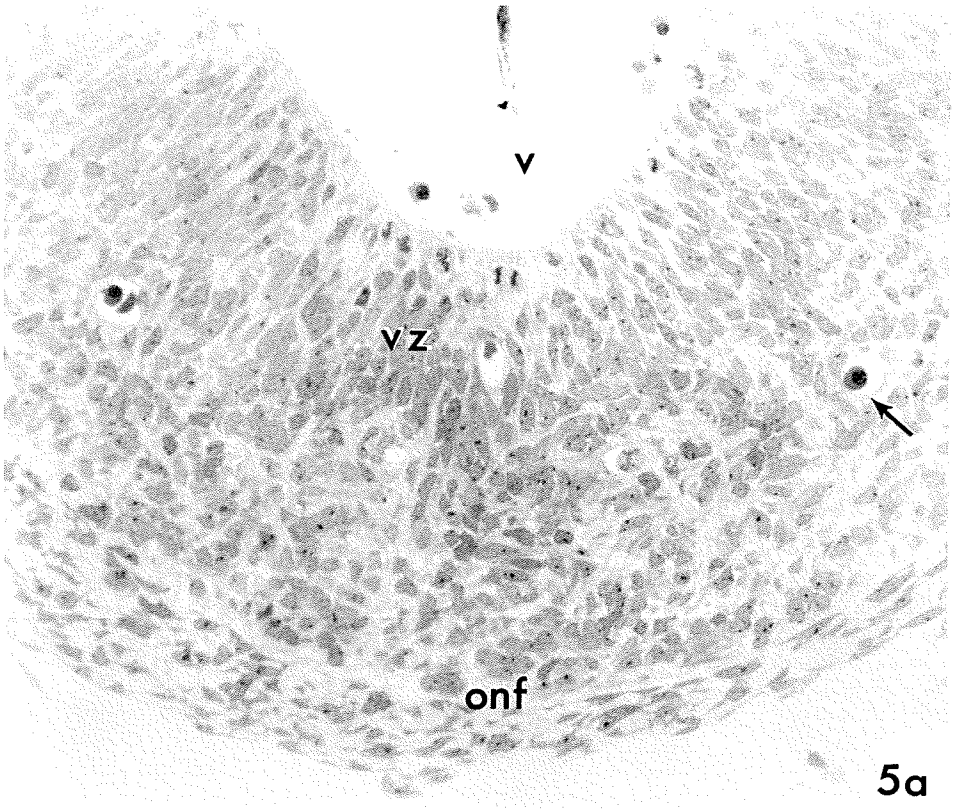

5a

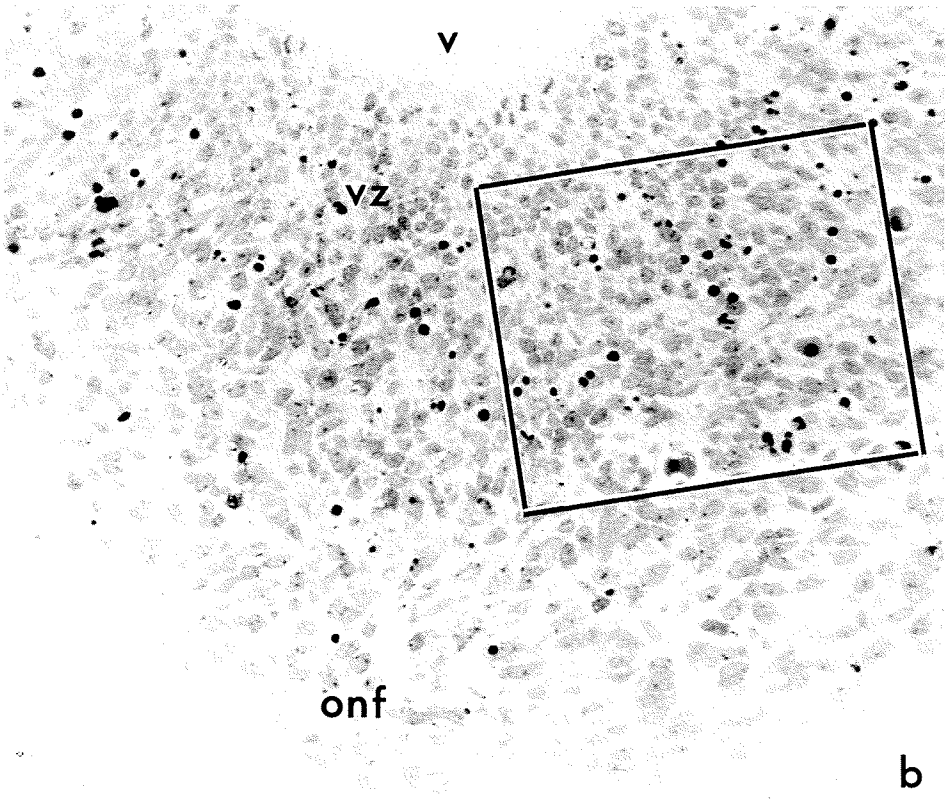

b

Figure 4-5: (continued)

(c) An enlarged area of the irradiated olfactory bulb shown in Figure 4-5b. Shrunken pyknotic cells can be seen. The arrows show irradiated blood vessels with intact endothelial linings. (x818.4)

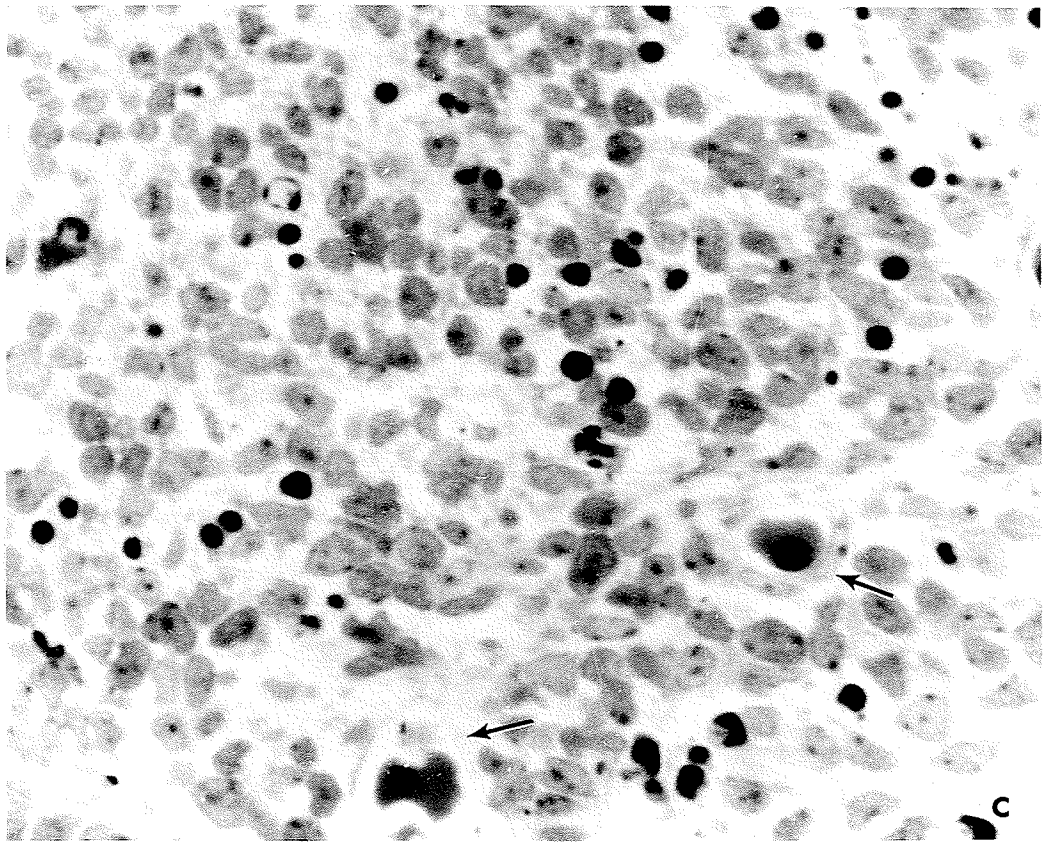
C

Figure 4-6: Coronal sections through the main olfactory bulbs of gestational day 15+48 hour (day 17) fetuses.

(a) A full coronal section of a gestational day 15+48 hour (day 17) main olfactory bulb control. As can be seen, some of the outermost layers of the main bulb can be identified at this stage. The area outlined represents the approximate regions shown in (b), and (c). Paraffin embedded; thionin stain. (x66.0)

(b) A higher magnification of the medial edge of a control 15+48 hour olfactory bulb. Paraffin embedded; thionin stain. (x343.2)

(c) A comparable magnification of the medial edge of a 15+48 hour irradiated olfactory bulb. Two specimens in this irradiated group demonstrated differences in the mitral cell layer, where cells were irregularily shaped, darker staining, and appeared to be lower in number as compared with controls. Paraffin embedded; thionin stain. (x343.2)

Glomerular layer (gl); external plexiform layer (ep); mitral layer (mi); regions of migrating cells (*); ventricular zone (vz).

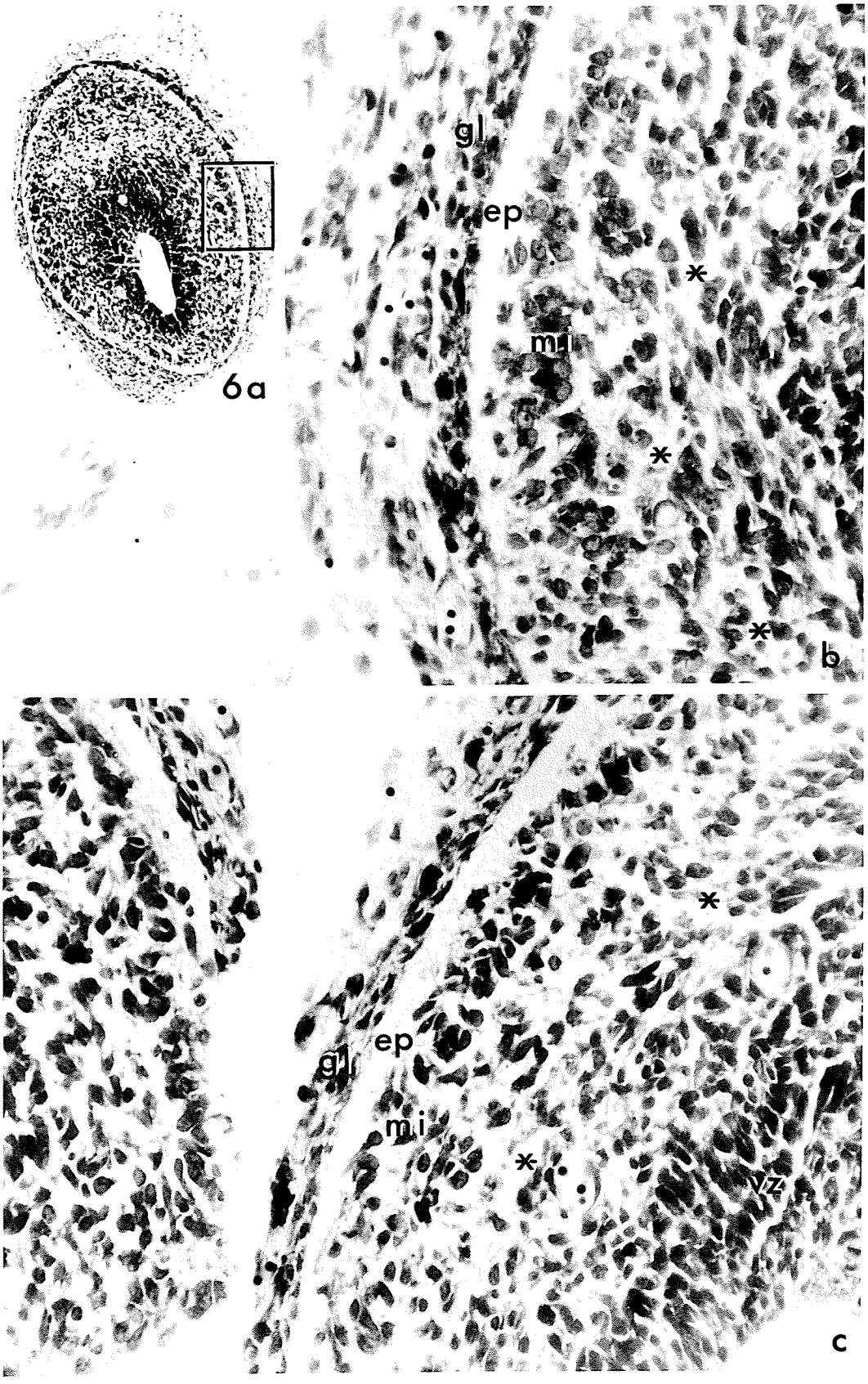
6a
gl
ep
m.i
b
gl
ep
m.i
vz
c

Figure 4-7: Coronal sections of the medial edge of the main olfactory bulbs from gestational day 15+5 day (day 20) fetuses. The full view of the main olfactory bulbs at this gestational stage can be seen in Figure 3-1.

(a) The medial edge of a control 15+5 day main olfactory bulb.
Paraffin embedded; thionin stain. (x343.2)

(b) The medial edge of an irradiated 15+5 day main olfactory bulb considered to be severely affected. All layers of the two severely affected irradiated bulbs appeared to have low cell densities, as compared to the control specimens (a). The most striking effect however, appeared in the mitral cell layer. Many of the cells of this layer appeared shrunken, darker staining, with lower cell packing densities than controls.
Paraffin embedded; thionin stain. (x343.2)

Glomerular layer (gl); external plexiform layer (ep); mitral layer (mi); internal plexiform layer (ip); region of migrating cells (*).

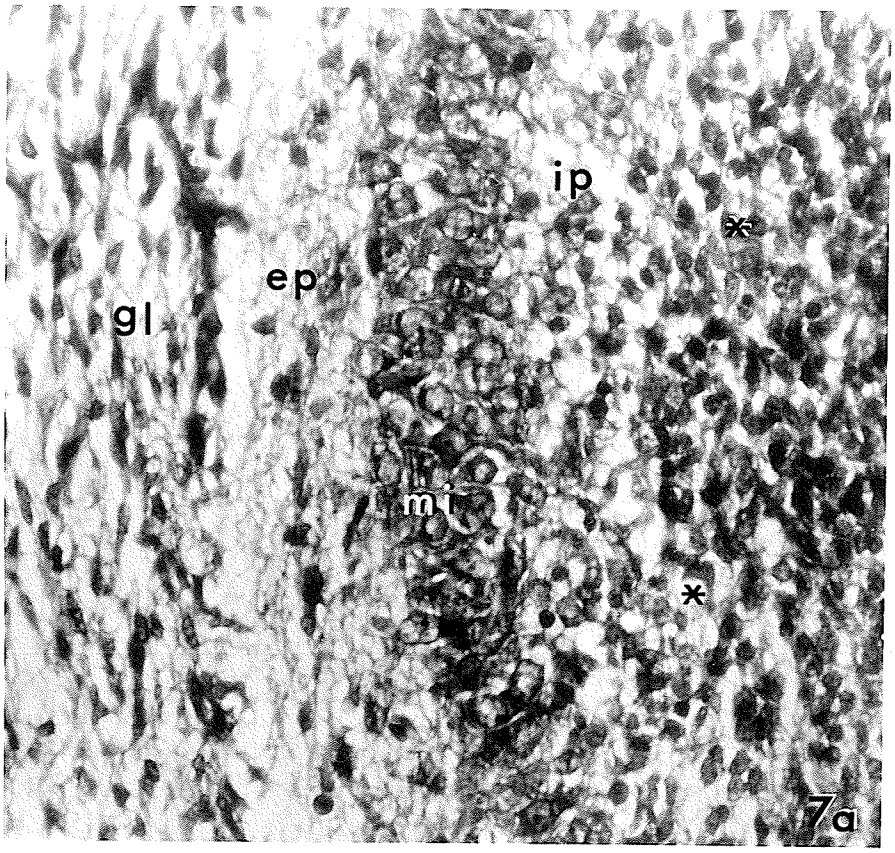
ip
ep
gl
mi
7a

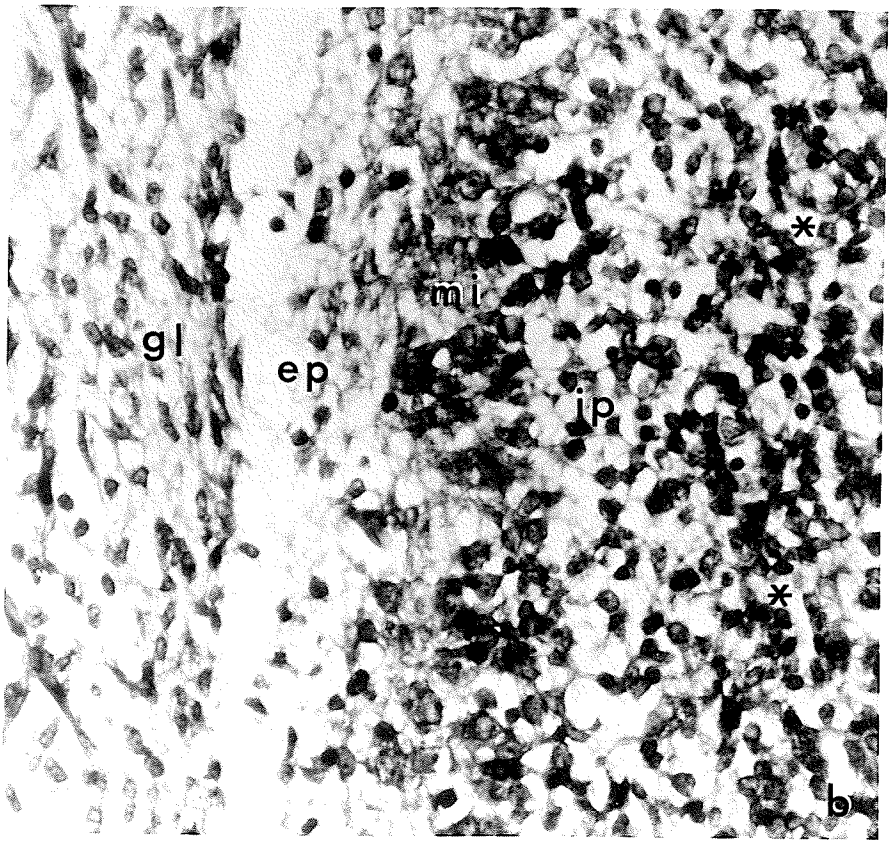
mi
gl
ep
ip
b

Figure 4-8: A coronal section showing the normal midsagittal crossing of the corpus callosum in a gestational day 15+5 day (day 20) control fetus.

Glial sling (gs); corpus callosum (cc).

Paraffin embedded, thionin stain. (x68.6)

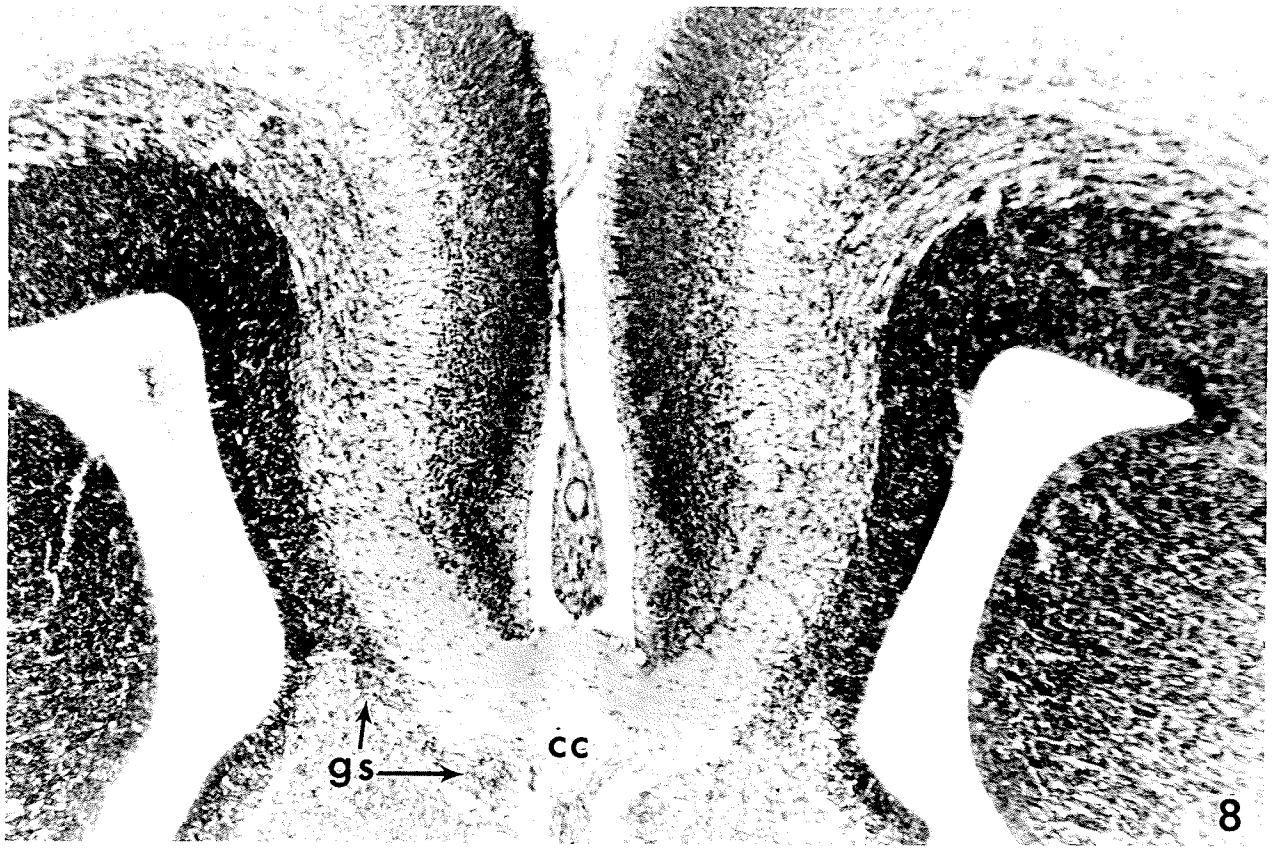
gs
cc
8

Figure 4-9: Coronal sections of the fetal rat hippocampal formation at various gestational intervals.

(a) The fetal hippocampal formation on gestational day 15+4 hours.
Lateral and third ventricles (v). The area outlined represents the area of enlargement for Figure 4-10.
Epon embedded; methylene blue - azure II stain. (x50.2)

(b) The fetal hippocampal formation on gestational day 15+48 hours (day 17).
Lateral and third ventricles (v); ventricular zone (vz); subicular pyramidal layer (pl); primordial dentate gyrus (*).
Paraffin embedded; thionin stain. (x66.0)

(c) The fetal hippocampal formation on gestational day 15+5 days (day 20).
Lateral ventricle (v); ventricular zone (vz); stratum oriens (so); the continuous pyramidal layer from the subiculum to Ammon's horn (pl); lacunosum-moleculare (lm); dentate gyrus (dg); fimbria (f).
Paraffin embedded; thionin stain. (x50.2)

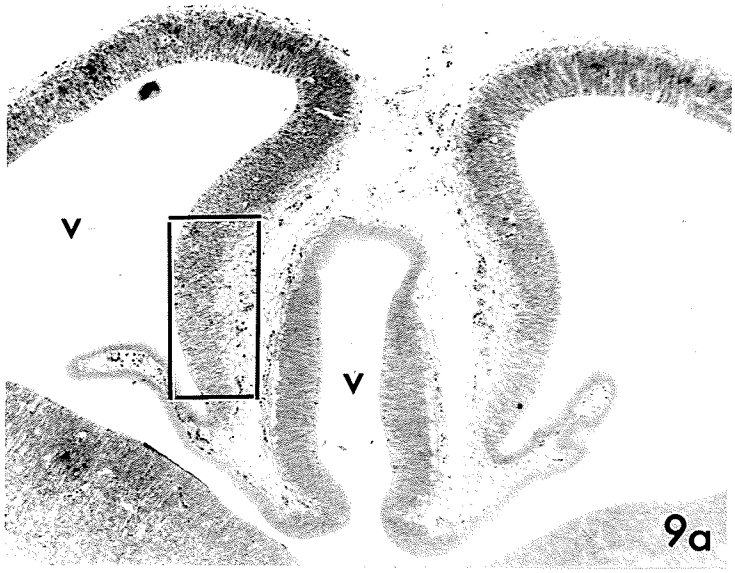
v
v
9a

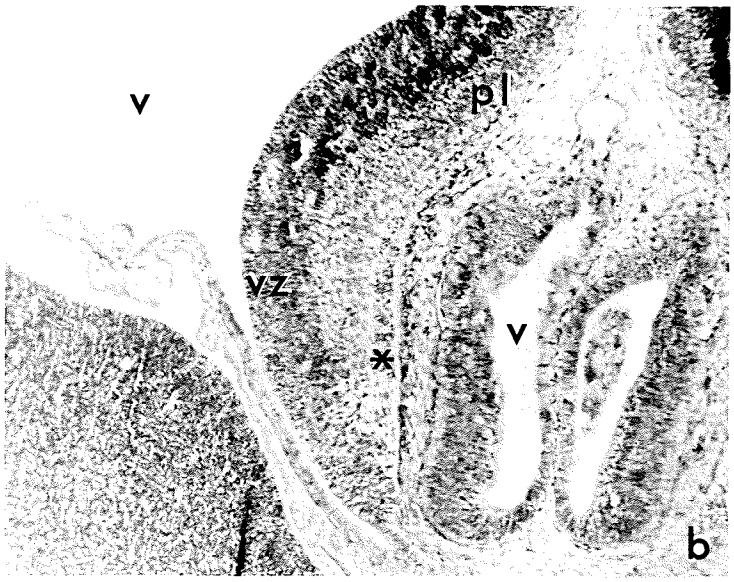
v
pl
vz
v
*
b

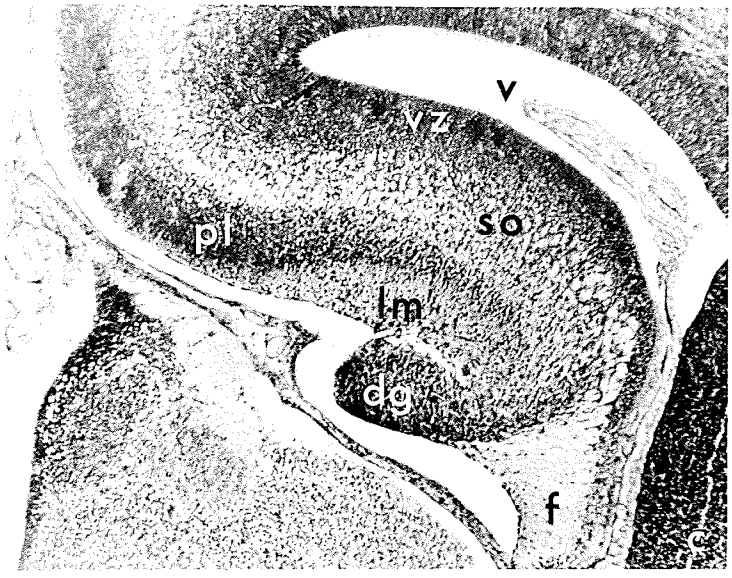
v
vz
pl
so
lm
dg
f

Figure 4-10: Coronal sections of the fetal hippocampal formation on gestation day 15+4 hours, as outlined in Figure 4-9a.

(a) The hippocampal formation of a control, gestational day 15+4 hour fetus.
Epon embedded; methylene blue - azure II stain.
(x330.0)

(b) The hippocampal formation of an irradiated gestational day 15+48 hour fetus. Pyknotic cells can be seen in the greatest numbers in the presumptive subicular region. The number of pyknotic cells decreases in the ventricular region of Ammon's horn, while essentially no pyknotic cells can be observed in the most ventral ventricular proliferative region of the dentate gyrus.
A decrease in mitotic activity at the juxtaventricular border of the ventricular zone is seen in this section as compared to the control (a).
Epon embedded; methylene blue - azure II stain.
(x330.0)

Lateral ventricle (v); ventricular zone (vz); marginal zone (mz).

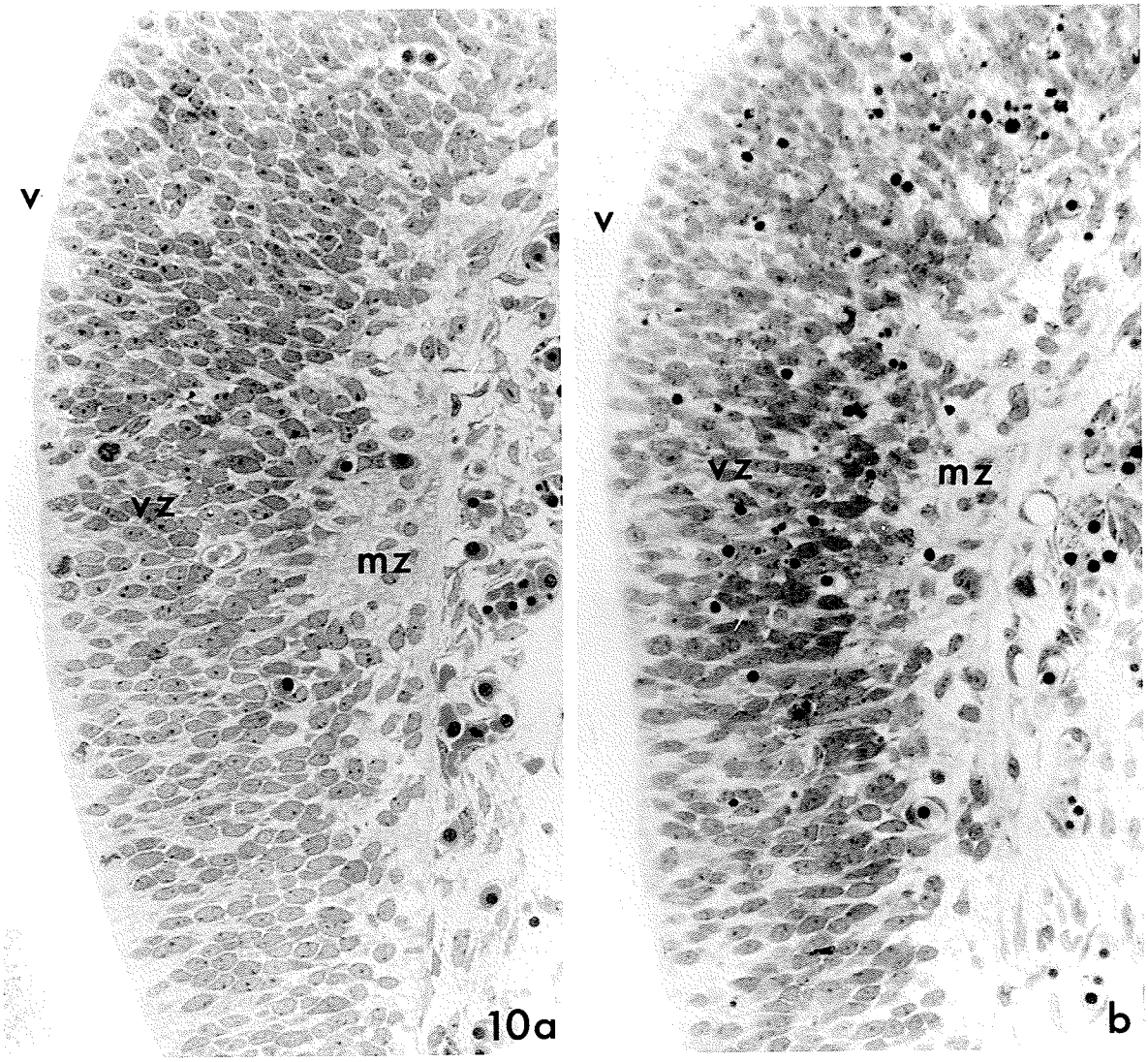
v
vz
mz
10a
v
vz
mz
b

Figure 4-11: Higher magnifications of the Ammon's horn ventricular zones shown in Figure 4-10. (Note: sections have been presented horizontally on this plate).

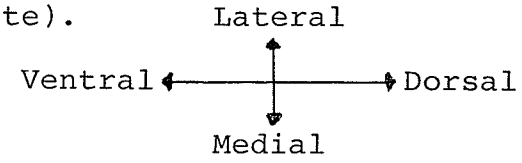

(a) Ammon's horn ventricular zone from a control 15+4 hour control fetus as shown in Figure 4-10a. (x686.4)

(b) Ammon's horn ventricular zone from an irradiated 15+4 hour fetus as shown in Figure 4-10b.

Shrunken pyknotic cells can be seen, as well as small dark staining flecks within the cytoplasm of ventricular cells. The flecks are more evident in regions where pyknosis is observed. These flecks, or cytoplasmic inclusions, are thought to represent ribosomal aggregations. As well, the decrease in the number of mitotic cells along the juxtaventricular border in the irradiated specimen is evident as compared with the control (a). The arrow in this figure shows an intact blood vessel.

Epon embedded; methylene blue - azure II stain. (x686.4)

Lateral ventricle (v); ventricular zone (vz): marginal zone (mz).

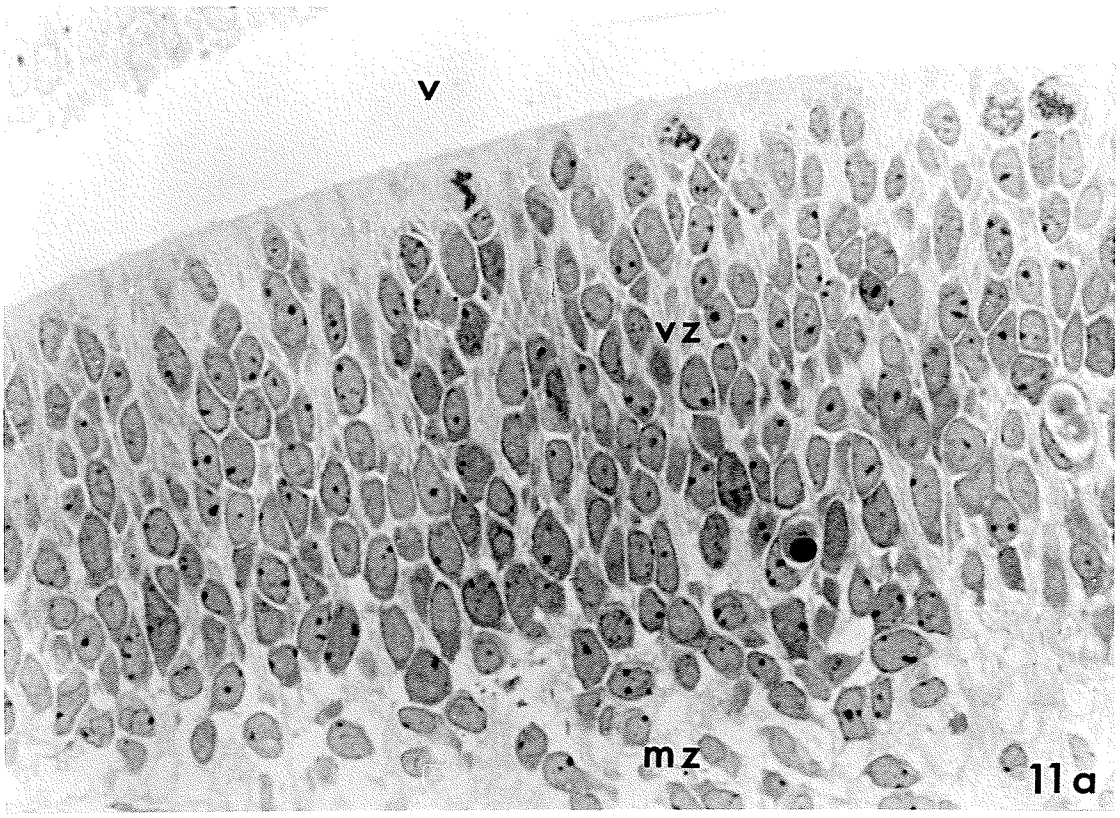
v
vz
mz
11a

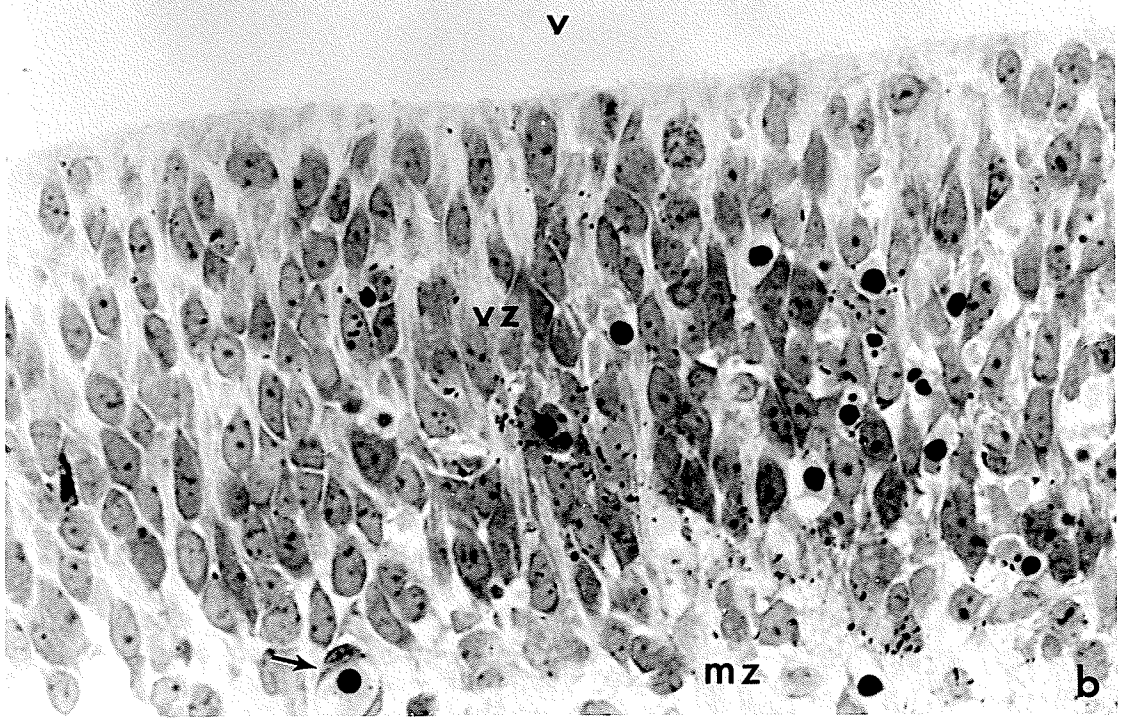
v
vz
mz
b

Figure 4-12: Coronal sections of the fetal rat cerebellum at various gestational intervals.

(a) The fetal cerebellum on gestational day 15+4 hours.
Superficial fibrous layer (sfl); nuclear zone (nz); transitional zone (tz); intermediate fibrous layer (ifl); cerebellar neuroepithelium (cn); metencoele (met).
Epon embedded; methylene blue - azure II stain.
(x58.1)

(b) The fetal cerebellum on gestational day 15+48 hours (day 17).
External germinal layer (egl); molecular layer (ml); Purkinje cell layer (pjl); cerebellar neuroepithelium (cn); germinal trigone (gt).
Epon embedded; methylene blue - azure II stain.
(x59.4)

(c) The fetal cerebellum on gestational day 15+5 days (day 20).
External germinal layer (egl); molecular layer (ml); Purkinje cell layer (pjl); nuclear zone (nz); cerebellar neuroepithelium (cn).
Paraffin embedded; thionin stain.
(x46.2)

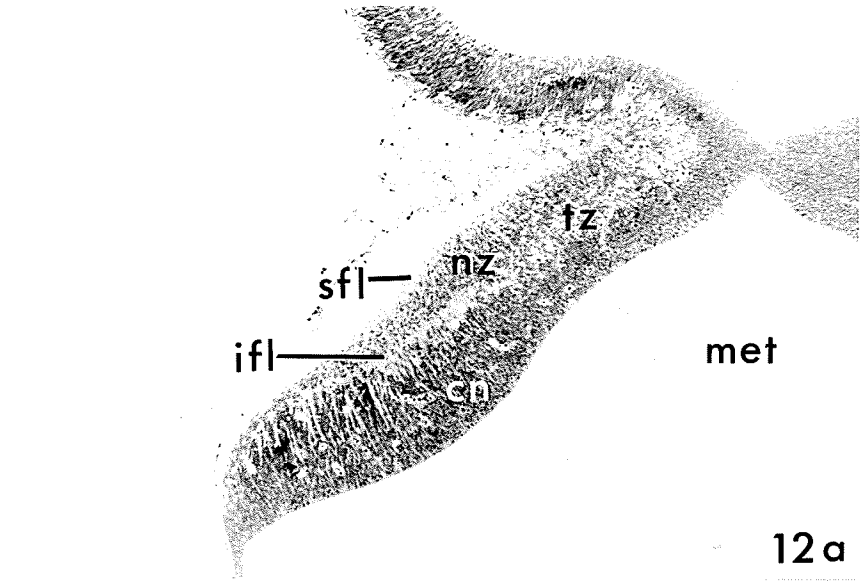

12a

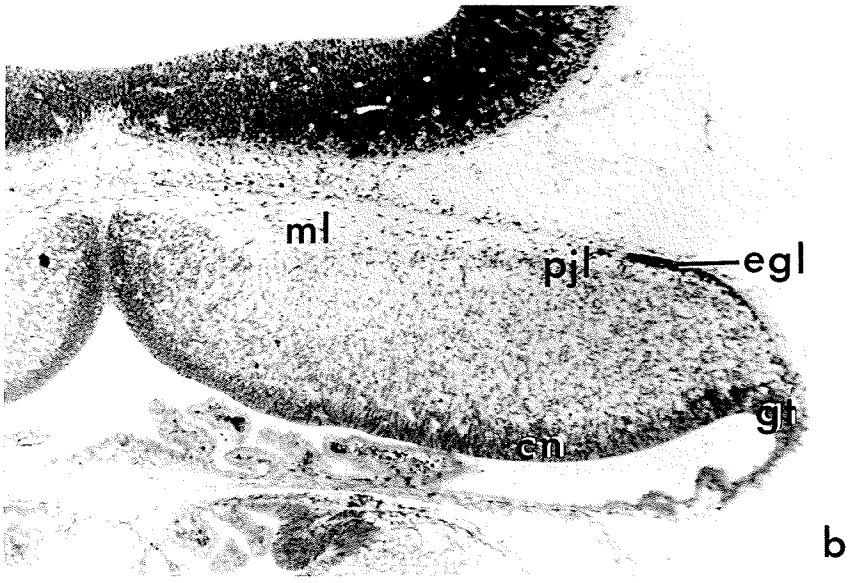

b

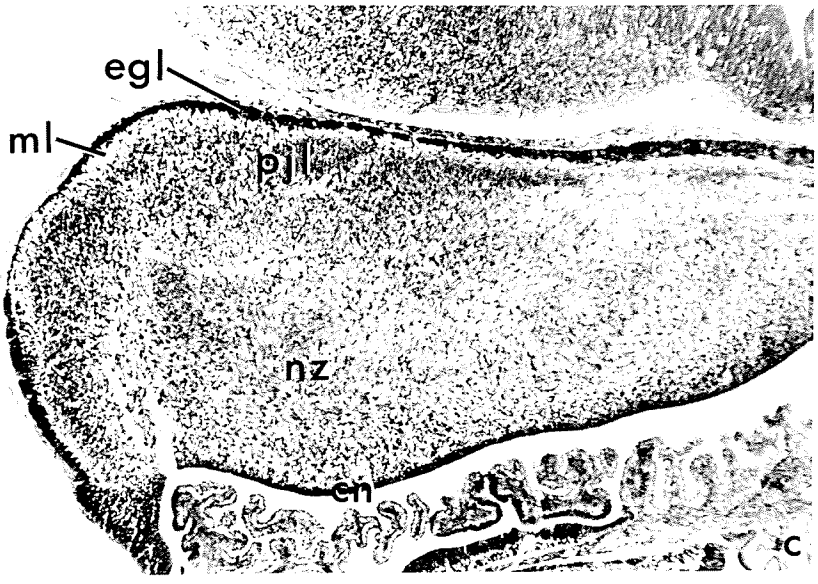

c

Figure 4-13: Coronal sections of the fetal rat cerebellar plates of gestational day 15+4 hour groups.

(a) An enlargement of a control 15+4 hour cerebellar plate as shown in Figure 4-12a. Epon embedded; methylene blue - azure II stain. (x171.6)

(b) An irradiated 15+4 hour cerebellar plate. Numerous pyknotic figures can be seen, particularly in the more lateral cerebellar neuroepithelial regions. A few pyknotic cells can also be seen in the nuclear zone with the most being observed in the medial limits of this zone, within and above the transitional zone.
Epon embedded; methylene blue - azure II stain. (x171.6)
Superficial fibrous layer (sfl); nuclear zone (nz); transitional zone (tz); intermediate fibrous layer (ifl); cerebellar neuroepithelium (cn); metencoele (met).

(c) See next plate.

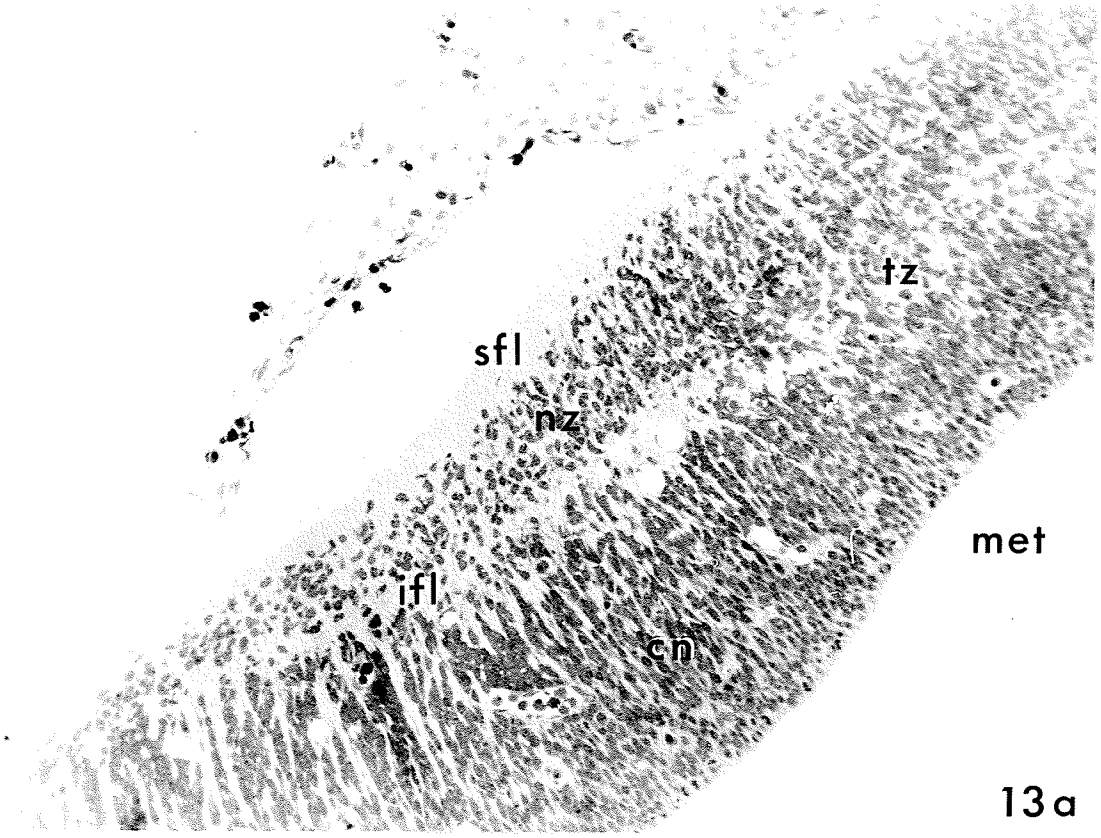

13a

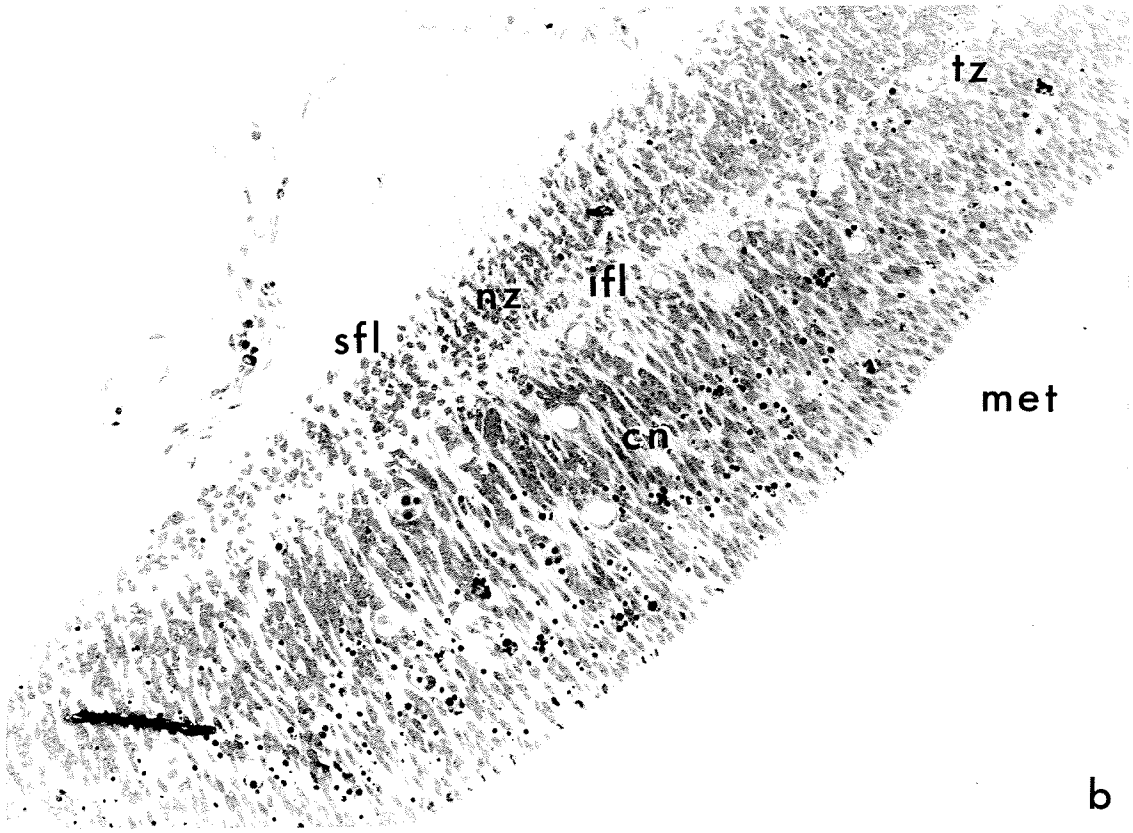

b

Figure 4-13: (continued)

(c) An enlarged area of the irradiated cerebellar plate shown in Figure 4-13b. Shrunken pyknotic cells can be seen. The arrows show irradiated blood vessels with intact endothelial linings. (x343.2)

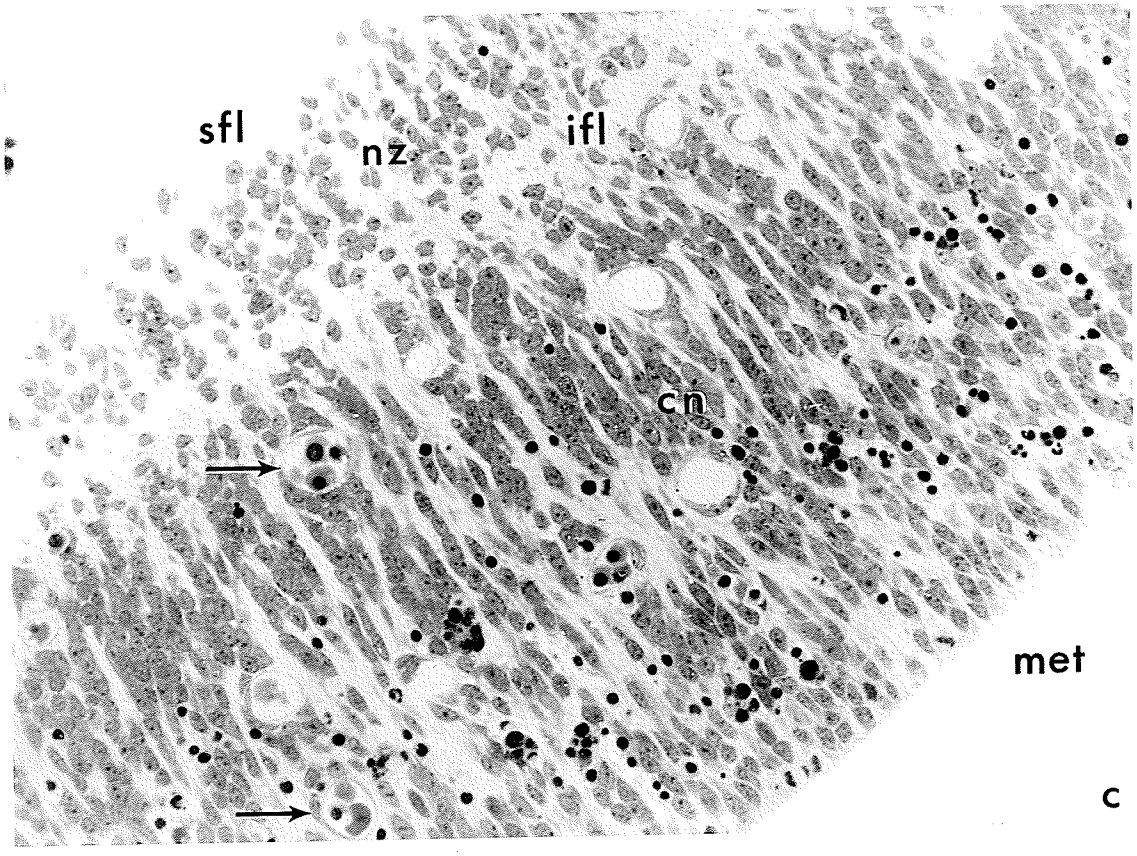
sfl
nz
ifl
cn
met
c

Table 4-14: **WEIGHTS OF PLACENTAS IRRADIATED ON GESTATIONAL DAY 15 AND RECOVERED 4 HOURS, 48 HOURS, AND 5 DAYS POST-IRRADIATION**

	PLACENTAL WEIGHTS (g)		
	15+4 HOURS	15+48 HOURS	15+5 DAYS
CONTROL	0.24 ± 0.004* (n = 140)	0.38 ± 0.005 (n = 149)	0.55 ± 0.007 (n = 142)
IRRADIATED	0.26 ± 0.003** (n = 149)	0.36 ± 0.004*** (n = 147)	0.53 ± 0.008 (n = 135)

* Mean ± S.E.M.

Student t-test comparisons. ** Significantly different from controls (P is less than 0.05).

*** Significantly different from controls (P is less than 0.001).

Figure 4-14: Chorionic plates and labyrinthine zones of placentas from gestational day 15+4 hour groups.

(a) The chorionic plate, labyrinthine zone, and a portion of the basal zone of a control 15+4 hour placenta.
Paraffin embedded; H&E stain. (x76.6)

(b) The chorionic plate, labyrinthine zone, and a portion of the basal zone of an irradiated 15+4 hour placenta. Note the large gaps or spaces (*) in the labyrinthine zone of this placenta.
Paraffin embedded; H&E stain. (x76.6)

Chorionic plate (chp); labyrinthine zone (lab); basal zone (bsl).

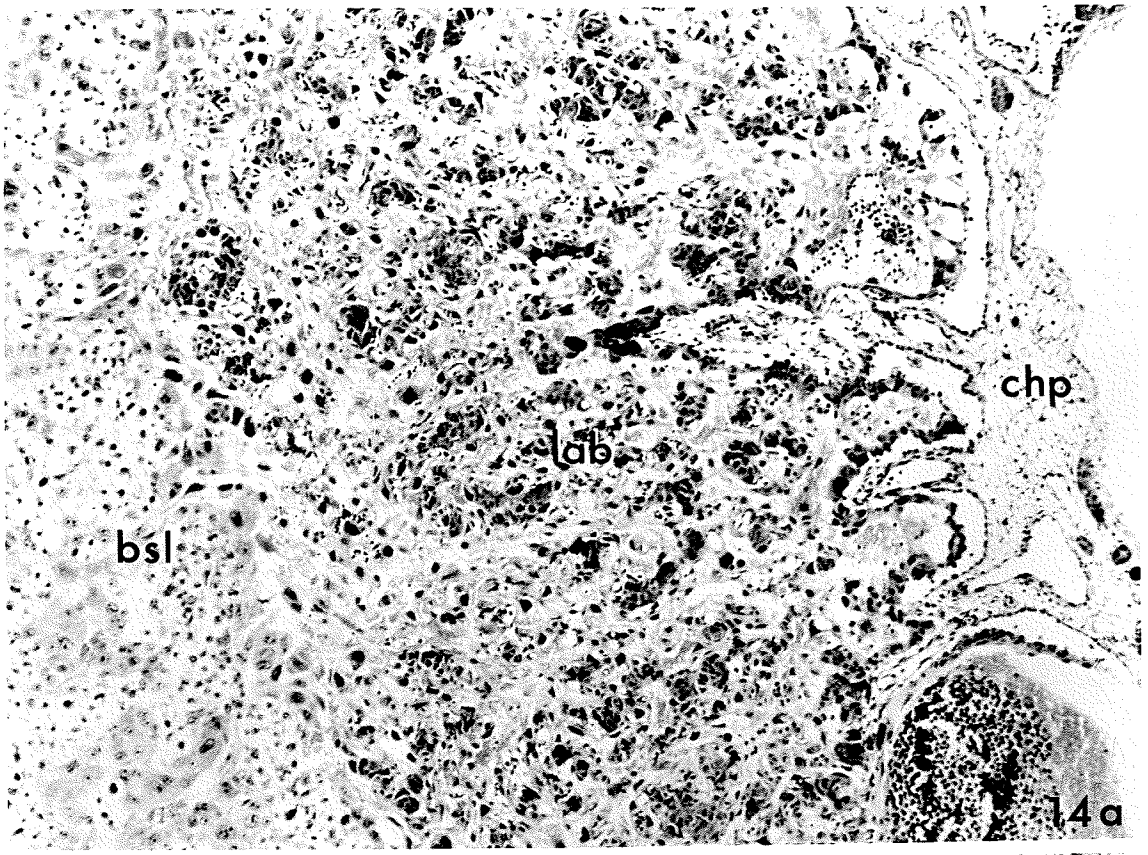
chp
lab
bsl
14a

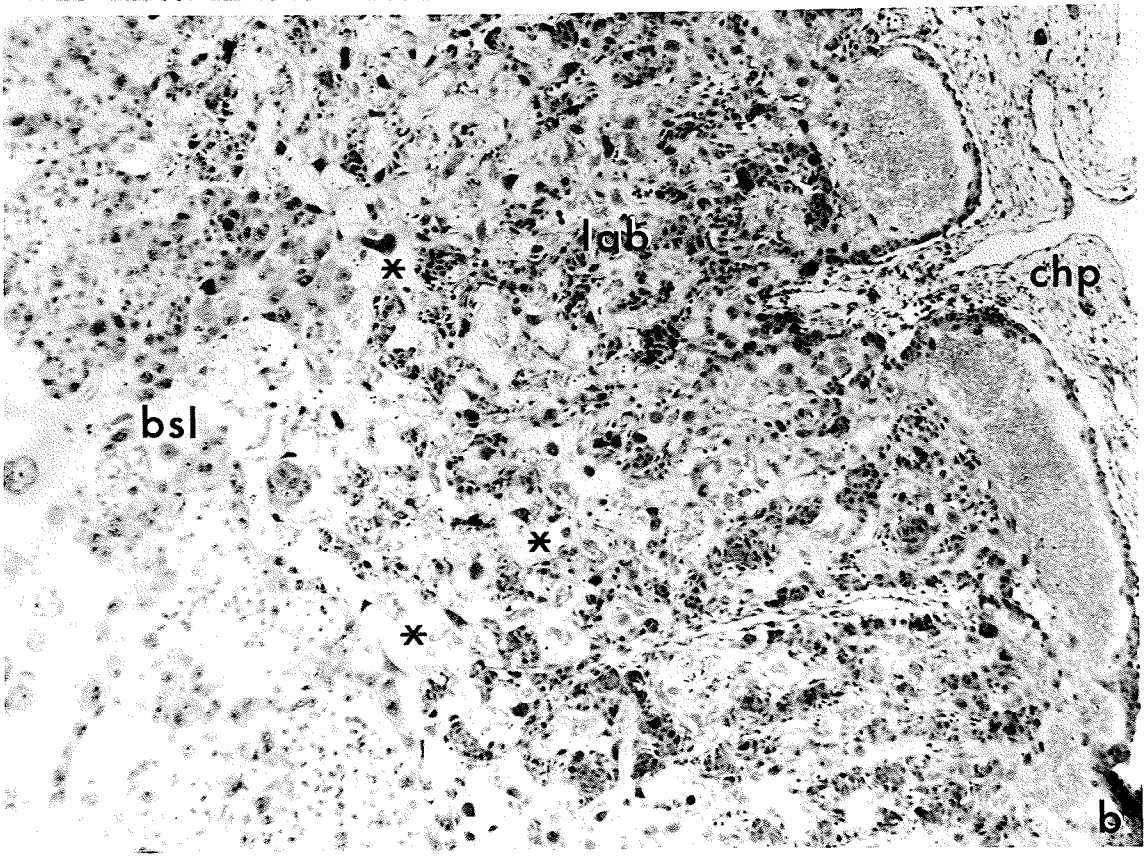
lab
chp
bsl
b

Figure 4-15: Higher magnifications of the labyrinthine zones of gestational day 15+4 hour placentas as shown in Figure 4-14.

(a) The labyrinthine zone of a control placenta. Paraffin embedded; H&E stain. (x316.8)

(b) The labyrinthine zone of an irradiated placenta. Higher magnification reveals that the fetal blood channels (arrows) are unaffected by irradiation while the maternal blood channels (*) are enlarged. Rather than an increase in maternal red blood cells, these maternal spaces appeared edematous as they stained a pale pink color with H&E stain. Paraffin embedded; H&E stain. (x316.8)

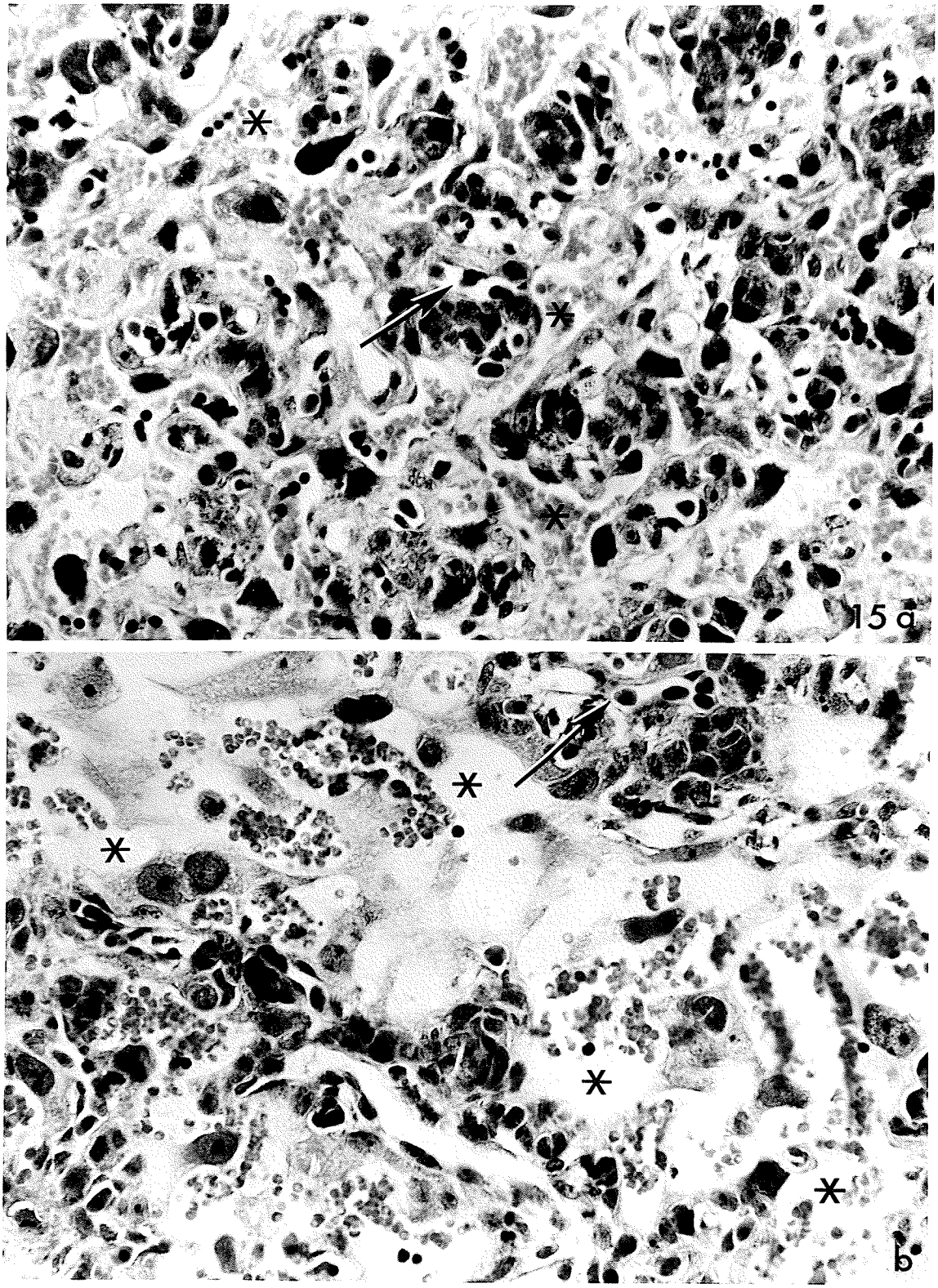
15a
b

Figure 4-16: Basal zones and decidua basalis layers of placentas fron gestational day 15+4 hour groups.

(a) The decidua basalis, basal zone, and a portion of the labyrinthine zone of a control 15+4 hour placenta.
Paraffin embedded; H&E stain. (x68.6)

(b) The decidua basalis, basal zone, and a portion of the labyrinthine zone of an irradiated 15+4 hour placenta. Large gaps or spaces (*) like those seen in the labyrinthine zones of irradiated placentas, were also seen in basal zones in these placentas. These spaces appeared to disrupt the normal cytological organization of the basal zone as compared with control placentas. As in the labyrinthine zone, these spaces appeared to be filled with a pale pink staining substance.
Paraffin embedded; H&E stain. (x68.6)

Decidua basalis (dec); basal zone (bsl); labyrinthine zone (lab); giant cells (G); glycogen cells (g); cytotrophoblastic (basophilic) cells (c).

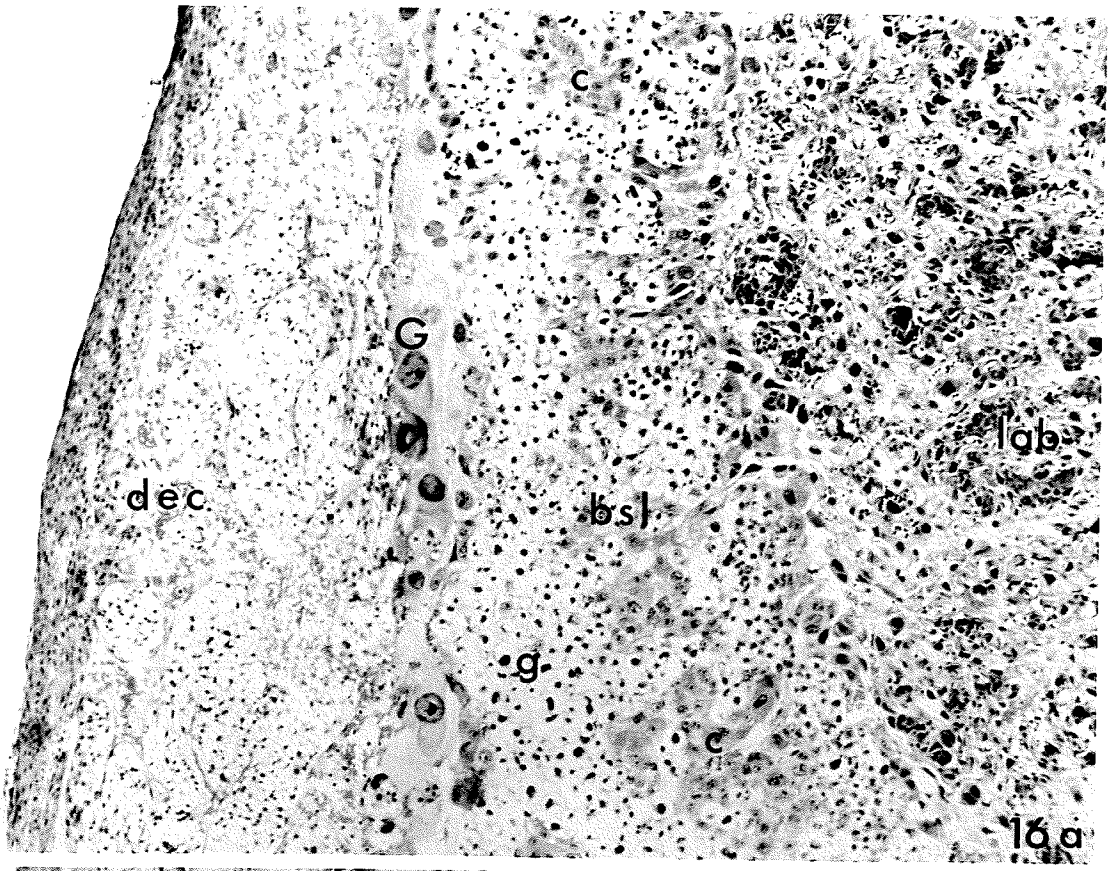
c
G
lab
dec
bsl
g
c
16a

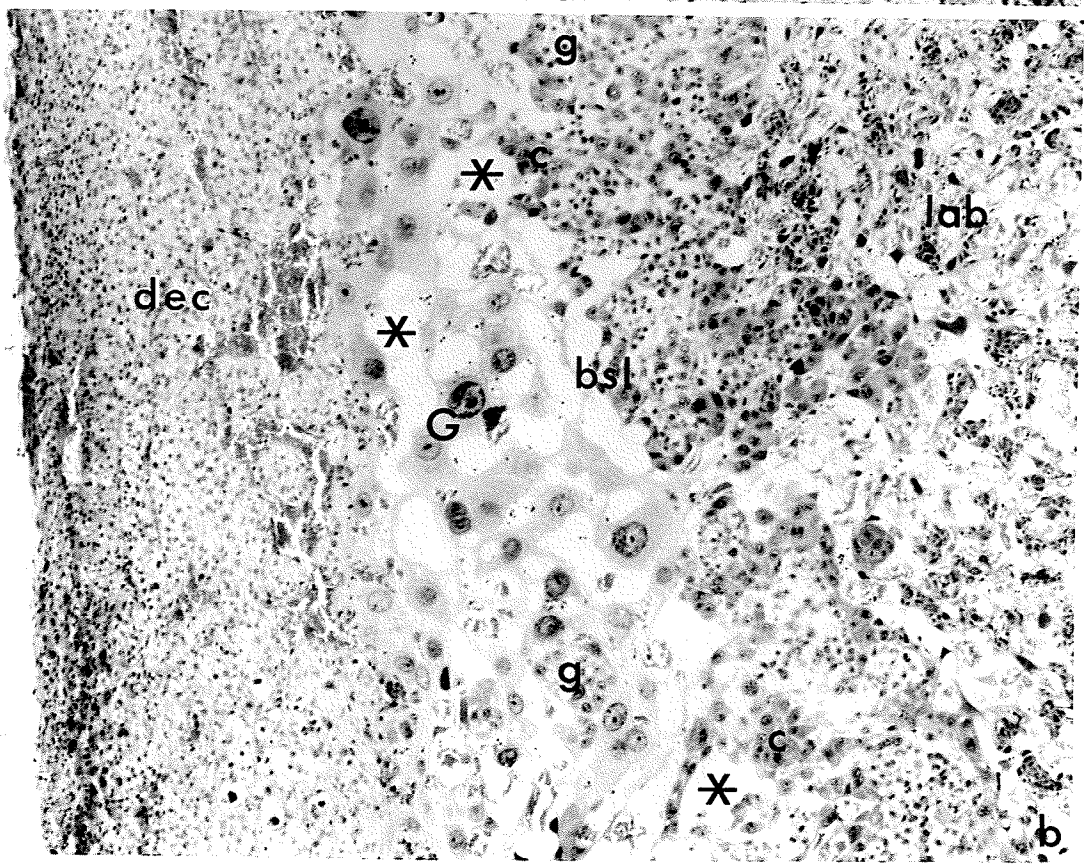
g
c
lab
dec
bsl
G
g
c
b

Figure 4-17: The placenta from gestational day 15+48 hour (day 17) groups.

(a) The fetal side of a 15+48 hour control placenta. This includes the chorionic plate (chp); the labyrinthine zone (lab); and a small portion of the basal zone (bsl). Paraffin embedded; H&E stain. (x68.6)

(b) The maternal side of a 15+48 hour control placenta which includes the decidua basalis (dec); the basal zone (bz); and a small portion of the labyrinthine zone (lab). Arrows indicate the small islands or pools of glycogen cells, which normally start to degenerate at this gestational age.
Paraffin embedded; H&E stain. (x68.6)

(c) See next plate.

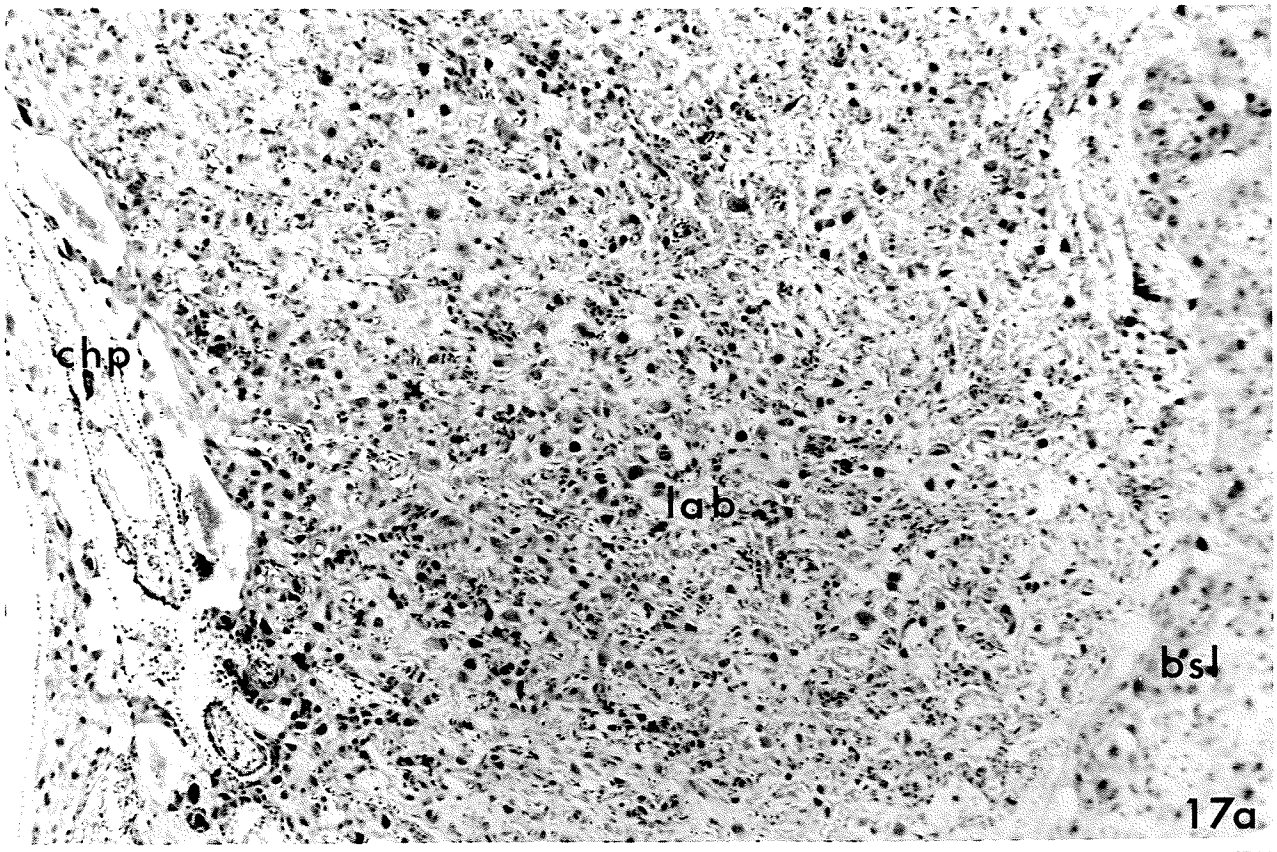
chp
lab
bsl
17a

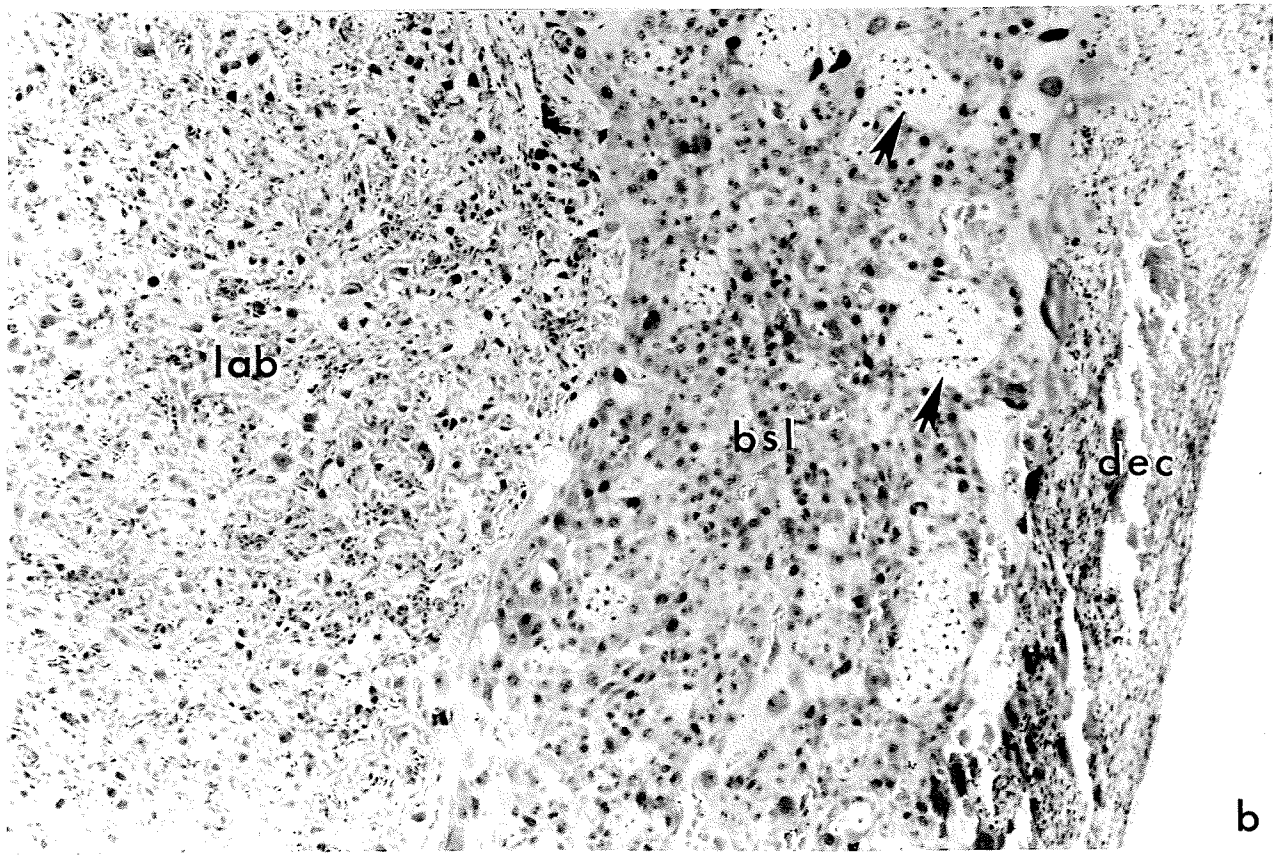
lab
bsl
dec
b

Figure 4-17: (continued)

(c) A high magnification view of the labyrinthine zone of an irradiated 15+48 hour (day 17) placenta. Within 6 of the 10 irradiated labyrinthine zones examined from this age group, localized areas of trophoblast stained a purplish-pink color instead of the characteristic blue stain that is typical of these cells in control specimens. For the particular specimen shown in this figure, the areas of altered staining propensity are outlined.

Paraffin embedded; H&E stain. (x316.8)

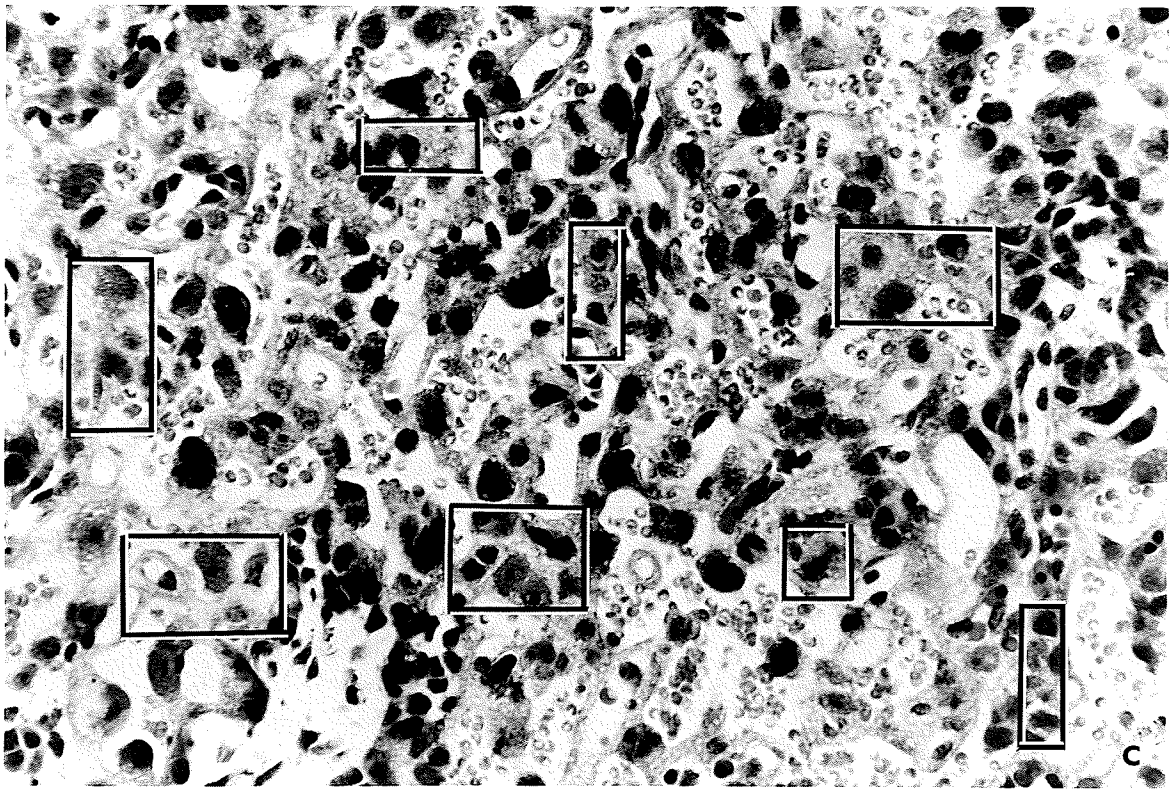
C

Figure 4-18: The placenta from gestational day 15+5 days (day 20) control groups.

(a) The fetal side of a 15+5 day control placenta. This includes the chorionic plate (chp), and the labyrinthine zone (lab).
Paraffin embedded; H&E stain. (x68.6)

(b) The maternal side of a 15+5 day control placenta which includes the decidua basalis (dec); the basal zone (bsl); and a small portion of the labyrinthine zone (lab). Arrows in this figure indicate the continued degeneration of glycogen cells from previous gestational stages.
Paraffin embedded; H&E stain. (x68.6)

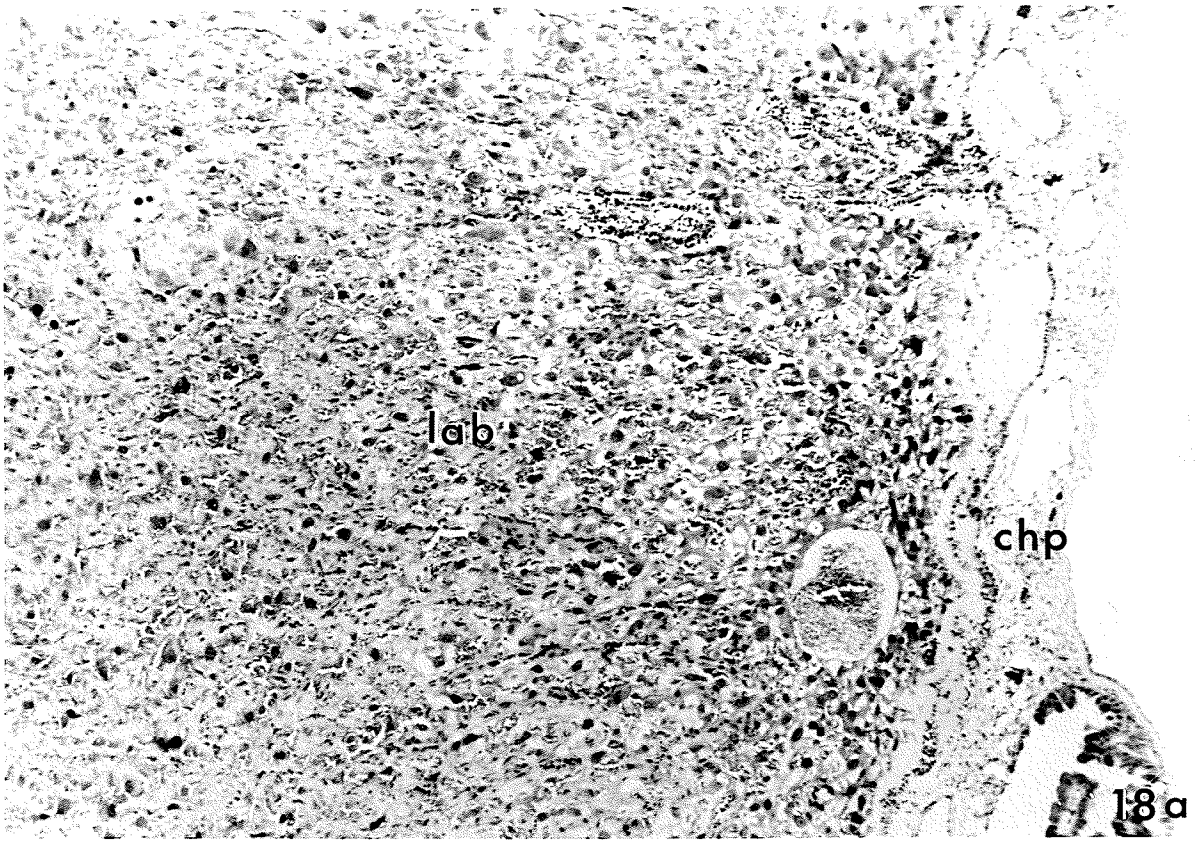
lab
chp
18a

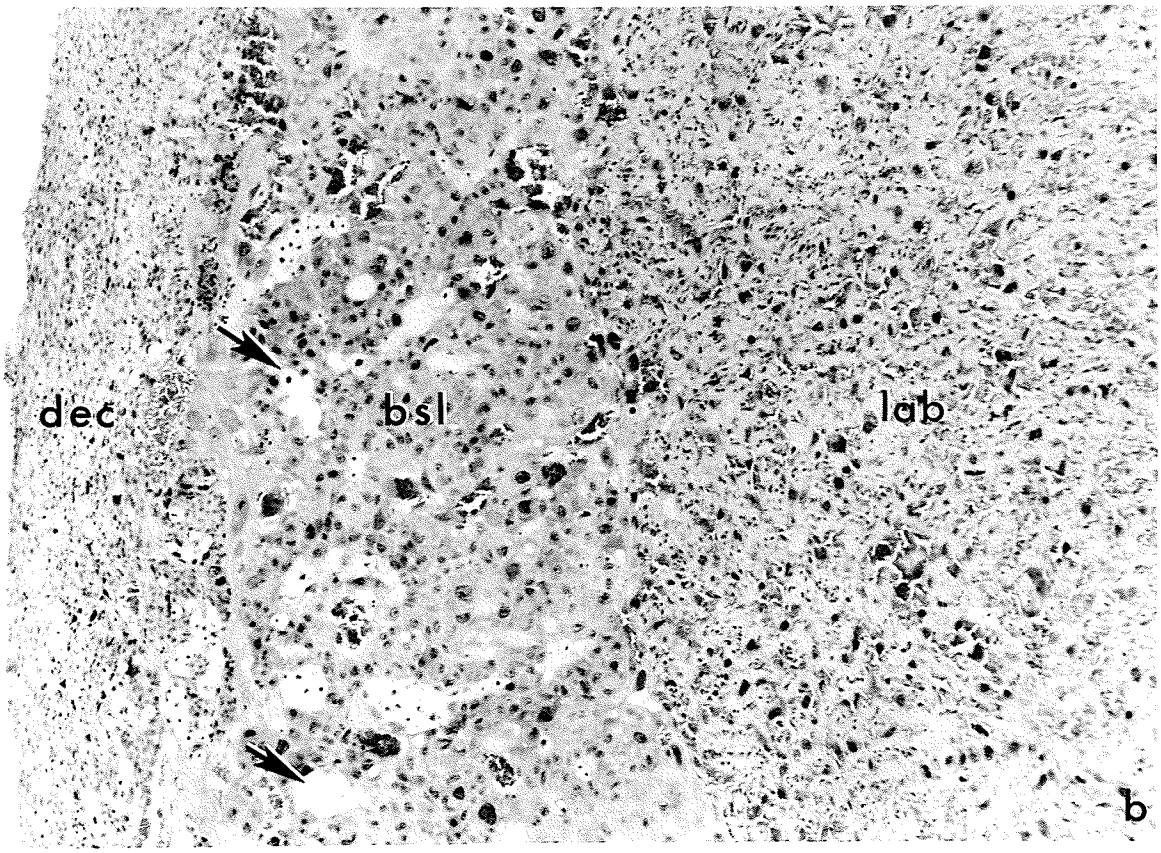
dec
bsl
lab
b

understanding of developmental anatomy, critical periods, and the mechanisms of teratogenesis (Rugh et al, 1964; Kalter, 1968; Rodier, 1986; Schull et al, 1990).

Although controlled experiments of irradiation teratogenesis have been conducted since 1935, there are still uncertainties about many of the mechanisms of radiation effects. This is probably due to the wide range of possible experimental combinations of dose, gestational timing, and biological endpoints of interest. In more recent years, dose levels below 1 Gy (100 rads) have been the focus of many investigations. However, due to the multiple possible combinations of experimental design, information regarding the teratogenicity of these lower dose ranges is fragmentary.

This study was designed to investigate a wide range of prenatal developmental events following a maternal irradiation with 0.5 Gy (50 rads) on gestational day 15. Unlike most studies which have investigated the biological endpoints of irradiation in the postnatal period, this study examined the prenatal or short-term effects of a relatively low dose of ionizing radiation. In this respect, many parameters explored in this study have not been reported in any previous investigations.

This study revealed that a 0.5 Gy (50 rad) irradiation on gestational 15 of the pregnant rat did not cause any significant changes in maternal weights 48 hours, or 5 days post-irradiation. As explained in Chapter 3, a sample of maternal weights in the 15+4 hour groups revealed

no weight changes for control or irradiated dams in the interval between sham or irradiation treatment and hysterotomy, therefore, recording of the weights of these animals was discontinued. As body weight may refect the general health of the maternal organism, it was concluded from this data that 0.5 Gy (50 rads) did not influence the health of dams in this study.

Norton and Kimler (1988) found that with a 1 Gy (100 rads) exposure on gestational day 15, pregnant rats failed to gain weight normally for a 24 hour period yet, resumed weight to control levels by parturition. In a subsequent study (Norton et al, 1991), the same results were found with a gestational day 15 exposure of 0.75 Gy (75 rads). Unfortunately, these studies had not been published until after we had completed maternal weighing procedures. Given the results of these studies, recording maternal weights at smaller, more frequent post-irradiation intervals might have provided more conclusive data on maternal health status following 0.5 Gy (50 rads).

As expected from previous reports, no significant radiation-induced changes were found in the number of viable fetuses per litter, nor the number of resorption or stillbirths per group, for any group examined. According to the literature, the threshold dose for altering the litter size on gestational day 15 is likely greater than 1 Gy (100 rads) (Brent, 1980; Takeuchi et al, 1981; Norton, 1986; Norton and Kimler, 1988).

Fetal weight data derived from this study support previously reported findings that a gestational day 15 exposure of 0.5 Gy (50 rads) results in a significant reduction in weight at birth as compared to controls (Norton and Donoso, 1985; Norton, 1986). In addition, the present results revealed that significant weight reductions can be detected in irradiated fetuses as early as 48 hours post-irradiation. This has not been reported in previous studies.

Crown-rump length measurements of the offspring are not usually included in the experimental protocol of teratological studies with irradiation. This is probably due to the fact that weight, as a fetal growth parameter, can be collected with greater speed and precision. As explained in Chapter 3, crown-rump measurements were not recorded for gestational day 15+5 day specimens. Significant reduction in the crown-rump measurements were found in the 15+48 hour irradiated group compared with controls, as might be expected given the reduced weights of these fetuses.

Surprisingly, fetal crown-rump lengths of the 15+4 hour irradiated group were significantly reduced as compared with controls, even though fetal weight appeared to be unchanged at this post-irradiation interval. This reduction of crown-rump length without a corresponding reduction of weight may indicate that crown-rump length is a more sensitive indicator of gestational day 15 irradiation

teratogenesis at early post-irradiation intervals. These results may also suggest that growth in length can normally occur within this four hour period of gestational day 15 in the absence of growth in weight. Information to either support or refute these theories could not be found in the teratology nor developmental literature.

A popular notion amongst irradiation teratologists is that generalized radiation-induced cell death is responsible for reduced mass and stunting of the post-irradiation offspring (Rugh et al, 1964). These investigators concede, however, that impediments of the normal chemical, enzymatic, or endocrine mechanisms responsible for fetal growth may also occur as a result of radiation exposure (Brent and McLaughlin, 1960; Rugh et al, 1964). The mechanisms responsible for radiation-induced growth retardation could not be determined from the material in this study.

No significant differences were found between the numbers of gross malformations observed for any irradiation group as compared with controls. Although previous reports of irradiation teratogenesis have established that gross congenital malformations are unlikely with a 0.5 Gy (50 rad) irradiation exposure on gestational day 15 (Brent, 1980; Kameyama and Hoshino, 1986), two novel pieces of information are derived from this study. First, comparisons of the incidence of observed deformities between gestational ages were not significant, therefore indicating that there were no cases of early malformation with late fetal stage

repair. Second, the fact that there were no observed developmental delays indicates that a 0.5 Gy (50 rad) irradiation on gestational day 15 does not cause any impediment to the normal rhythm of developmental events.

According to the normal sequence of developmental events occurring during gestational day 15 (Table 2-1), only a few of the defects listed in Table 4-9 for irradiated groups could be related to a gestational day 15 irradiation insult. These could include the cleft palates of the irradiated 15+48 hours group, and the eyelid malformations of the 15+5 day irradiated group. Severe malformations of the brain and cranium, like the partial exencephalies observed in this study, are more likely to occur with gestational day 8 exposures; during the induction of the neural plate (Hicks, 1953; Hicks et al, 1957 and 1959; Hicks and D'Amato, 1980). Similarly, anopthalmia is most commonly observed with exposures on gestational days 9 through 10 (Wilson and Karr, 1951; Hicks, 1953; Hicks et al, 1957; Cowan and Geller, 1960; Hicks and D'Amato, 1966; Brizzee et al, 1982; Takeuchi and Takeuchi, 1986).

The litter sex ratios were assessed in the gestational day 15+5 day groups as some very early studies suggested that ionizing radiation could alter the sex ratio (Job et al, 1935). As well, other studies have suggested that there may be sexual differences in the incidence of radiation-induced malformations. For example, Rugh et al (1964) found that female offspring were more affected in

terms of radiation-induced stunting with a prenatal exposure of 100 rads (1 Gy) before gestational day 9. Sexing of the 15+5 day fetuses in this study revealed that a 0.5 Gy (50 rad) exposure on gestational day 15 did not significantly alter the sex ratio. As only 3 fetuses showed gross anomalies in this group (2 males and 1 female), no apparent sexual distribution of anomalies was apparent.

Of the 244 whole brains examined from the combined irradiated and control groups, no differences in gross brain morphology were detected. As mentioned previously, brains yielded from visibly smaller irradiated fetuses (approximately 7 irradiated specimens from all groups combined) appeared small when compared with controls. Other than small size, however, morphology appeared proportional and intact. These findings are consistent with the notion that a gestational day 15 exposure with doses lower than 100 rads (1 Gy) have a low probability of yielding visibly malformed brains (Brent, 1980; Kameyama and Hoshino, 1986).

For all regions of the brain examined in this study, pyknotic cells were readily apparent in 100% of the gestational day 15+4 hour irradiated specimens. Previous studies indicate that the peak incidence of post-irradiation pyknosis occurs 4 to 6 hours following exposure of 25 to 200 rads (0.25 to 2 Gy) in telencephalic regions (Hicks and D'Amato, 1961 and 1980; Brizzee et al, 1982; Tribukait and Cekan, 1982). It could not be concluded from this study whether the 4 hour post-irradiation interval represented

the time of peak incidence for pyknotic cells in any brain regions examined.

For essentially all brain regions studied, pyknotic cells were restricted to proliferative ventricular zones. Very rarely were pyknotic cells observed in the mitotically active regions of the proliferative zones, or in regions of assumed post-migratory destinations of cells for any brain region. An exception to this observation occurred in the cerebellum where a few pyknotic cells were observed in the 15+4 hour nuclear zone (a post-migratory region), and the transitional zone (a pre-migratory zone). It should be noted, however, that the numbers of pyknotic cells observed in nuclear and transitional zones were at all times, dramatically lower than those seen in the cerebellar proliferative zones of the same specimens.

Occasional pyknotic cells were also observed in the superficial limits of the main olfactory bulbs. Again, however, pyknotic cells seen in these superficial regions were considerably rare. Generally therefore, it may be assumed from these observations that for all brain regions studied, cells in the M phase of the cell cycle as well as those which had attained their post-migratory positions (G zero phase cells) were the most radioresistant to a 0.5 Gy (50 rad) exposure on gestational day 15. Cells in other stages of the cell cycle, and post-mitotic cells could not be differentiated at this gestational time period with conventional light microscopy. It was assumed that

the pyknotic cells observed were proliferative stem cells of the G2 phase, and undifferentiated neural and/or glial cells of the early G1 phase, as described in previous studies (Hicks and D'Amato, 1966 and 1980; Altman, 1969a; Bayer and Altman, 1974 and 1975; Hoshino and Kameyama, 1988).

Based on the available information regarding the cellular events in the brain on gestational day 15, early G1 phase cells of the cerebral cortex at this time may include pre-migratory and migratory large neurons and/or glial cells of lamina VI and possibly the subplate (Berry and Rogers, 1965; Berry, 1974; Marin-Padilla, 1978; Raedler et al, 1980; Schultze and Korr, 1981; Smart and McSherry, 1982). As well as the G2 phase proliferative cells of the olfactory bulbs, pyknotic cells observed in the main olfactory bulbs ventricular zones may represent the pre-migratory and migratory mitral and tufted cells destined for the mitral layer and the external plexiform layer, respectively. The few pyknotic cells seen in the superficial regions of the bulb could possibly represent either late-migratory or post-migratory tufted or mitral cells, or glial cell elements of the main olfactory bulb (Bayer, 1983).

Although the regional borders of the hippocampal formation are difficult to distinguish at this gestational stage, pyknotic cells in this structure were assumed to represent G2 phase proliferative cells of the subicular and Ammon's horn ventricular zones. Affected G1 phase cells of these regions may represent the deep pyramidal cells

of the subiculum, as well as the large neurons of Ammon's horn, excluding the pyramidal cells of the Ammon horn pyramidal cell layer. As the proliferative ventricular area believed to give rise to the cells of the dentate gyrus demonstrated few pyknotic figures in any irradiated specimen at this post-irradiation interval, it was deduced that polymorphic and pyramidal cells of the dentate hilus as well as large neurons of the dentate molecular layer, which all begin to arise on gestational day 15, were unaffected by a 0.5 Gy (50 rad) exposure (Bayer and Altman, 1974; Bayer, 1980a; Bayer, 1980b). In addition to the G2 proliferative cells of the cerebellar neuroepithelium, it is likely that pyknotic cells of this region represent pre-migratory, late arising deep cerebellar nuclei neurons and Purkinje cells. The few pyknotic cells observed in the nuclear zones of the irradiated cerebelli may represent a radiosensitive post-migratory class of deep cerebellar neuron or nuclear zone glial cell. Pyknotic transitional zone cells were assumed to represent the pre-migratory, undifferentiated Purkinje cells of this region (Altman and Bayer, 1978a).

With the exception of the hippocampal formation, the number of mitotically active cells observed at the juxtaventicular borders of proliferative ventricular zones were subjectively assessed as similar to control levels in all brain regions examined 4 hours post-irradiation. Studies of the telencephalon have revealed that reductions in the number of mitotic cells can be observed at 1 to

2 hour post-irradiation intervals following 50 to 200 rads (0.5 to 2 Gy) exposures. Resumption of mitotic activity to control levels occurs within 2 to 5 hours post-irradiation (Hicks and D'Amato, 1961; Hayashi and Kameyama, 1979; Brizzee et al, 1982; Tribukait and Cekan, 1982; Kameyama and Hoshino, 1986; Hoshino and Kameyama, 1988). Based on assumptions derived from the literature on acute irradiation effects, it can therefore be said that following a 0.5 Gy (50 rad) irradiation on gestational day 15, mitotic activity may be temporarily reduced, but evidence of such reductions are not evident by a 4 hour post-irradiation interval in the cerebral cortex, main olfactory bulb, and cerebellum.

Differences between the acute 4 hour post-irradiation response of the hippocampal formation as compared to other brain regions are noteworthy. First, the hippocampal formation is the only brain area studied which demonstrated a regionally variable distribution of pyknotic cells. As noted previously, the regional distibution of pyknotic cells indicates that radiosensitivity of the formation is highest in the subicular region, followed by the Ammon's horn region on gestational day 15. The presumtive proliferative region of the dentate gyrus appeared radioresistant at this post-irradiation interval, based on the extremely low incidence of pyknotic cells observed in this region. The hippocampal formation was the only brain area examined which demonstrated a lower incidence of mitotic figures as compared with controls.

In the Ammon horn region, small cytoplasmic

inclusions were also observed in the ventricular zone cells at the 4 hour post-irradiation interval. As mentioned, studies on the post-irradiation acute effects on the telencephalon reveal that mitotic activity of this region resumes within 2 to 5 hours post-irradiation, approximately concurrent to the estimated time of peak pyknotic cell frequency (Hicks and D'Amato, 1961 and 1980; Brizzee et al, 1982; Kameyama and Hoshino, 1986; Hoshino and Kameyama, 1988). As well, Hayashi and Kameyama (1979) found in a study of the mouse telencephalon with irradiation exposures of 25 to 100 rads (0.25 to 1 Gy), that cytoplasmic ribosomal aggregations were evident prior to the appearance of nuclear pyknosis in early fetal stage irradiated specimens.

Assuming that the cytoplasmic inclusions seen in the Ammon's horn ventricular cells represented ribosomal aggregations, and that the acute post-irradiation sequence of events is similar in the telencephalon and hippocampal formation, observations made in this study of the 4 hour post-irradiation hippocampal formation may indicate that this region revealed a prolonged acute effect response, compared to other brain regions examined. In other words, at the 4 hour post-irradiation interval in the hippocampal formation, the full picture of acute post-irradiation responses of cells in this region may just begin to be evident. As Bayer (1980b) found that the hippocampal formation ventricular neuroepithelium was most radiosensitive on gestational day 15, examination of this region at short post-irradiation

intervals, beyond the 4 hour post-irradiation interval, may reveal a more accurate picture of pyknotic cell frequencies, and thus, a more accurate estimation of the relative radiosensitivities of various developmental areas of this brain region.

Finally, with respect to the acute 4 hour post-irradiation assessments, no evidence of macrophage activity was evident in any brain region examined. This indicates that cellular debris clearance of the traumatized brain regions had not commenced by this post-irradiation interval. This finding is consistent with previous observations made in acute telencephalic post-irradiation studies, where clearance of cellular debris was not evident until the 24 hour post-irradiation interval (Brizzee et al, 1982).

By the 48 hour post-irradiation interval, no qualitative differences existed between the control and irradiated brain regions with exception of the main olfactory bulbs of two irradiated specimens. In these two specimens, many of the mitral cells seen in the post-migratory mitral cell layer demonstrated irregular morphology and a darker staining propensity, compared with mitral cells of control olfactory bulbs. As the main olfactory bulbs on gestational day 15 are giving rise to approximately 80% of the mitral cells of the mitral cell layer (Bayer, 1983), it was assumed that irregularities of mitral cells seen in these two specimens may constitute an irradiation effect. However, chi-square analysis of two anomalous findings out of 13 irradiated

specimens was not statistically significant.

In addition to the above, one control specimen in the 15+48 hour group demonstrated retarded development of the hippocampal formation as described in Chapter 4. Although the reason for this anomalous control finding cannot be determined conclusively, it was assumed that it may represent a normal control incidence of brain malformation.

By the 15+5 day post-irradiation interval, differentiation between control and irradiated specimens proved to be similar to findings derived from the 15+48 hour groups. Qualitative assessment of the cerebral cortex, corpus callosum, hippocampal formation, and the cerebellum at the 15+5 day post-irradiation interval revealed no differences between the control and irradiated specimens. Again, however, mitral cell changes were observed in 4 out of 15 irradiated specimens which proved statistically significant with chi-square comparison.

Two of the four affected irradiated specimens showed an overall reduction in brain size so consequently, olfactory bulb size of these fetuses was also reduced, compared with controls. The olfactory bulbs of these two specimens demonstrated an overall decrease of laminae cell densities, with the most stiking depletions occurring in the mitral cell layer. Throughout the mitral cell layer of these specimens, many mitral cells appeared shrunken, irregularly shaped, and dark-staining, compared with the

controls. In the other two affected olfactory bulbs of this series, deficits were restricted to localized areas of the mitral cell layer. Cells in these circumscribed regions were similar in appearance to those observed in more seriously affected bulbs. As well as these qualitative differences observed, mitral cell counts of the affected specimens revealed a significant depletion of mitral cells as compared with the controls; with the severely affected bulbs showing close to a 50% reduction of mitral cells, and the less seriously affected bulbs showing an 18% depletion of mitral cells.

The apparent differences between the irradiation effects seen in the olfactory bulbs of those severely affected and those more subtly affected, may be due to differences in the developmental stage of these fetuses at the time of irradiation exposure. Although all irradiation in this study occurred on gestational day 15, differences in the developmental timetables of fetuses on gestational day 15 likely existed. Differences in the developmental status of fetuses between litters for the same gestational day would be expected due to the likely variability in the timing of animal mating and fertilization. Differences in the developmental age of offspring within the same litter also occurs due to variability in fertilization time and variability in implantation time. Because blood supply is not uniform throughout the uterus, variability in the nutritional supply to the embryos also exists, which can

influence the timing of developmental events, and/or alter the regenerative potential in some fetuses (Rugh, 1968; Hicks and D'Amato, 1966).

In the two more severely affected specimens, all main olfactory bulb layers seemed to be depleted in relative cell density. This may indicate that the irradiation insult to these specimens occurred when the olfactory neuroepithelium was still in its proliferative phase, prior to giving rise to the neural and glial elements of the main olfactory bulb layers. Consequently, the depleted number of olfactory neuroepithelial cells resulted in an overall depletion of cells in all olfactory bulb layers. Similar multilaminar deficits of the cortical plate have been demonstrated with irradiation of the cerebral cortex neuroepithelium during its proliferative phase (Berry and Eayrs, 1963; Berry, 1974). In the two more subtly affected specimens, only the mitral cell layers were affected. In this case, irradiation insult to the olfactory lobes of these specimens likely occurred after the major proliferative phase of the neuroepithelium, and during the specific generation phase of mitral cells. Consequently only the mitral cells arising at that particular gestational moment would be affected.

Although the above explanation implies that irradiation-induced cell depletion observed in the mitral layer in these animals could be accounted for on the basis of G2 proliferative cell depletion or early G1 mitral cell

depletion, other plausible explanations exist according to the literature on irradiation-induced teratogenesis of the nervous system. Delayed migration of mitral cells, radial glia cell death, or post-migratory cell death secondary to damage to the stroma and/or inadequate synaptogenesis could all account for the mitral cell depletions observed in these specimens (Lewis, 1979; Brent, 1986; Kameyama and Hoshino, 1986; Konermann, 1986; Schull et al, 1990).

The significance of the changes in mitral cell staining propensity and shape could not be determined with conventional light microscopy at this gestational interval. These changes could represent a permanent distortion of mitral cell morphology as a consequence of direct radiation exposure to the cells, delayed maturation of mitral cells, or a pre-pyknotic state of mitral cells resulting from either a radiation-induced interruption of the stroma, and/or impaired post-migratory synaptic connectivity (Lewis, 1979; Hall, 1988).

Mitral cell depletion and morphological changes of the mitral cells following <u>in utero</u> exposure to irradiation have not been previously reported. Very few irradiation studies have been conducted on the post-irradiation effects of the olfactory bulbs, and those which have considered the olfactory bulbs have involved exposure dosages well above 100 rads (1 Gy). Changes in the mitral cell layer were not a reported finding in the sister investigation of this study (Persaud and Bruni, 1990).

Approximately 80% of mitral cells arise from the olfactory ventricular zone on gestational days 15 and 16 (Bayer, 1983), therefore, mitral cells could be a credible target for the antiproliferative effects of a 0.5 Gy (50 rad) exposure to ionizing radiation on gestational day 15. Normally, the remaining complement of mitral cells continue to arise until gestational day 18 (Bayer, 1983). It is conceivable that mitral cell depletions and morphological changes were not observed in the postnatal period following exposure to 0.5 Gy (50 rads) on gestational day 15 (Persaud and Bruni, 1990) if, in fact, the olfactory ventricular zone is also capable of mitral cell restitution until gestational day 18. Evidence in the literature as to whether the olfactory ventricular zone is capable of restitution of lost cells could not be found.

If, in fact, mitral cell depletion constitutes a permanent long term effect of a 0.5 Gy (50 rad) exposure of ionizing radiation on gestational day 15, this defect could have serious functional and behavioral implications for the rat in the postnatal period. In the rat, mitral cells participate in an intricate circuit within the olfactory bulb, making multiple connections with essentially all other neurons of the main olfactory bulb. This complex circuit of intrabulbar connections is believed to constitute the mechanism for the amplification of olfactory stimuli. The mitral cells are considered the main output neurons of the olfactory bulb. Their axons constitute the bulk

of the efferent olfactory fiber system, which in very general terms, make connections with brain regions responsible for olfactory discrimination, emotion responses to olfactory stimuli, and the coordination of smell, touch, taste, and motor activity (Zeman and Innes, 1963, Bayer; 1983). Essentially, it may be assumed that the rat, as a macrosmatic animal, would demonstrate deficits in many instinctive and volitional behaviors if mitral cells of the olfactory bulbs were depleted or impaired.

Another significant finding of the 15+5 day irradiated group was that derived from cortical zone measurements. Besides the normal developmental trends outlined in Chapter 4, three-way analysis of variance comparisons indicated a significant difference between cortical zone measurements of the irradiated vs control specimens. One-way analysis of variance comparisons confirmed that significant thinning of the subventricular zones occurred in both frontal and parietal cortices of gestational day 15+5 day irradiated fetuses. Occipital cortical areas were unaffected by treatment with 0.5 Gy (50 rads) on gestational day 15. Prenatal measurement of irradiated cortical zones has not been done in previous studies.

Thinning of the subventricular zone could be due to a depleted number of migrating neurons passing through this zone to their laminar destinations, or a depleted number of glial percursor cells, as this zone is considered to constitute a major glial cell pool (Berry, 1974; Lewis,

1979; Sturrock and Smart, 1980; Caviness, 1989). Given the other zone measurements derived in this study, it would appear that the latter is the most likely cause of subventricular zone thinning of irradiated 15+5 day fetuses. Gestational day 20 (15+5 days) represents the final stages of neuronal production and migration to laminae III and II of the cortical plate (Berry and Rogers, 1965; Berry, 1974). Given that the ventricular zone measurements of all irradiated cortical regions on this gestational day were the same as controls, one does not expect that the production of the normal complement of laminae III and II neurons would be impaired. Likewise, it seems improbable that a reduced complement of migrating neurons exists in irradiated subventricular zones at this time.

Numerous studies on the postnatal effects of prenatal irradiation have revealed reductions in the cortical plate thickness of irradiated offspring with both high and low dose ranges. Cortical plate thinning has been primarily attributed to radiation-induced neuronal depletion with a subsequent reduction of neuropil density for this region (Hicks, 1953; Hicks et al, 1957 and 1959; Cowan and Geller, 1960; Hicks and D'Amato, 1961 and 1966; Takeuchi et al, 1981; Brizzee et al, 1982; Norton and Donoso, 1985; Kameyama and Hoshino, 1986; Konermann, 1986; Reyners et al, 1986; Norton and Kimler, 1988; Schull et al, 1990; Fukui et al, 1991).

The role of glial cell radiosensitivity, and

the possible contribution of depleted glial cells to radiation-induced cortical plate thinning has not been established, and remains a controversial point (Dr. R.P. Jensh, personal communication). The findings of this study do not preclude the possibility that radiation-induced thinning of the cortical plate in the postnatal period is due to prenatal neuronal depletion, postnatal neuronal depletion secondary to reduced synaptogenesis and/or disruption of the stroma, or reduced neuropil. However, the lack of significant differences in thickness measurement or qualitative differences in the cell packing densities of existing cortical plate regions, and the ventricular zones of irradiated cerebral cortices, compared with controls on gestational day 20 (15+5 days), indicate that neuronal depletion is not a probable outcome of a 0.5 Gy (50 rad) exposure on gestational day 15. Rather, as indicated from this data, depletion of cortical plate glia would more likely contribute to postnatal thinning of frontal and parietal cortical regions.

The significance of subventricular thinning in frontal and parietal regions, with no significant differences in occipital regions is unknown. These trends may simply reflect normal patterns and gradients of cortex growth on gestational day 15, or at the gestational period of cortex measurement (day 20).

A few comments on the overall picture of irradiation effects to the developing prenatal brain demonstrated in this study are required. Although all brain regions examined

revealed signs of radiosensitivity at the 4 hour post-irradiation interval, no significant differences between irradiated and control specimens (with exception to the mitral cell changes and the cortical measurement changes observed) existed in subsequent post-irradiation intervals. In some respects, this is congruent with the literature on nervous system effects of prenatal irradiation. Studies on the acute effects of telencephalon irradiation have indicated that signs of post-irradiation repair of tissues begin approximately 24 hours following irradiation at low dose ranges (Hoshino and Kameyama, 1988). As shown in this study, no indications of acute irradiation trauma such as cell pyknosis, altered mitotic rate, or increased macrophage activity were observed by the 48 hour post-irradiation interval for cerebral cortex, olfactory bulbs, hippocampal formation, or cerebellum.

With exception of the mitral cell changes of the main olfactory bulbs, and subventricular zone thinning of the cerebral cortices in the 15+5 day specimens, one is tempted to conclude from these results that post-irradiation recovery had occurred for most brain regions examined. However, abundant literature concerning postnatal cytological changes in the brain following prenatal irradiation, as well as the cortical, hippocampal, and cerebellar changes observed in Persaud and Bruni's study (1990), which utilized the same 0.5 Gy (50 rad) exposure on gestational day 15, indicate that any conclusions as to recovery may be erroneous.

Rather, a more plausible conclusion is that the fetus is not an adequate model for demonstrating the full impact of a 0.5 Gy (50 rad) irradiation exposure on gestational day 15 to the developing nervous system; nor does the fetal model provide a complete picture of the genesis of cytological lesions which are manifested in the postnatal period. As indicated by our mitral cell findings, some degree of cell differentiation appears to be a prerequisite for detecting radiation-induced changes. Other investigators have provided credibility for this conclusion in their findings that prenatal irradiation effects become more evident with increasing age of the irradiated offspring (Brizzee et al, 1982; Goerttler, 1982; Brent, 1986; Persaud and Bruni, 1990). Essentially, cytologically normal appearing tissue in the prenatal period, does not mean that subsequently expressed damage can be excluded with security.

In addition to the above, one must also recognize the possible draw-backs of methodologies used, and the subjective evaluation inherent in all scientific study. First, the sample sizes used to determine brain manifestations may not be adequate to reveal a realistic incidence of irradiation effects. Second, conventional light microscopy, particularily when combined with paraffin sectioning and singular staining techniques, imposes an inherent limitation on the possible breadth of observable effects. Finally, as revealed in Chapter 4, for brain regions examined at prenatal gestational intervals, most cells at these stages

were homogeneous in appearance and had not attained any organized spatial distribution, making differentiation between cell types, and definition of regional borders a relatively subjective exercise.

The final component of this study to be discussed are the findings from the placenta. At the 4 hour post-irradiation interval, placental weights were found to be significantly greater than controls. Microscopic evaluation of 9 out of 10 irradiated placentas revealed enlargement of maternal blood channels in both labyrinthine and basal zones as compared with the controls. Although the cytological constituents of these placental zones appeared disorganized in some of the irradiated specimens, cells appeared intact and no pyknosis was observed. Swelling of the maternal blood spaces was assumed to be due to an edematous response of the maternal blood channels, secondary to irradiation trauma. The increased weights of the placentas at this post-irradiation interval were assumed to be related to the apparent increase in fluid volume of the placentas at this time. One may expect that inflamation of this magnitude may interrupt placental blood flow; however, this could not be confirmed within this study.

By the 48 hour post-irradiation interval, placental weights were significantly less than the controls. Histological studies revealed a difference in the staining propensity of circumscribed areas of labyrinthine zone trophoblast. Within these circumscribed regions, trophoblast cells stained

a pale purplish-pink color, instead of the characteristic blue color of these cells seen in unaffected regions and in the controls. These areas of altered staining appeared primarily in the region of labyrinth close to the chorionic plate. Other than these areas of altered staining, no other qualitative differences were detected, as compared with controls. Cellular staining changes were noted in 6 out of 10 irradiated placentas which proved significant. Changes from the normally basophilic nature of labyrinthine trophoblast to a more acidophilic staining propensity may represent a decrease or disruption in the DNA or RNA constituents of these cells (Wheater et al, 1987). It may be assumed that the general integrity of the trophoblast cells in these regions had changed, and possibly, the normal mitotic activity of this region was altered. No increased incidence of pyknotic cells was observed at this post-irradiation interval, therefore, whether these cellular changes represented a pre-pyknotic state could not be determined. Although the exact nature or cause for these changes could not be determined with certainty in these specimens, it is probable that damage to these regional localizations of cells was due to excessive mechanical stress placed upon them from edematous maternal blood channels of earlier stages. As growth of the placenta is primarily due to the hypertrophy and hyperplasia of the labyrinthine zone at this gestational stage (Bridgman, 1948b, Blackburn et al, 1965; Davies and Glasser, 1968), it is assumed that decreased mitotic activity

of affected labyrinthine regions could account for the decreased weight of irradiated placentas at this post-irradiation interval.

By the 5 day post-irradiation interval, no significant differences existed in placental weights, or the morphological and histological appearance of irradiated placentas as compared with control.

The placental weight changes and microscopic changes observed in this study have not been previously reported in the literature for any irradiation dose level. Studies of the placenta have been quite rare. Those which have been conducted have concluded that the placenta is radioresistant, and that the placenta plays an insignificant role in irradiation teratogenesis. Seventy-two hours post-irradiation is the earliest post-irradiation interval at which placentas have been assessed in related studies, and placental weight information has not been provided (Foraker et al, 1955; Brent, 1960; Rugh, 1965).

In part, this study is in agreement with previous reports of irradiation effects on the placenta. Histological assessment did not reveal any observable cytological damage or changes in the placenta which could have resulted from direct radiation exposure. Rather, placental weight changes at the 4 and 48 hour post-irradiation intervals, as well as the histological changes seen at the 48 hour interval appear to represent secondary effects of whole body maternal exposure. However, as placental integrity is temporarily

compromised following a 0.5 Gy (50 rad) irradiation exposure on gestational day 15, one may suspect that this may have an impact on the developing fetus.

As outlined by Rosso (1980), reduced nutrient transfer to the fetus can result from either reduced placental blood flow or reduced placental size. Consequently, fetal growth retardation may result. As mentioned, previous irradiation studies of the placenta have concluded that the placenta does not play a role in irradiation teratogenesis (Brent, 1960). However, gestational dates of exposure and post-irradiation assessment intervals do not correspond to those used in this study. Although fetal growth retardation is believed by most irradiation teratologists to be caused by the antiproliferative effects of ionizing radiation acting directly on the fetus (Brent and McLaughlin, 1960; Rugh et al, 1964), a temporary impediment of placental transfer of nutrients may also contribute to the persistent growth reductions seen in offspring irradiated during the fetal period.

Because of these placental findings, it is believed that future systematic studies on radiation effects on the placenta could contribute valuable information to the field of irradiation teratogenesis.

6. SUMMARY

This study reveals that a 0.5 Gy (50 rad) gamma irradiation exposure on gestational day 15 had no impact on maternal health, litter size, fetal lethality rate, gross morphological development, or the litter sex ratio. Fetal growth parameters are affected, with crown-rump measurement reductions evident in irradiated fetuses as early as the 4 hour post-irradiation interval.

Evidence of irradiation-induced pyknosis in the cerebral cortices, main olfactory bulbs, hippocampal formations, and cerebelli of all 4 hour post-irradiation specimens reveals that these regions are radiosensitive on gestational day 15. However, at subsequent fetal stages few post-irradiation effects were observed.

This study showed reductions of olfactory bulb mitral cells in a significant number of 5 day post-irradiation specimens. These findings have not been reported in previous irradiation teratology studies. Since the mitral cells are the main output neurons of the rat olfactory bulbs, we suggest that reductions of these cells may affect the postnatal behavior of the irradiated rat offspring.

Measurements of the developmental cortical zones in 5 day post-irradiation fetuses revealed significant reductions in the subventricular zones of frontal and parietal cortical regions, compared with controls. A gestational day 15 irradiation with 0.5 Gy (50 rads) did not affect thickness measurements of occipital cortical zones.

Cortical thinning has been a well documented postnatal outcome of both high and low level prenatal irradiation. In most postnatal studies, neuronal depletion has been assumed to be the cause of cortical thinning following prenatal irradiation. The relative radiosensitivity of glial cells and their role in cortical depletion, however, remains a controversial issue. This study indicates that the subventricular zone, which serves as a major pool of glial cells, is thinned in frontal and parietal regions with a 0.5 Gy (50 rad) irradiation on gestational day 15. This implies that glial precursor cells are particularily radiosensitive, and may contribute to cortical irradiation manifestations in the postnatal period.

Although no other significant brain changes were detected at the 48 hour, and 5 day post-irradiation intervals, we are cautious to conclude that recovery has occurred in these other brain regions. Persaud and Bruni (1990) found that there were postnatal changes in the cerebral cortex, hippocampal formation, and cerebellum following a gestational day 15 irradiation with 0.5 Gy (50 rads). This and other irradiation studies indicate that the fetus may not be an adequate model for demonstrating the full impact of a 0.5 Gy (50 rad) irradiation exposure on gestational day 15 to the developing nervous system; nor does the fetal model provide a complete picture of the genesis of cytological lesions which are manifest in the postnatal period. Further maturation of these brain regions appears to be required

before irradiation-induced effects can be observed.

Few previous studies have assessed the effects of irradiation on the placenta. This study reveals that cytological constituents of the placenta are not affected by direct irradiation exposure, however, the placenta is indirectly affected by whole body maternal exposure. Since we have shown that the placenta is temporarily compromised following a 0.5 Gy (50 rad) irradiation exposure on gestational day 15, one may suspect that this may have an impact on the developing fetus. Further studies are needed to evaluate the role of the placenta on irradiation-induced teratogenesis.

***

TABLE A.2 EQUIVALENT SQUARES OF RECTANGULAR FIELDS

Long axis (cm)	Short axis (cm)																								
	1	2	3	4	5	6	7	8	9	10	11	12	13	14	15	16	17	18	19	20	22	24	26	28	30
1	1·0																								
2	1·4	2·0																							
3	1·6	2·4	3·0																						
4	1·7	2·7	3·4	4·0																					
5	1·8	3·0	3·8	4·5	5·0																				
6	1·9	3·1	4·1	4·8	5·5	6·0																			
7	2·0	3·3	4·3	5·1	5·8	6·5	7·0																		
8	2·1	3·4	4·5	5·4	6·2	6·9	7·5	8·0																	
9	2·1	3·5	4·6	5·6	6·5	7·2	7·9	8·5	9·0																
10	2·2	3·6	4·8	5·8	6·7	7·5	8·2	8·9	9·5	10·0															
11	2·2	3·7	4·9	5·9	6·9	7·8	8·6	9·3	9·9	10·5	11·0														
12	2·2	3·7	5·0	6·1	7·1	8·0	8·8	9·6	10·3	10·9	11·5	12·0													
13	2·2	3·8	5·1	6·2	7·2	8·2	9·1	9·9	10·6	11·3	11·9	12·5	13·0												
14	2·3	3·8	5·1	6·3	7·4	8·4	9·3	10·1	10·9	11·6	12·3	12·9	13·5	14·0											
15	2·3	3·9	5·2	6·4	7·5	8·5	9·5	10·3	11·2	11·9	12·6	13·3	13·9	14·5	15·0										
16	2·3	3·9	5·2	6·5	7·6	8·6	9·6	10·5	11·4	12·2	13·0	13·7	14·3	14·9	15·5	16·0									
17	2·3	3·9	5·3	6·5	7·7	8·8	9·8	10·7	11·6	12·4	13·2	14·0	14·7	15·3	15·9	16·5	17·0								
18	2·3	4·0	5·3	6·6	7·8	8·9	9·9	10·8	11·8	12·7	13·5	14·3	15·0	15·7	16·3	16·9	17·5	18·0							
19	2·3	4·0	5·4	6·6	7·8	8·9	10·0	11·0	11·9	12·8	13·7	14·5	15·3	16·0	16·7	17·3	17·9	18·5	19·0						
20	2·3	4·0	5·4	6·7	7·9	9·0	10·1	11·1	12·1	13·0	13·9	14·7	15·5	16·3	17·0	17·7	18·3	18·9	19·5	20·0					
22	2·3	4·0	5·5	6·8	8·0	9·1	10·3	11·3	12·3	13·3	14·2	15·1	16·0	16·8	17·6	18·3	19·0	19·7	20·3	20·9	22·0				
24	2·4	4·1	5·5	6·8	8·1	9·2	10·4	11·5	12·5	13·5	14·5	15·4	16·3	17·2	18·0	18·8	19·6	20·3	21·0	21·7	22·9	24·0			
26	2·4	4·1	5·5	6·9	8·1	9·3	10·5	11·6	12·6	13·7	14·7	15·7	16·6	17·5	18·4	19·2	20·1	20·9	21·6	22·4	23·7	24·9	25·0		
28	2·4	4·1	5·6	6·9	8·2	9·4	10·5	11·7	12·8	13·8	14·8	15·9	16·8	17·8	18·7	19·6	20·5	21·3	22·1	22·9	24·4	25·7	27·0	28·0	
30	2·4	4·1	5·6	6·9	8·2	9·4	10·6	11·7	12·8	13·9	15·0	16·0	17·0	18·0	18·9	19·9	20·8	21·7	22·5	23·3	24·9	26·4	27·7	29·0	30·0

All dimensions are in cm

--- PROGRAM SUP11 - THERAPLAN V03 ---
% Depth Dose Data for THERATRON COBALT

Source-Surface Distance 75.0 cm
COBALT 60 HVL = 10.50 MM
Field size defined at 75.0 cm
Dosimetry normalized at 75.5 cm

Depth	4.0 X 4.0	5.0 X 5.0	6.0 X 6.0	7.0 X 7.0	8.0 X 8.0	9.0 X 9.0	10.0 X 10.0	11.0 X 11.0	12.0 X 12.0	13.0 X 13.0	14.0 X 14.0	15.0 X 15.0	16.0 X 16.0	18.0 X 18.0	20.0 X 20.0	25.0 X 25.0
0.0	50.0	50.0	50.0	50.0	50.0	50.0	50.0	50.0	50.0	50.0	50.0	50.0	50.0	50.0	50.0	50.0
0.5	100.0	100.0	100.0	100.0	100.0	100.0	100.0	100.0	100.0	100.0	100.0	100.0	100.0	100.0	100.0	100.0
1.0	97.1	97.4	97.6	97.7	97.8	97.9	98.0	98.1	98.1	98.2	98.2	98.2	98.2	98.2	98.2	98.3
1.5	94.1	94.6	94.9	95.2	95.4	95.5	95.7	95.8	95.9	95.9	96.0	96.0	96.0	96.1	96.1	96.3
2.0	91.2	91.9	92.4	92.7	93.0	93.2	93.4	93.6	93.7	93.7	93.8	93.9	93.9	94.0	94.1	94.3
2.5	88.1	88.9	89.5	89.9	90.3	90.6	90.8	91.0	91.2	91.3	91.4	91.5	91.6	91.7	91.8	92.1
3.0	85.1	86.0	86.7	87.2	87.7	88.0	88.3	88.6	88.7	88.9	89.0	89.2	89.3	89.5	89.7	89.9
3.5	82.2	83.1	83.9	84.5	85.0	85.4	85.7	86.0	86.2	86.4	86.6	86.8	86.9	87.1	87.3	87.7
4.0	79.3	80.3	81.1	81.8	82.4	82.8	83.2	83.5	83.8	84.0	84.2	84.4	84.6	84.8	85.1	85.5
4.5	76.3	77.4	78.4	79.1	79.8	80.3	80.7	81.0	81.3	81.6	81.8	82.0	82.2	82.5	82.8	83.3
5.0	73.4	74.7	75.7	76.5	77.2	77.8	78.2	78.6	78.9	79.2	79.5	79.7	79.9	80.3	80.6	81.1
5.5	70.6	71.9	72.9	73.9	74.6	75.2	75.7	76.2	76.5	76.9	77.2	77.4	77.6	78.0	78.4	79.0
6.0	67.9	69.1	70.3	71.2	72.0	72.7	73.3	73.8	74.2	74.6	74.9	75.2	75.4	75.8	76.2	76.9
6.5	65.3	66.6	67.8	68.8	69.6	70.3	70.9	71.4	71.9	72.3	72.6	72.9	73.1	73.6	74.0	74.7
7.0	62.8	64.1	65.4	66.4	67.2	68.0	68.6	69.1	69.6	70.0	70.4	70.7	70.9	71.4	71.8	72.6
7.5	60.3	61.7	62.9	64.0	64.9	65.6	66.3	66.8	67.3	67.7	68.1	68.5	68.7	69.3	69.8	70.6
8.0	57.9	59.3	60.5	61.6	62.5	63.3	64.0	64.6	65.1	65.5	65.9	66.3	66.6	67.2	67.7	68.7
8.5	55.6	57.0	58.3	59.4	60.3	61.1	61.8	62.4	63.0	63.4	63.8	64.2	64.5	65.2	65.7	66.7
9.0	53.3	54.8	56.1	57.2	58.2	59.0	59.7	60.4	60.9	61.4	61.8	62.2	62.5	63.2	63.7	64.8
9.5	51.2	52.7	54.0	55.1	56.1	57.0	57.7	58.3	58.9	59.3	59.8	60.2	60.6	61.2	61.8	62.9
10.0	49.1	50.6	51.9	53.1	54.1	55.0	55.7	56.3	56.9	57.4	57.9	58.3	58.6	59.3	59.9	61.0
10.5	47.3	48.7	50.0	51.2	52.2	53.1	53.8	54.5	55.0	55.5	56.0	56.4	56.8	57.5	58.1	59.2
11.0	45.5	46.9	48.2	49.4	50.4	51.2	52.0	52.6	53.2	53.7	54.2	54.6	55.0	55.7	56.4	57.5
11.5	43.8	45.2	46.5	47.6	48.6	49.4	50.2	50.8	51.4	52.0	52.5	52.9	53.3	54.0	54.6	55.8
12.0	42.1	43.5	44.7	45.9	46.8	47.7	48.4	48.1	48.7	50.2	50.7	51.2	51.6	52.3	53.0	54.2
12.5	40.4	41.8	43.0	44.1	45.1	45.9	46.7	47.4	48.0	48.5	49.1	49.5	49.9	50.7	51.3	52.6
13.0	38.0	40.2	41.4	42.5	43.4	44.3	45.0	45.7	45.3	46.9	47.4	47.8	48.3	49.0	49.7	51.0
13.5	37.2	38.5	39.8	40.8	41.8	42.6	43.4	44.1	44.7	45.3	45.8	46.2	46.7	47.5	48.1	49.4
14.0	35.7	37.0	38.2	39.2	40.1	41.0	41.0	42.5	43.1	43.7	44.2	44.7	45.1	45.9	46.6	47.9
14.5	34.1	35.4	36.6	37.6	38.5	39.4	40.2	40.9	41.5	42.1	42.6	43.1	43.6	44.4	45.1	46.5
15.0	32.6	33.9	35.1	36.1	37.0	37.9	38.7	39.4	40.0	40.6	41.1	41.6	42.1	42.9	43.6	45.0

Appendix IIa

FIXATIVE
2.5% Glutaraldehyde - 2% Paraformaldehyde in 0.12 m Phosphate Buffer with 0.02 mM $CaCl_2$

Paraformaldehyde (5%)	200 ml
50% Glutaraldehyde (Biological Grade)	25 ml
0.4 M Standard Phosphate Buffer	150 ml
0.5% $CaCl_2$	2 ml
Add distilled water to make	500 ml

The solution was filtered through #44 filter paper before use.

STOCK SOLUTIONS
5% Paraformaldehyde

Paraformaldehyde	10 gm
Distilled water	200 ml
1 N NaOH	4-6 drops

The distilled water was heated until slightly steaming, and then the paraformaldehyde was added. Once the paraformaldehyde was dissolved, the NaOH was added until the solution was clear.

0.4 M Standard Phosphate Buffer

Sodium phosphate monobasic	5.3 gm
Potassium phosphate dibasic anhydrous	28.0 gm
Add distilled water to make	500.0 ml

DEXTROSE RINSE SOLUTION
8% Dextrose in 0.12 M Phosphate Buffer with 0.02 mM $CaCl_2$

Dextrose	8.0 gm
Phosphate buffer 0.4 M.	30.0 ml
$CaCl_2$ 0.5%	0.4 ml
distilled water to make	100.0 ml

EPON EMBEDDING
For Epon 812 with a W.P.E. of 143.9

	200 ml.	100 ml.
Epon 812	99.0 gm	49.5 gm
DDSA	45.5 gm	22.75 gm
MNA	55.5 gm	27.75 gm
BDMA	3.0 ml	1.5 ml

EPON EMBEDDING PROCEDURE FOR LIGHT MICROSCOPY

* The time of each rinse may vary with size of tissue block. Time schedules listed below are adequate for fetal brains at gestational day 20. It is preferable to rotate tissues during all rinses.

1) overnight in dextrose rinse solution.

2) 30 minutes in distilled water.

3) 2 changes of 30 minutes each in 30% ETOH.

4) 45 minutes or overnight in 70% ETOH.

5) 45 minutes in 95% ETOH.

6) 30 minutes in 100% ETOH.

7) 2 changes of 30 minutes each in 100% MeOH.

8) 3 changes of 30 minutes each in 100% propylene oxide.

9) 9 hours of 50/50 ratio of propylene oxide/Epon.

10) overnight at 25/75 ratio of propylene oxide/Epon.

11) 100% Epon for 24 hours on rotator.

12) 100% Epon - capsule embedded - overnight at 37°C.

13) capsules - 48 hours at 60°C.

The blocks were left to cure for approximately 2 weeks before sectioning.

MANUAL PROCESSING FOR PARAFFIN EMBEDDING OF FETAL BRAINS

* The following procedure was found adequate for infiltration of paraffin in fetal brains at gestational day 20. For steps 1) to 4) inclusive, tissues were agitated in their respective rinses.

1) 2 changes of 70% ETOH for 30 minutes each.

2) 2 changes of 95% ETOH for 30 minutes each.

3) 2 changes of 100% ETOH for 30 minutes each.

4) 2 changes of Chloroform for 1 hour each.

5) 4 changes of Paraffin for a total of 3 to 4 hours.

   i) 1st paraffin change - in hot water bath under fume hood. Approximately 1 hour.

   ii) 2nd paraffin change - in hot water bath under fume hood. Approximately 1 hour.

   iii) 3rd paraffin change - uncovered in vaccum oven at 15 lbs. pressure. Approximately 1 hour.

   iv) 4th paraffin change - uncovered in vaccum oven at 15 lbs. pressure. Approximately 1 hour.

6) Embed in paraffin blocks.

THIONIN STAINING FOR THE PARAFFIN EMBEDDED TISSUE

1) 2 changes of Xylol for 2 minutes each.

2) 1 change of 100% ETOH for 5 minutes.

3) 1 change of 95% ETOH for 5 minutes.

4) 1 change of 70% ETOH for 5 minutes.

5) 1 change of distilled water for 5 minutes.

6) 1 change of thionin stain for 4 to 6 seconds
   (Note: time may vary with different density tissues)

7) 3 changes of distilled water for 5 minutes each.

8) 3 changes of 70% ETOH for 5 minutes each.

9) 1 changes of 95% ETOH for 2 minutes.

(thionin staining continued)

10) 2 changes of 100% ETOH for 2 minutes each.

11) 2 changes of Xylol for 2 minutes each.

* can be cover-slipped immediately.

Appendix IId

HAEMATOXYLIN AND EOSIN STAINING PROCEDURE

1) 2 changes of Xylol for 2 minutes each.

2) 2 changes of 100% ETOH for 2 minutes each.

3) 1 change of 95% ETOH for 2 minutes.

4) 1 change of distilled water for 5 minutes.

5) 1 change of Harris Haematoxylin for 4 minutes.

6) Water wash for 5 minutes.

7) 2 to 3 dips of 1% acid alcohol.

8) Water wash for 5 minutes.

9) 1 change of Lithium Carbonate (saturated aqueous) for 2 minutes.

10) Water wash for 5 minutes.

11) 1 change of Eosin for 2 minutes.

12) 10 dips in distilled water.

13) 15 dips in 70% ETOH.

14) 20 dips in 95% ETOH.

15) 2 changes of 100% ETOH for 2 minutes each.

16) 2 changes of Xylol for 2 minutes each.

* can be cover-slipped immediately.

MORPHOLOGICAL CRITERIA - GESTATIONAL DAY 15
(g.d. 15+4 hours)

Maternal # _____ # live offspring _____

dead offspring _____ # resorptions _____

	YES	NO
1) skull shape normal (pronounced mesencephalic and cervical flexures; head size about equal to body)		
2) eyes are developed i) bilateral symmetry		
ii) same size		
iii) eyelids not formed		
3) ears i) bilateral symmetry		
ii) ear auricle just beginning to develop		
4) mouth i) mandible formed but is much smaller than maxilla		
ii) tongue beginning to form (can be seen when mouth is open)		
iii) palate open		
5) papillae i) minimum of 4 to 6 rows of maxillary vibrissary papillae		
ii) 2 papillae above eye		
iii) 3 mammary papillae appearing along milk line		
iv) a few hair papillae may be appearing on trunk		
6) scent gland or papillae appear at angle of mouth		

(15+4 Hours Continued) YES NO

7) forelimbs
i) bilateral symmetry

ii) forepaws are webbed
(a slight degree of digit
differentiation evident)
Forepaws more advanced in
development than hindpaws

8) hindlimbs
i) bilateral symmetry

ii) hindpaws are webbed
(no obvious digit
differentiation as yet)

9) gut herniation evident
(covered by an epithelial
sac)

10) umbilical cord intact

11) spine/torso straight
i) both anterior and posterior
neuropores should be closed

12) tail straight (should
extend beyond tip of snout)

13) cloaca open

14) liver and heart should
be visible through skin

15) CROWN- RUMP LENGTHS

1)____ 2)____ 3)____ 4)____ 5)____ 6)____ 7)____

8)____ 9)____ 10)____ 11)____ 12)____ 13)____

14)____ 15)____ 16)____ 17)____ 18)____ 19)____

20)____

COMMENTS:

MORPHOLOGICAL CRITERIA - GESTATIONAL DAY 17
(g.d. 15+48 hours)

Maternal # _____ # live offspring _____

dead offspring _____ # resorptions _____

	YES	NO
1) skull shape normal (mesencephalic and cervical flexures still obvious at this stage)		
2) eyes (formation complete) i) bilateral symmetry		
ii) same size		
iii) eyelids forming (membranous ring, slightly elevated)		
3) ears i) bilateral symmetry		
ii) ear auricle partially covering external auditory meatus		
4) mouth i) mandible almost same size as maxilla		
ii) tongue normal (may be slightly protruding from mouth) - papillae forming on dorsal aspect		
iii) palate partially fused anteriorly and dorsally, still open in middle region		
5) papillae i) minimum of 8 rows of maxillary vibrissary papillae		
ii) 2 vibrissary papillae over eye		
iii) 1 between eye and ear		

(15+48 Hours Continued) YES NO

iv) 3 mammary papillae along milk line

v) hair papillae over body and some appearing on the head

6) 3 scent glands along line of jaw

7) forelimbs
i) bilateral symmetry

ii) full separation of digits

8) hindlimbs
i) bilateral symmetry

ii) webbing of digits with variable degree of digit separation

9) gut herniation visible and covered by an epithelial sac

10) umbilical cord intact

11) spine/torso straight

12) tail straight (reaches tip of snout)

13) genital tubercle present

14) cloaca closed

15) CROWN- RUMP LENGTHS

1)____ 2)____ 3)____ 4)____ 5)____ 6)____ 7)____

8)____ 9)____ 10)____ 11)____ 12)____ 13)____

14)____ 15)____ 16)____ 17)____ 18)____ 19)____

20)____

COMMENTS:

MORPHOLOGICAL CRITERIA- GESTATIONAL DAY 20
(g.d. 15+5 days)

Maternal # _____ # live offspring _____

dead offspring _____ # resorptions _____

	YES	NO
1) skull shape normal		
2) eyes i) bilateral symmetry		
ii) same size		
iii) eyelid formed (palpabral fissure closed)		
3) ears i) bilateral symmetry		
ii) auricle formed over external auditory meatus		
4) mouth i) normal externally (mandible and maxilla development complete)		
ii) tongue normal (papillae present)		
iii) palate closed		
5) papillae i) minimum of 10 rows of maxillary vibrissary papillae (with whiskers)		
ii) 2 vibrissary papillae over eye (whiskers)		
iii) 1 between eye and ear		
iv) 3 mammary papillae along milk line		
v) hair papillae over body and head		

(15+5 DAYS CONTINUED) YES NO

6) 3 scent glands along line of jaw

7) forelimbs

i) bilateral symmetry

ii) 5 toes (clawed)

iii) paw pads formed

8) hindlimbs

i) bilateral symmetry

ii) 5 toes (clawed)

iii) paw pads formed

9) gut herniation totally reduced

10) umbilical cord intact

11) spine/torso straight

12) tail straight (reaches to mid-torso region)

13) genital tubercle developed

FEMALES _____ # MALES _____
(1.0 mm.) (2.0 mm.)

14) CROWN - RUMP LENGTHS

1)____ 2)____ 3)____ 4)____ 5)____ 6)____ 7)____

8)____ 9)____ 10)____ 11)____ 12)____ 13)____

14)____ 15)____ 16)____ 17)____ 18)____ 19)____

20)____

COMMENTS:

BIBLIOGRAPHY

Altman, J. (1969a). Autoradiographic and histological studies of postnatal neurogenesis III. Dating the time of production and onset of differentiation of cerebellar microneurons in rats. J. Comp. Neurol., 136: 269-294.

Altman, J. (1969b). Autoradiographic and histological studies of postnatal neurogenesis IV. Cell proliferation and migration in the anterior forebrain, with special reference to persisting neurogenesis in the olfactory bulb. J. Comp. Neurol., 137: 433-458.

Altman J. and Bayer, S. (1978a). Prenatal development of the cerebellar system in the rat I. Cytogenesis and histogenesis of the deep cerebellar nuclei and the cortex of the cerebellum. J. Comp. Neurol., 179: 23-48.

Altman, J. and Bayer, S. (1978b). Prenatal development of the cerebellar system in the rat II. Cytogenesis and histogenesis of the inferior olive, pontine gray, and the precerebellar reticular nuclei. J. Comp. Neurol., 179: 49-76.

Altman, J., and Das, G.D. (1966). Autoradiographic and histological studies of postnatal neurogenesis. J. Comp. Neurol., 126: 337-390.

Alvarez-Buylla, A. (1990). Commitment and migration of young neurons in the vertebrate brain. Experientia, 46: 879-882.

Angevine, J.B., and Sidman, R.L. (1961). Autoradiographic study of cell migration during histogenesis of cerebral cortex in the mouse. Nature, 192: 766-768.

Bayer, S.A. (1980a). Development of the hippocampal region in the rat I. Neurogenesis examined with 3H-thymidine autoradiography. J. Comp. Neurol., 190: 87-114.

Bayer, S.A. (1980b). Development of the hippocampal region in the rat II. Morphogenesis during embryonic and early postnatal life. J. Comp. Neurol., 190: 115-134.

Bayer, S.A. (1983). Radiographic studies of neurogenesis in the rat olfactory bulb. Exper. Brain Res., 50: 329-340.

Bayer, S.A., and Altman, J. (1974). Hippocampal development in the rat: Cytogenesis and morphogenesis examined with autoradiography and low-level x-irradiation. J. Comp. Neurol., 158: 55-80.

Bayer, S.A., and Altman, J. (1975). The effects of x-irradiation on the postnatally-forming granule cell populations in the olfactory bulb, hippocampus, and cerebellum of the rat. Exper. Neurol., 48: 167-174.

Berry, M. (1974). Development of the cerebral neocortex of the rat. In Gottlieb, G. (ed.) Aspects of Neurogenesis. Academic Press, New York, pp. 7-67.

Berry, M., and Eayrs, J.T. (1963). Histogenesis of the cerebral cortex. Nature, 197: 984-985.

Berry, M., and Rogers, A.W. (1965). The migration of neuroblasts in the developing cerebral cortex. J. Anat., 99: 691-709.

Blackburn, W.R., Kaplan, H.S., McKay, D.G. (1965). Morphologic changes in the developing rat placenta following prednisolone administration. Am. J. of Obstet. and Gynecol., 92: 234-246.

Boulder Committee (1970). Embryonic vertebrate central nervous system: Revised terminology. Anat. Rec., 166: 257-262.

Brent, R.L. (1960). The indirect effect of irradiation on embryonic development II. Irradiation of the placenta. Am. J. Dis. Child., 100: 103-108.

Brent, R.L. (1980). Radiation teratogenesis. Teratology, 21: 281-298.

Brent, R.L. (1986). The effects of embryonic and fetal exposure to x-ray, microwaves, and ultrasound. Clinic in Perinatology, 13: 615-648.

Brent, R.L. and Bolden, B.T. (1967). The indirect effect of irradiation on embryonic development III. The contribution of ovarian irradiation, uterine irradiation, oviduct irradiation, and zygote irradiation to fetal mortality and growth retardation in the rat. Radiation Research, 30: 759-773.

Brent, R.L. and Bolden, B.T. (1968). Indirect effect of x-irradiation on embryonic development: Utilization of high doses of maternal irradiation on the first day of gestation. Radiation Research, 36: 563-570.

Brent, R.L. and McLaughlin, M.M. (1960). The indirect effect of irradiation on embryonic development I. Irradiation of the mother while shielding the embryonic site. Am. J. Dis. Child., 100: 94-102.

Bridgman, J. (1948a). A morphological study of the development of the placenta of the rat I. An outline of the development of the placenta of the white rat. J. Morphol., 83: 61-85.

Bridgman, J. (1948b). A morphological study of the development of the placenta of the rat. II. A histological and cytological study of the development of the chorioallantoic placenta of the white rat. J. Morphol., 83: 195-223.

Brill, A.B. (1982) Low-Level Radiation Effects: A Fact Book. The Society of Nuclear Medicine, New York, pp. 25-36.

Brizzee, K.R. (1967). Quantitative histological studies on delayed effects of prenatal x-irradiation in rat cerebral cortex. J. Neuropathol. and Exper. Neurol., 26: 584-600.

Brizzee, K.R., and Brannon, R.B. (1972). Cell recovery in foetal brain after ionizing radiation. Int. J. Radiat. Biol., 21: 375-388.

Brizzee, K.R., Ordy, J.M. and D'Agostino, A.N. (1982). Morphological changes of the central nervous system after radiation exposure in utero. In Developmental Effects of Prenatal Irradiation. Gustav Fischer- Stuttgart, New York, pp. 145-201.

Brown, N.A. and Fabro, S. (1981). Quantitation of rat embryonic development in vitro: a morphological scoring system. Teratology, 24: 65-78.

Caviness, V.S. (1989). Normal development of the cerebral neocortex. Developmental Neurobiol., 12: 1-10.

Christie, G.A. (1964). Developmental stages in somite and post-somite rat embryos, based on external appearance, and including some features of the macroscopic development of the oral cavity. J. Morph., 114: 263-286.

Clarke, R.H., and Southwood, T.R.E. (1989). Risks from ionizing radiation. Nature, 338: 197-198.

Cobb, C.E. (1989). Living with radiation. National Geographic, (April edition): 403-437.

Cowan, D. and Geller, L.M. (1960). Long-term pathological effects of prenatal x-irradiation on the central nervous system of the rat. J. Neuropathol. and Exper. Neurol., 19: 488-527.

D'Amato, C.J. and Hicks, S.P. (1980). Development of the motor system: effects of radiation on developing corticospinal neurons and locomotor function. Exper. Neurol., 70: 1-23.

Das, G.D. (1977). Experimental analysis of embryogenesis of cerebellum in rat. I. Subnormal growth following x-ray radiation on day 15 of gestation. J. Comp. Neurol., 176: 419-434.

Davies, J. and Glasser, S.R. (1968). Histological and fine structural observations on the placenta of the rat. Acta Anat., 69: 542-608.

Edwards, J.A. (1968). The external development of the rabbit and rat embryo. Advances in Teratology, 3: 239-263.

Ferrer, I., Xumetra, A., and Santamaria, J. (1984). Cerebral malformations induced by prenatal x-irradiation: an autoradiographic and golgi study. J. Anatomy, 138: 81-93.

Foraker, A.G., Denham, S.W., and Mitchell, D.D. (1955). Histochemical studies of the effect of irradiation of the placenta. Arch. Pathol., 59: 82-89.

Fukui, Y., Hoshino, K., Hayasaka, I., Inouye, M., and Kameyama, Y. (1991). Developmental disturbance of rat cerebral cortex following prenatal low-dose gamma irradiation: a quantitative study. Exper. Neurol., 112: 292-298.

Gadisseux, J.F., Evrard, P., Misson, J.P., and Caviness, V.S. (1889). Dynamic structure of the radial glial fiber system of the developing murine cerebral wall. An immunocytochemical analysis. Developmental Brain Research, 50: 55-67.

Gadisseux, J.F., Kadhim, H.J., van den Bosch de Aguilar, P., Caviness, V.S., and Evard, P. (1990). Neuron migration within the radial glial fiber system of the developing murine cerebrum: an electron microscope autoradiographic analysis. Developmental Brain Research, 52: 39-56.

Goerttler, K. (1982). The effect of external irradiation on the prenatal development. Pathomorphological bases. In Developmental Effects of Prenatal Irradiation. Gustav Fischer-Stuttgart, New York, pp. 15-26.

Gray, G.E., Leber, S.M., and Sanes, J.R. (1990). Migratory patterns of clonally related cells in the developing central nervous system. Experientia, 46: 929-940.

Halasz, N. (1986). Early x-irradiation of rats. Methodological

description and morphological observations on the olfactory bulb. Journal of Neuroscience Methods, 18: 255-268.

Hall, E.J. (1988). Radiation for the Radiobiologist. Third edition. J.B. Lippincott Company, Philadelphia.

Hayashi, Y. and Kameyama, Y. (1979). Early pathological changes of mantle cells of the telencephalon by low-dose x-irradiation in mouse embryos and fetuses. Congenital Anomalies, 19: 37-46.

Hernandez-Verdum, D. (1974). Morphogenesis of the syncytium in the mouse placenta. Cell Tissue Research, 148: 381-396.

Hicks, S.P. (1953). Developmental malformations produced by radiation: a timetable of their development. Amer. J. Roentgen Rad. Ther. Nuc. Med., 69: 272-293.

Hicks, S.P., Brown, B.L. and D'Amato, C.J. (1957). Regeneration and malformation in the nervous system, eye, and mesenchyme of the mammalian embryo after radiation injury. Amer. J. Pathol., 33: 459-474.

Hicks, S.P. and D'Amato, C.J. (1961). How to design and build abnormal brains using radiation during development. In Disorders of the Developing Nervous System. Edited by W.S. Fields, Charles C. Thomas Publishers, Illinois, pp. 60-97.

Hicks, S.P. and D'Amato, C.J. (1963). Low dose radiation of the developing brain. Science, 141: 903-905.

Hicks, S.P. and D'Amato, C.J. (1966). Effects of ionizing radiation on fetal development. In Advances In Teratology I. Logos Press Ltd., London, pp. 196-250.

Hicks, S.P. and D'Amato, C.J. (1980). Effects of radiation on development, especially of the nervous system. The Am. J. of Forensic Med. and Pathol., 4: 309-317.

Hicks, S.P., D'Amato, C.J., and Lowe, M.J. (1959). The development of the mammalian nervous system. I. Malformations of the brain, especially the cerebral cortex, induced in rats by radiation. J. Comp. Neurol., 113: 435-470.

Hinds, J.W. (1968a). Autoradiographic study of histogenesis in the mouse olfactory bulb I. Time of origin of neurons and neuroglia. J. Comp. Neurol., 134: 287-304.

Hinds, J.W. (1968b). Autoradiographic study of histogenesis in the mouse olfactory bulb II. Cell proliferation and migration. J. Comp. Neurol., 134: 305-322.

Hoshino,K. and Kameyama, Y. (1988). Developmental stage-dependent radiosenitivity of neural cells in the ventricular zone of telencephalon in mouse and rat fetuses. Teratology, 37: 257-262.

Ivy, G.O. and Killackey, H.P. (1981). The ontogeny of the distribution of callosal projection neurons in the rat parietal cortex. J. Comp. Neurol., 195: 367-389.

Jacobson. S. and Trojanowski, J.Q. (1974). The cells of origin of the corpus callosum in rat, cat, and rhesus monkey. Brain Res., 74: 149-155.

Jensen, K.F. and Altman, J. (1982). The contribution of late-generated neurons to the callosal projection in the rat: A study with prenatal x-irradiation. J. Comp. Neurol., 209: 113-122.

Jensh, R.P. Departments of Anatomy and Radiology, Jefferson Medical College, Thomas Jefferson University, Philadelphia, Pennsylvania.

Jensh, R.P. (1986). Effects of prenatal irradiation on postnatal psychophysiological development. In Handbook of Behavioral Teratology. Edited by, E.P. Riley and C.V. Vorhees, Plenum Press, New York, pp. 471-485.

Jensh, R.P., Brent, R.L. and Vogel, W.H. (1986). Studies concerning the effects of low level prenatal x-irradiation on postnatal growth and adult behavior in the wistar rat. Int. J. Radiat. Biol., 50: 1069-1081.

Jensh, R.P., Brent, R.L., and Vogel, W.H. (1987). Studies of the effect of 0.4-Gy and 0.6-Gy prenatal x-irradiation on postnatal adult behavior in the wistar rat. Teratology, 35: 53-61.

Job, T.T., Leibold, G.J., and Fitzmaurice, H.A. (1935). Biological effects of roentgen rays: The determination of critical periods in mammalian development with x-rays. The Am. J. of Anat., 56: 97-117.

Kalter, H. (1968). Teratology of the Central Nervous System. The University of Chicago Press, Chicago, pp. 90-138.

Kameyama, Y. and Hoshino, K. (1986). Sensitive phases of CNS development. In Radiation Risks to the Developing Nervous System. Gustav Fischer- Stuttgart, New York, pp. 75-92.

Kirby, D.R.S., and Bradbury, S. (1965). The hemochorial mouse placenta. Anat. Rec., 152: 279-282.

Konermann, G. (1982). Consequences of prenatal radiation exposure on perinatal and postnatal development: morphological, biochemical, and histochemical aspects. In Developmental Effects of Prenatal Irradiation. Gustav Fischer- Stuttgart, New York, pp. 237-249.

Konermann, G. (1986). Brain development in mice after prenatal irradiation: modes of effect manifestation; Dose-response relationships and the RBE of neutrons. In Radiation Risks to the Developing Nervous System. Gustav Fischer Verlag, Stuttgart, New York, pp. 93-116.

Levitt, P., Cooper, M.L., and Rakic, P. (1981). Coexistence of neuronal and glial precursor cells in the cerebral ventricular zone of the fetal monkey: an ultrastructure immunoperoxidase analysis. J. Neurosci., 1: 27-39.

Lewis, P.D. (1979). The application of cell turnover studies to neuropathology. Recent Advances in Neuropathol., 1: 41-65.

Liesi, P. (1990). Extracellular matrix and neuronal movement. Experientia, 46: 900-907.

Luskin, M.B., Pearlman, A.L., and Sanes, J.R. (1988). Cell lineage in the cerebral cortex of the mouse studied in vivo and in vitro with a recombinant retrovirus. Neuron, 1: 635-647.

Marin-Padilla, M. (1978). Dual origin of the mammalian neocortex and evolution of the cortical plate. Anat. Embryol., 152: 109-126.

McClellan, R.O. (1988). Prospects for new information relevant to radiation protection from studies of experimental animals. Health Physics, 55: 279-293.

McConnell, S.K. (1990). The specification of neuronal identity in the mammalian cerebral cortex. Experientia, 46: 922-929.

Mole, R.H. (1979). Radiation effects on pre-natal development and their radiological significance. Brit. J. Radiol., 52: 89-101.

Mossman, K.L., and Hill, L.T. (1982). Radiation risks in pregnancy. Obstet. and Gynecol., 60: 237-242.

Mullenix, P., Norton, S., and Culver, B. (1975). Locomotor damage in rats after x-irradiation in utero. Exper.

Neurol., 48: 310-324.

Muntener, M., and Hsu, Y.C. (1977). Development of trophoblast and placenta of the mouse. Acta Anat., 98: 241-252.

National Research Council (1980). The Effects on Populations of Exposure to Low Levels of Ionizing Radiation. National Academic Press, Washington, D.C., pp. 477-514.

Norton, S. (1986). Behavioral changes in preweaning and adult rats exposed prenatally to low ionizing radiation. Toxicol. and Applied Pharmacol., 83: 240-249.

Norton, S., and Donoso, J.A. (1985). Forebrain damage following prenatal exposure to low-dose x-irradiation. Exper. Neurol., 87: 185-197.

Norton, S. and Kimler, B.F. (1987). Correlation of behavior with brain damage after in utero exposure to toxic agents. Neurotoxicol. and Teratol., 9: 145-150.

Norton, S. and Kimler, B.F. (1988). Comparison of functional and morphological deficits in the rat after gestational exposure to ionizing radiation. Neurotoxicol. and Teratol., 10: 363-371.

Norton, S., Kimler, B.F., and Mullenix, P.J. (1991). Progressive behavioral changes in rats after exposure to low levels of ionizing radiation in utero. Neurotoxicol. and Teratol., 13: 181-188.

Ordy, J.M., Brizzee, K.R. and Young, R. (1982). Prenatal Co 60-irradiation effects on visual acuity, maturation of the fovea in the retina, and the striate cortex of squirrel monkey offspring. In Developmental Effects of Prenatal Irradiation. Gustav Fischer- Stuttgart, New York, pp. 205-217.

Paxinos, G., Tork, I., Tecott. L.H., Valentino, K.L. (1991). Atlas of the Developing Rat Brain. Academic Press Inc., Harcourt Brace Jovanovich Publishers, San Diego.

Pellegrino, L.J., Pellegrino, A.S., and Cushman, A.J. (1981). Stereotaxic Atlas of the Rat Brain. Second edition. Plenium Press, New York.

Persaud, T.V.N. and Bruni, J.E. (1990). In vitro and in vivo studies of the health effects of ionizing radiation on the development of the CNS in the rat. (Unpublished report).

Prasad, K.N. (1974). Effects of irradiation on the nervous system. From Human Radiation Biology. Harper and Row Publishers Inc., Maryland, pp. 257-274 and 319-339.

Price,J. and Thurlow, L. (1988). Cell lineage in the rat cerebral cortex: a study using retroviral mediated gene transfer. Development, 104: 473-482.

Raedler, E., Raedler, A., and Feldhaus, S. (1980). Dynamic aspects of neocortical histogenesis in the rat. Anat. Embryol., 158: 253-269.

Rakic, P. (1986). Normal and abnormal migration during brain development. In Radiation Risks to the Developing Nervous System. Gustav Fischer Verlag, Stuttgart, New York, pp. 35-44.

Rakic, P. (1988). Specification of cerebral cortical areas. Science, 241: 170-176.

Rakic, P. (1990). Principles of neural cell migration. Experientia, 46: 882-891.

Reyners, H., Reyners, E.G., and Maisin, J.R. (1986). The role of the glia in late damage after prenatal irradiation. In Radiation Risks to the Developing Nervous System. Gustav Fischer Verlag, Stuttgart, New York, pp. 117-131.

Ritenour, E.R. (1986). Health effects of low level radiation: Carcinogenesis, teratogenesis, and mutagenesis. Seminars in Nuclear Medicine, XVI: 106-117.

Rodier, P.M. (1986). Behavioral effects of antimitotic agents administered during neurogenesis. In Handbook of Behavioral Teratology. Edited by E.P. Riley and C.V. Vorhees, Plenum Press, New York, pp. 185-209.

Roizin, L., Rugh, R, and Kaufman, M.A. (1962). Neuropathologic investigations of the x-irradiated embryo rat brain. J. Neuropathol. and Exper. Neurol., 21: 219-243.

Rosso, P. (1980). Placental growth, development, and function in relation to maternal nutrition. Federation Proc., 39: 250-254.

Rugh, R. (1965). Effects of ionizing radiations, including radioisotopes, on the placenta and embryo. Birth Defects Original Article Series, 1: 64-73.

Rugh, R. (1968). The Mouse: Its Reproduction and Development. Burgess Publishing Company, Minneapolis, pp. 299.

Rugh, R., Duhamel, L., Osborne, A.W., and Varma, A. (1964). Persistent stunting following x-irradiation of the fetus. Am. J. Anat., 115: 185-198.

Russell, L.B., and Russell, W.L. (1950). The effect of radiation on the preimplantation stages of the mouse embryo. Anat. Res., 108: 521.

Schmidt, S.L. and Lent, R. (1987). Effects of prenatal irradiation on the development of cerebral cortex and corpus callosum of the mouse. J. Comp. Neurol., 264: 193-204.

Schull, W.J., Norton, S., and Jensh, R.P. (1990). Ionizing radiation and the developing brain. Neurotoxicol. and Teratol., 12: 249-260.

Schultze, B., and Korr, H. (1981). Cell kinetic studies of different cell types in the developing and adult brain of the rat and the mouse: a review. Cell Tissue Kinet., 14: 309-325.

Shepard, T.H. (1989). Catalog of Teratogenic Agents. Sixth Edition. John Hopkins University Press, Baltimore.

Silver, J., Lorenz, S.E., Wahlsten, D. and Coughlin, J. (1982). Axonal guidance during development of the great cerebral commissures: Descriptive and experimental studies, in vivo, on the role of preformed glial pathways. J. Comp. Neurol., 210: 10-29.

Smart, I.H.M., and McSherry, G.M. (1982). Growth patterns in the lateral wall of the mouse telencephalon. II. Histological changes during and subsequent to the period of isocortical neuron production. J. Anat., 134: 415-442.

Sturrock, R.R., and Smart, I.H.M. (1980). A morphological study of the mouse subependymal layer from embryonic life to old age. J. Anat., 130: 391-415.

Takeuchi, I.K., Kawabata, M., and Takeuchi, Y.K. (1981). Effects of prenatal x-irradiation on the postnatal growth and the brain weights of rats. Congen. Anom., 21: 245-251.

Takeuchi, I.K. and Takeuchi, Y.K. (1986). Congenital hydrocephalus following x-irradiation of pregnant rats on an early gestational day. Neurobehav. Toxicol. and Teratol., 8: 143-150.

Tamaki, Y. and Inouye, M. (1976). Brightness discrimination learning in a Skinner box in prenatally irradiated

rats. Physiol. Behav., 16: 343-348.

Tribukait, B. and Cekan, E. (1982). Dose-effect relationship and the significance of fractionated and protracted radiation for the frequency of fetal malformations following x-irradiation of pregnant C3H mice. In Developmental Effects of Prenatal Irradiation. Gustav Fischer- Stuttgart, New York, pp. 29-34.

Upton, A.C. (1982). The biological effects of low-level ionizing radiation. Scientific American, 246, 2: 41-49.

Walsh, C., and Cepko, C.L. (1990). Cell lineage and cell migration in the developing cerebral cortex. Experientia, 46: 940-947.

Wheater, P.R., Burkitt, H.G., and Daniels, V.G. (1987). Functional Histology. Churchill Livingstone Publishers, New York.

Wilson, J.G. (1964). In Teratology: Principles and Techniques. Edited by J.G. Wilson and J. Warkany, University of Chicago Press, Chicago, 251-277.

Wilson, J.G., and Karr, J.W. (1951). Effects of irradiation on embryonic development: X-rays on the 10th day of gestation in the rat. The Am. J. of Anat., 88: 1-33.

Wise, S.P. (1975). The laminar organization of certain afferent and efferent fiber systems in the rat somatosensory cortex. Brain Res., 90: 139-142.

Wise, S.P. and Jones, E.G. (1976). The organization and postnatal development of the commissural projection of the rat somatic sensory cortex. J. Comp. Neurol., 168: 313-344.

Yamazaki, J.N. (1966). A review of the literature on the radiation dosage required to cause manifest central nervous system disturbances from in utero and postnatal exposure. Pediatrics, 37: 877-903.

Yorke, C.H. and Caviness, V.S. (1975). Interhemispheric neocortical connections of the corpus callosum in the normal mouse: A study based on anterograde and retrograde methods. J. Comp. Neurol., 164: 233-246.

Zeman, W. and Innes, J.R.M. (1963). Craigie's Neuroanatomy of the Rat. Academic Press, New York.